

9th International Symposium on Swift Heavy Ions in Matter

Abstract book

May 18 - 21, 2015
Darmstadt, Germany



Conference Venue

darmstadtium (level 3, room 3.09, Helium)
Schlossgraben 1
64283 Darmstadt

Conference Office

darmstadtium (level 3, room 3.10, Hydrogenium)
Stefanie Lüttges
Sabine Seubert
Phone: +49- 6151-7806808
Mobil: +49-174 – 3281484
Email: shim2015@gsi.de

Registration

Sunday, May 17, 4 – 6 pm
Monday, May 18, 8 – 9 am

Wifi / WLAN

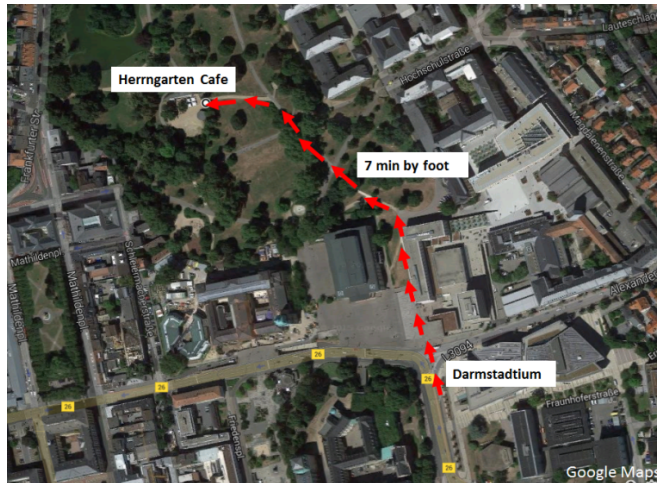
At the conference center free Wifi access will be available.
SSID: SHIM2015
Password: shim2015

Local Organizers

M. Bender	C. Malot	D. Severin
S. Hagmann	L. Movsesyan	A. Spende
J. Krieg	P. Neumayer	M.E. Toimil-Molares
K. Kupka	H. Rothard	M. Tomut
T. Litvinova	I. Schubert	C. Trautmann
S. Lüttges	S. Seubert	G. Taucher-Scholz

Meals

Coffee breaks will be served at the foyer (level 3). Drinks and pretzels will be provided during the poster sessions. Lunches (Monday to Wednesday) will be served at Herrngarten Cafe.



Social Program

- **Welcome reception:** Sunday, May 17, 6 - 9 pm

takes place at Herrngarten Cafe (see map).

- **Evening tour at Mathildenhöhe:** Tuesday, May 19, 7 pm

We offer a guided walking tour (~ 1h) at Mathildenhöhe. Please indicate at the registration, if you would like to join. The tour is limited to 25 persons.

- **Excursion:** Wednesday, May 20, 1:30 pm

Option A: *Grube Messel* (~ 3.5 h)

Guided tour of Messel pit fossil site (Grube Messel), a UNESCO World Heritage site. www.grube-messel.de

Buses to Messel will depart in front of the conference center at 1:30 pm.

Option B: *Mathildenhöhe* (~ 2h)

Guided walking tour of Artists Colony on Mathildenhöhe, a prominent center of *Art Nouveau*, including visit of the museum. www.mathildenhoehe.eu

Meeting point for the Mathildenhöhe tour will be in front of Darmstadtdium at 1:30 pm.

Please indicate your choice at the registration. Note, the Messel tour is limited to 100 persons.

- **Conference Dinner:** Wednesday, May 20

The Conference Dinner will be served at Frankenstein Castle.

frankenstein-restaurant.de

Buses will depart directly from Grube Messel to Frankenstein Castle at 5:10 pm.

An extra bus to the dinner leaves in front of the conference center at 5:40 pm.

- **GSI Tour:** Thursday, May 21, 1:20 pm

www.gsi.de

For the GSI Tour on Thursday, May 21, buses depart at 1:20 pm in front of the conference center. At GSI, snacks and drinks will be provided.

Scientific Program

Conference Chairpersons

C. Trautmann (GSI, Darmstadt, Germany)

H. Rothard (CIMAP, Caen, France)

International Scientific Committee

P. Apel (Dubna, Russia)

A. Itoh (Kyoto, Japan)

D. Avasthi (Delhi, India)

A. Iwase (Osaka, Japan)

E. Balanzat (Caen, France)

X. Ma (Lanzhou, China)

W. Bolse (Stuttgart, Germany)

R. Papaleo (Porto Alegre, Brazil)

S. Bouffard (Caen, France)

M. Toulemonde (Caen, France)

D. Dauvergne (Lyon, France)

C. Trautmann (Darmstadt, Germany)

M. Durante (Darmstadt, Germany)

A. Warczak (Krakow, Poland)

Invited Speakers

Walter Assmann, *Munich, Germany*

Toshiyuki Azuma, *Riken, Japan*

Michaël Beuve, *Lyon, France*

Marie-Claude Clochard, *Palaiseau, France*

Emily Lamour, *Paris, France*

Emmanuel Dartois, *Orsay, France*

Véronique Ferlet-Cavrois, *Noordwijk, Netherlands*

Siegfried Klaumünzer, *Berlin, Germany*

Nikita Medvedev, *Hamburg, Germany*

Isabelle Monnet, *Caen, France*

Olli Pakarinen, *Helsinki, Finland*

Markus Schöffler, *Frankfurt, Germany*

Thomas Stöhlker, *Darmstadt, Germany*

YuYu Wang, *Lanzhou, China*

Kazuhiro Yasuda, *Kyushu Univ, Japan*

Matt Zepf, *Belfast, UK*

Orals

Invited talks: **25 min plus 5 min** for discussion

Oral talks: **15 min plus 5 min** for discussion

The organizers will provide a Windows 7 PC and RGB cable. For this computer, presentation slides should be provided as powerpoint (ppt, pptx) or pdf file for smooth operation. Speakers are requested to identify themselves to the chairperson of the session and upload the final version of their talk during the preceding coffee break. Speakers can use their own laptop but should check the compatibility with the available system well in advance of the session. If needed, speakers are requested to bring adapting connectors (e.g. for Macintosh laptops).

Posters

Poster sessions will be held on Monday and Tuesday (May 18 and 19). Posters to be presented on Monday (Session A) can be placed on Monday after 12 pm and must be dismantled Tuesday before midday. Posters to be presented on Tuesday (Session B) can be placed on Tuesday after 12 pm and must be dismantled on Wednesday before midday. Any poster left after the indicated times will be discarded. Presenters are expected to be close to their poster for discussions. **Four best student posters will be awarded. The winners will be announced during the Conference Dinner.**

Poster Specifications: Poster boards are designed for **DIN A0** in portrait orientation (height larger than width, **maximum poster size 90cm x 120cm**). Poster pins will be provided at the conference desk.

Manuscripts for SHIM proceedings

- Three paper copies have to be submitted to the organizers by the first day of the conference
- In addition, manuscripts have to be submitted electronically to the special proceedings submission system of Elsevier at:
http://ees.elsevier.com/nimb_proceedings/default.asp
When asked for the "Article Type" please make sure to select **SHIM-2015**.
- Deadline for submission is May 31, 2015
- More info on manuscripts are available under
<http://indico.gsi.de/internalPage.py?pagelId=11&confId=2825>

Vendor Exhibition

Opened during conference hours from Monday to Wednesday (May 18-20).

Scientific Program

* Primary author
Presenting author

Monday, May 18, 2015

- 09:00 **Conference Opening**
Welcome to Darmstadt
Reinhard Neumann
- Session 1 - Chair: Akio Itoh (Kyoto University)**
- 09:30 **I1 - Fragmentation of He and Ne dimers by swift heavy ions**
Markus Schöffler (Goethe-University Frankfurt)
- 10:00 **O1 - Quasi-equilibrium in charge state evolution for swift heavy ions after passing through carbon foils**
Makoto Imai (Kyoto University)
- 10:20 **I2 - Primary processes: from ion-solid to ion-ion collisions**
Emily Lamour (Institut des NanoSciences de Paris - UPMC)
- 10:50 **O2 - Fragmentation mechanism of neon dimer induced by O₆⁺ ions**
Xinwen Ma (Chinese Academy of Sciences)
- 11:10 --- Coffee break ---
- Session 2 - Chair: Maik Lang (University of Tennessee)**
- 11:40 **I3 - In-situ single event effect tests of electronic components for space applications**
Véronique Ferlet-Cavrois (European Space Agency)
- 12:10 **O3 - Swift heavy ion irradiation damage in Ti-6Al-4V and Ti-6Al-4V-1B: Study of the microstructure and mechanical properties**
Aida Amroussia (Michigan State University)
- 12:30 **O4 - Effects of Damage Annealing on Thermo-Mechanical Properties of High-Temperature Heavy Ion Irradiated Graphite**
Marilena Tomut (GSI Darmstadt)
- 12:50 **O5 - Influences of heavy ion parameters on single event effects in semiconductor devices**
Jie Liu (Chinese Academy of Sciences)
- 13:10 --- Lunch ---

Session 3 – Chair: Pavel Apel (Joint Institute for Nuclear Research)

14:30 **I4 - Radiografted track-etched polymer membranes for research and application**

Marie-Claude Clochard (École Polytechnique, Palaiseau)

15:00 **O6 - AuAg alloy and porous Au nanowires and nanowire networks created by electrodeposition in ion-track etched polymer templates for plasmonic applications**

Ina Schubert (GSI Darmstadt)

15:20 **O7 - Giant rectification effect in PET suspended graphene nanopore**

Huijun Yao (Chinese Academy of Sciences)

15:40 **O8 - Modification of carbon nanomembranes and graphene with ions**

Marika Schleberger (Universität Duisburg-Essen)

16:00 --- *Coffee break* ---

16:30 Poster Session A (until 18:00)

Session Special – Chair: Hermann Rothard (CIMAP-Ganil CNRS)

18:00 **I5 - 56 Years of Ion Tracks: Where Do We Stand?**

Siegfried Klaumünzer (Helmholtz-Zentrum Berlin)

18:30 **I6 - Atomic Physics, Plasma Physics, and Applied Science at the Future FAIR Facility**

Thomas Stöhlker (GSI Darmstadt)

Tuesday, May 19, 2015

Session 4 – Chair: Ricardo Papaléo (Pontifical Catholic University of Rio Grande do Sul)

- 08:30 **I7** - Simulations of transient electronic and atomic kinetics: energy dissipation in highly excited dielectrics
Nikita Medvedev (Center for Free Electron Laser Science, DESY)
- 09:00 **O9** - SAXS and SANS characterization of ion irradiation in polymers
Daniel Schauries (Australian National University)
- 09:20 **O10** - Aliphatic polymers oxidative ageing under Swift Heavy Ion irradiation: LET, dose and dose rate effects
Yvette Ngono-Ravache (CIMAP)
- 09:40 **O11** - Effect of spatial confinement on the chemical damage induced by ion bombardment on ultrathin polymer films
Raquel Thomaz (Pontifical Catholic University of Rio Grande do Sul)
- 10:00 --- Coffee break ---

Session 5 - Chair: Marcel Toulemonde (CIMAP, Caen)

- 10:30 **I8** - Swift Heavy Ion irradiation of III-N semiconductors: ion tracks and point defect formation
Isabelle Monnet (CIMAP)
- 11:00 **O12** - Local formation of nitrogen-vacancy centers in diamond by swift heavy ions
Thomas Schenkel (Lawrence Berkeley National Laboratory)
- 11:20 **I9** - Molecular dynamics simulations of swift heavy ion induced damage and recovery processes
Olli Pakarinen (University of Helsinki)
- 11:50 **O13** - Comprehensive analysis of the recrystallization effect induced by swift heavy ions in silicon carbide
Abdenacer Benyagoub (CIMAP-GANIL)
- 12:10 --- Lunch ---

Session 6 - Chair: Devesh Avashti (IUAC, New Delhi)

13:30 **I10 - From water radiolysis to hadrontherapy: Nanox a multi-scale model for biological effects**

Michaël Beuve (Université de Lyon)

14:00 **O14 - High energy heavy ion microbeam for interdisciplinary research**

Guanghua Du (Institute of Modern Physics, CAS)

14:20 **O15 - Spatiotemporal dynamics of repair proteins at DNA damage induced by particles of different energy and LET**

Burkhard Jakob (GSI Darmstadt)

14:40 **I11 - The sound of protons - Ionoacoustics for ion range determination**

Walter Assmann (LMU München)

15:10 --- *Coffee break* ---

15:40 Poster Session B (until 17:10)

Session 7 - Chair: Flyura Djurabekova (Helsinki Institute of Physics)

17:10 **I12 - Ultrafast temporal response of materials to proton irradiation**
Matt Zepf (Queens University Belfast; Helmholtz Institut Jena)

17:40 **O16 - Ion-shaped Metallic Nanoparticles: Fundamental Aspects and Applications**

Pierre-Eugene Coulon (École Polytechnique, Palaiseau)

18:00 **O17 - Investigation of swift heavy ion induced modifications of size of embedded Au nanoparticles by atomistic simulations**

Saif Khan (Inter-University Accelerator Centre, New Delhi)

18:20 **O18 - PW-laser produced MeV proton beams stopped in WDM plasmas (H,He,Ar,N,Xe)**

Claude Deutsch (LPGP UParis-Sud)

19:00 --- *Evening Tour at Mathildenhöhe (registered participants only)* ---

Wednesday, May 20, 2015

Session 8 – Chair: Isabelle Monnet (CIMAP)

- 08:30 **I13** - Ion-induced hillock formation: kinetic and potential energy contributions of highly charged ions and swift heavy ions
Yuyu Wang (Institute of Modern Physics, Lanzhou)
- 09:00 **O19** - Crystalline hillock formation of oxides irradiated with swift heavy ions -TEM study-
Norito Ishikawa (Japan Atomic Energy Agency)
- 09:20 **O20** - Y2Ti2O7 and Me23C6 nanoparticles in swift heavy ion irradiated ODS alloys
Vladimir Skuratov (JINR, Dubna)
- 09:40 **O21** - Swift Heavy Ion Irradiation of Dense GeO2 Glass at Ultrahigh Pressure: Formation and Stabilization of a Disordered NiAs-Type Structure
Raul Palomares (University of Tennessee)
- 10:00 --- Coffee break ---

Session 9 – Chair: Marika Schleberger (Universität Duisburg-Essen)

- 10:30 **I14** - Swift heavy ion modifications of astrophysical water ice
Emmanuel Dartois (Institut d'Astrophysique Spatiale-CNRS, Orsay)
- 11:00 **O22** - Time-of-flight Secondary Neutral & Ion Mass Spectrometry using swift Heavy Ions
Andreas Wucher (Universität Duisburg-Essen)
- 11:20 **O23** - Synergy effect between electronic and collisional sputtering: The case of amorphous silicon nitride irradiated with energetic C₆₀ ions
Kenji Kimura (Kyoto University)
- 11:40 **O24** - Ion induced reactivity in systems of astrophysical interest
Alicja Domaracka (Université de Caen-Basse Normandie)
- 12:00 --- Lunch ---
- 13:30 --- Excursion ---
- Conference Dinner at Burg Frankenstein ---

Thursday, May 21, 2015

Session 10 – **Chair:** Frederique Pellemoine (Michigan State University)

- 09:00 **I15 - Transmission Electron Microscopy Study on Ion Tracks in Ceria**
Kazuhiro Yasuda (Kyushu University)
- 09:30 **O25 - Recent advances in characterisation of ion tracks using small angle x-ray scattering measurements**
Patrick Kluth (The Australian National University)
- 09:50 **O26 - Structural modifications induced by swift heavy ions in Al₂O₃**
Clara Grygiel (CIMAP-GANIL)
- 10:10 **O27 - Systematic study of the phase behavior of f-block oxides irradiated with swift heavy ions**
Cameron Tracy (University of Michigan)
- 10:30 **O28 - Commissioning of the PRIOR prototype at GSI**
Dmitry Varentsov (GSI Darmstadt)
- 10:50 --- Coffee break ---

Session 11 - **Chair:** Jie Liu (Chinese Academy of Sciences)

- 11:20 **I16 - Resonant coherent excitation under swift heavy ion channeling**
Toshiyuki Azuma (RIKEN AMO Physics laboratory)
- 11:50 **O29 - Determination of electronic stopping powers of 0.05-1 MeV/u 131Xe-ions in C-, Ni- and Au-absorbers with calorimetric low temperature detectors**
Artur Echler (University of Giessen)
- 12:10 **O30 - Design and fabrication of waveguides and optical gratings in crystals and glasses via swift heavy ion irradiation**
Istvan Banyasz (Wigner Research Centre for Physics)
- 12:30 **O31 - In-Situ SEM-Investigation of SHI induced Modification of Surfaces and Thin Films**
Wolfgang Bolse (Universität Stuttgart)
- 12:50 --- Final remarks ---
- 13:00 --- End of conference ---
- 13:20 --- Departure to GSI – Snacks at GSI ---

Fragmentation of He and Ne dimers by swift heavy ions

SCHÖFFLER, Markus 1*; SANN, Hendrik 1; MECKEL, M. 1; STUCK, C. 1; LENZ, Ute 1; METZ, Daniel 1; JUNG, Anika 1; ODENWELLER, Matthias 1; NEUMANN, Nadine 1; ULRICH, Birte 1; COSTA FRAGA, Rui Alexandre 1; PETRIDIS, Nikos 1; SCHÖSSLER, S. 1; ULLMANN-PLÉGER, Klaus 1; GRISENTI, Robert 1; CZASCH, Achim 1; JAGUTZKI, Ottmar 1; SCHMIDT, Lothar 1; JAHNKE, Till 1; SCHMIDT-BÖCKING, Horst 1; BECHT, J. 1; GASSERT, Helena 1; MERABET, H. 2; RANGAMA, J. 3; ZHOU, C. L. 3; CASSIMI, Armin 3; LÜDDE, Hans-Jürgen 4; DÖRNER, Reinhard 1; KIM, Hong-Keun 1; TITZE, Jutta 1; TRINTER, Florian 1; WAITZ, Markus 1; VOIGTSBERGER, Jörg 1

1 Institut für Kernphysik, Goethe-University Frankfurt, 60438 Frankfurt am Main, Germany; 2 Department of Mathematics, Statistics and Physics, College of Arts and Sciences, P.O. Box: 2713 Doha, Qatar; 3 CIMAP Caen, GANIL, Bd Henri Becquerel, BP 55027 – 14076 Caen Cedex 05, France; 4 Institut für theoretische Physik, Goethe-University Frankfurt, 60438 Frankfurt am Main, Germany

All atoms and molecules can – even in their ground state – form clusters, weakly bound molecules, held together by the van der Waals force. The smallest of this type is the dimer, composed of two atoms/molecules. While the Ne dimer is a representative for rare gas dimers in general, the He dimer is a quite exotic object, with a broad internuclear distribution, stretching up to several 100 a. u. Here we investigated the ionization and fragmentation dynamics of He₂ and Ne₂ induced by ion impact (11.4 MeV/u, S14+). We employ the technique of COLTRIMS reaction microscopes to determine the momenta of all fragments in coincidence.

Thereby different pathways are accessible depending on how the electrons have been removed from the atomic sites. The two dominant mechanisms are:

1.) The direct mechanism: Here the projectile ionizes each of the two atoms individually. The dimer's constituents have ionization properties similar to those of a single atom, completely different than what is known for a covalent bound molecule. The ionization dynamics strongly varies with the impact parameter b . But its measurement is rather difficult, if possible at all. Especially for large b , which dominate ionization, are believed not resolvable. Here the nuclear scattering is smaller than the typically exchanged momentum with the electron. Leading to ambiguities, the impact parameter is inaccessible through any momentum transfer measurement between the nuclei. Here we show that the large internuclear distance of rare gas dimers opens a new way to this puzzling question. Focusing on the two electron release, the impact parameter dependent ionization probability $P(b)$ leads to a maximum angle between the molecular axis and the ion beam. Further tilts result in the ionization of only one atom.

2.) In some cases, an ionized atom stays electronically excited. This energy is efficiently released via the Interatomic Coulombic decay (ICD). Predicted in 1997 and in photoionization experiments observed in 2004, ICD is an extremely efficient source for the production of low energetic electrons. It probably plays a significant role for radiation damage in living tissue and for ion radiation therapy.

18 May 2015 at 10:00

Quasi-equilibrium in charge state evolution for swift heavy ions after passing through carbon foils

IMAI, Makoto 1*; SATAKA, Masao 2; MATSUDA, Makoto 3; OKAYASU, Satoru 3;
KAWATSURA, Kiyoshi 4; TAKAHIRO, Katsumi 5; KOMAKI, Ken-ichiro 6; SHIBATA, Hiromi
7; NISHIO, Katsuhisa 3

1 Dep. Nuclear Engineering, Kyoto Univ.; 2 Tsukuba Univ.; 3 Japan Atomic Energy Agency;
4 Kansai Gaidai Univ.; 5 Kyoto Institute of Technology; 6 RIKEN; 7 Osaka Univ.

Non-equilibrium and equilibrium charge state distributions for 2.0 MeV/u Sq^+ ($q = 6-16$) and Cq^+ ($q = 2-6$) ions after penetrating carbon foils have been investigated experimentally. Those wide ranges of the initial charge states have proved that charge state distributions, mean charge states, and distribution widths for projectile ions without K-shell holes, Sq^+ ($q = 6-14$) and Cq^+ ($q = 2-4$), once coincided at a target thickness of 6.9 and 5.7 micro-g/cm², respectively, showing a "quasi-equilibrium", and simultaneously evolved to establish a real equilibrium when the foil thickness was increased further. Those for projectile ions with K-shell hole(s), S15, 16+ and C5, 6+, evolved differently and directly to the real equilibrium, established at a target thickness of around 100 micro-g/cm² or greater for S ions and at over 10 micro-g/cm² for C ions. The quasi- and real-equilibrium mean charge states for 2.0 MeV/u S ions were 12.3 and 12.68, respectively, whereas those for 2.0 MeV/u C ions were 5.48 and 5.57. Simulations using ETACHA code and solution of simpler rate equations showed that the quasi-equilibrium was brought by a difference between the reaction-rates for K- and L-shell processes.

Primary processes: from ion-solid to ion-ion collisions

LAMOUR, Emily 1*; LÉVY, Anne 1; MACÉ, Stéphane 1; PRIGENT, Christophe 1;
TRASSINELLI, Martino 1; ROZET, Jean-Pierre 1; STEYDLI, Sébastien 1; VERNHET,
Dominique 1

1 Institut des NanoSciences de Paris - UPMC

Fast Highly Charged Ions (HCIs) going through matter induce material modifications and, in turn, their stopping power, charge state and excited states are affected by the material encountered. Here, we report on experimental studies, performed at GANIL, on the production and transport of HCIs excited states in thin solid targets in the so-called high velocity domain. Solids of various thicknesses to investigate the transport effects have been used but also atomic targets to control the primary process that populates the projectile excited states. With the development of quantum transport theories to treat, on the same footing, all the competing processes, we have reached an unprecedented precision in the description of the ion transport in matter in this perturbative regime.

On the other hand, in the non-perturbative regime, where the ion stopping power is maximum, the probabilities related to all the primary electronic processes are of the same order of magnitude. This leads to "interference effects" and makes the determination of experimental cross sections of single elementary collision processes extremely difficult. To overcome this issue, we propose a project, named FISIC*, that will allow studying ion-ion collisions under well controlled conditions. Our goal is to reach experimentally the true three-body system and then add additional electrons, one by one, to explore the quantum dynamics of N-body systems. Those experiments are now possible with the avenue of the new large scale facilities such as GANIL/SPIRAL2 and FAIR/CRYRING.

* FISIC for Fast Ion-Slow Ion Collisions

Fragmentation mechanism of neon dimer induced by O6+ ions

MA, Xinwen 1*; ZHU, Xiaolong 1; FENG, Wentian 1; YAN, Shuncheng 1; GUO, Dalong 1; GAO, YONG 1; CHENG, Xiaowen 1; ZHANG, Xujie 2; ZHAO, Dongmei 1; XU, Shenyue 1; WANG, Hanbing 1; QIAN, Dongbin 1; HUANG, Zhongkui 1; ZHANG, Ruitian 1

1 Institute of Modern Physics, Chinese Academy of Sciences; 2 Henan University of Science and Technology, School of Physics and Engineering

Since the prediction of the Interatomic Coulombic Decay (ICD) by Cederbaum et al. in 1997 [1], the rare gas atomic dimers have been widely investigated by photon impact. However, the investigation of dimers with the ions and electrons as the projectile is still scarce [2-6]. For neon dimer, only a few works involved with heavy ions were reported [4]. Utilizing the reaction microscope [7], we investigated the fragmentation of neon dimer induced by highly charged O6+ ion at the projectile energy of 240 keV.

In the present work, we clearly observed four peaks in the spectrum of kinetic energy release (KER) for Ne+-Ne+ pair, which locate at 4.5, 7.3, 8.5, and 9.7 eV, and are marked by A, B, C, and D successively. By comparing with the potential curve of Ne2

[8], we clarified the fragmentation mechanisms of them. The peak A results from the coulombic explosion (CE) and ICD, while the peak B results from radiation charge transfer (RCT) of one-site states Ne2+(2p4)-Ne. The peaks C and D can be ascribed to the contribution of the radiationless charge transfer [9]. These two peaks were the first time observed in transfer ionization and pure double electron capture processes induced by heavy ions.

This work was partially supported by the 973 Program of China under Grants No. 2010CB832902 and by the NSFC of China under Grants Nos. 10979007, 10974207 and 11274317.

References

- [1] L. S. Cederbaum et al 1997 Phys. Rev. Lett. 79, 4778.
- [2] J. Matsumoto et al 2010 Phys. Rev. Lett. 105, 263202.
- [3] J. Titze et al 2011 Phys. Rev. Lett. 106, 033201.
- [4] H.-K. Kim et al 2013 Phys. Rev. A 88, 042707; 2014 Phys. Rev. A 89, 022704.
- [5] S. Yan et al 2013 Phys. Rev. A 88, 042712; 2014 Phys. Rev. A 89, 062707
- [6] W. Iskandar et al 2014 Phys. Rev. Lett. 113, 143201.
- [7] X Ma et al 2011 Phys. Rev. A 83, 052707.
- [8] S D Stoychev et al 2008 J. Chem. Phys. 129, 074307.
- [9] K. Kreidi et al 2008 Phys. Rev. A 78, 043422.

In-situ single event effect tests of electronic components for space applications

FERLET-CAVROIS, Véronique 1*

1 European Space Agency (ESA/ESTEC)

The space environment is inhospitable to humans and the spacecrafts utilised by us to access space, its systems, subsystems and EEE component. An important element of the space environment is the abundance of high energy particles, constituting the natural space radiation environment. The space radiation environment detrimentally affects EEE components flown on space missions. The impact on electronic components vary from slow degradation of electrical parameters, due to cumulative effects, or sudden unwanted events due to transient effects.

In this presentation, we will show several cases of single event effects (SEE) and the associated radiation hardness assurance (RHA) issues. The presentation will be divided in three parts:

- In a first part, we will illustrate a major difficulty usually encountered in space projects, which is the traceability of the design and fabrication process when procuring parts from semiconductor manufacturers, and consequently the representativeness of the SEE tests performed before flight. Any modification in the design or process will induce a different SEE response, potentially catastrophic. Examples of this type of SEE issue encountered in the frame of space projects will be presented: (a) latch-up in a SRAM memory, (b) burn-out in a quad CMOS driver, used as a clock driver for CCDs.
- In a second part, SEE in two component types, Flash-based FPGAs, and Floating-gate memories, will be detailed. Both show re-programming failures after irradiation. The impact on their flight mission is though significantly different: it will directly affects the memory primary function, while FPGA are usually not reprogrammed in flight, except in few exceptional situations. The failure mechanisms, as well as other effects, such as single event upsets and transients (SEU and SET) will be shown from both broad beam and microprobe experiments.
- Finally, the example of new types of power devices, based on silicon carbide, will be highlighted and compared to silicon ones. The failure mechanism in silicon carbide is resolutely different from silicon based devices, and will necessitate to adapt SEE test methods and RHA rules.

Based on these examples, we will conclude with general considerations on failure sources in EEE components used in space and methods to prevent these failures.

18 May 2015 at 12:10

Swift heavy ion irradiation damage in Ti-6Al-4V and Ti-6Al-4V-1B: Study of the microstructure and mechanical properties

AMROUSSIA, Aida 1*; GRYGIEL, CLARA 2; MITTIG, Wolfgang 3; MONNET, Isabelle 2;
PELLEMOINE, Frederique 4; J. BOEHLERT, Carl 1; DURANTEL, Florent 2

1 Department of Chemical Engineering and Materials Science, Michigan State University; 2 CIMAP-GANIL; 3 MSU-NSCL; 4 Michigan State University - Facility for Rare Isotope Beams

Due to their excellent mechanical properties, corrosion resistance, fatigue strength, low density and low activation under irradiation, titanium (Ti) alloys are currently being considered for use as a structural material for the beam dump shell for the Facility for Rare Isotope Beams (FRIB): A new generation accelerator with high power heavy ion beams. The capability of the FRIB to operate at full beam power depends on the beam dump being able to absorb up to a 325 kW beam power (with primary Beam from O to U). Ti-6Al-4V (grade 5) is the preferred candidate for this beam dump shell material. A significant increase of beam dump lifetime with respect to fatigue due to thermal cycling can be expected for the rotating beam dump if Ti-6Al-4V with an addition of 1% boron (Ti-6Al-4V-1B) is used [1]. Two sets of samples of both Ti-6Al-4V and Ti-6Al-4V-1B were irradiated at the IRRSUD beam line at the GANIL CIMAP, Caen France with swift heavy ion beams respectively ^{36}Ar (36MeV, $S_e=7.5\text{keV/nm}$) and ^{131}Xe (92MeV, $S_e=19.7\text{keV/nm}$). The samples were polished and etched before irradiation and selected areas on the surfaces of the samples were characterized before and after irradiation using Scanning Electron Microscopy and Electron Backscatter Diffraction. In addition, Vickers hardness and nano-indentation measurements were also used to probe the change in hardness and elastic modulus as a function of the depth. This talk will describe irradiation setups and the post irradiation techniques used to characterize the material. The results indicate a low-radiation damage sensitivity in both materials.

This material is based upon work supported by the U.S. Department of Energy Office of Science under Cooperative Agreement DE-SC0000661, the State of Michigan and Michigan State University.

[1] W. Chen, C. J. Boehlert (2009). Materials Transactions, Vol. 50, No. 7 pp. 1690 to 1703.

Effects of Damage Annealing on Thermo-Mechanical Properties of High-Temperature Heavy Ion Irradiated Graphite

TOMUT, Marilena 1*; HORNY, Nicolas 2; SCHEIN, Mike 3; TRAUTMANN, Christina 1; CHIRTOC, Mihai 2; ZABELS, Robert 4; ILZE, Manika 4; JANIS, Manik 4; AVILOV, Mikhail 5; FERNANDES, Sandrina 3; MITTIG, Wolfgang 6; PELLEMOINE, Frederique 5

1 GSI, Darmstadt; 2 GRESPI-CATHERM, Univ. Reims, France; 3 FRIB, MSU, East Lansing, MI, US; 4 Institute of Solid State Physics, University of Latvia, Riga, Latvia; 5 Facility for Rare Isotope Beams - Michigan State University; 6 MSU-NSCL

Beam induced hardening and thermal conductivity degradation plays an important role in the failure of targets, beam catchers, beam windows and collimators for the new generation of high power accelerators (Large Hadron Collider, Facility for Antiproton and Ion Research, Facility for Rare Isotope Beam). Operating at high temperatures is expected to anneal significantly the radiation damage. The goal of this work is to investigate the effect of damage recovery on thermal diffusivity and hardening behavior of high-temperature ion-irradiated graphite by Raman spectroscopy, photo-thermal radiometry and nanoindentation. Information on ion-induced thermal conductivity degradation of materials is in general extremely scarce. We present the first experimental data on thermal diffusivity of isotropic graphite thin foils irradiated with 8.6 MeV/u ^{197}Au ions, at temperatures up to 1600 °C, done by innovatively using a photothermal radiometry method for this type of samples. Nanoindentation tests have been performed for following the influence of the irradiation temperature on the hardness and Young modulus of the same ion exposed graphite samples. At high irradiation temperatures, the degradation of thermal diffusivity and the ion induced hardening are less pronounced due to enhanced vacancy mobility. Our results advocate operation temperatures above 1000 °C for graphite targets and beam catchers.

Influences of heavy ion parameters on single event effects in semiconductor devices

LIU, Jie 1*; ZHANG, Zhangang 1; HOU, Mingdong 1; SUN, Youmei 1; SU, Hong 1; YAO, Huijun 1; MO, Dan 1; DU, Guanghua 1; LUO, Jie1; ZHAI, Pengfei 1; ZENG, Jian 1; CHEN, Yonghui 1; GENG, Chao 1; CAO, Dianliang 1; LIU, Wenqiang 1; GU, Song 1; LIU, Tianqi 1; XI, Kai 1; LIU, Jiande 1; WANG, Bin 1; YE, Bing 1; DUAN, Jinglai 1

1 Institute of Modern Physics, Chinese Academy of Sciences

Single event effects (SEEs) in semiconductor devices is a phenomenon of increase importance with the development in device technology. In this work, the SEE tests have been carried out by heavy ions from HIRFL accelerator. The Geant4 simulations have been performed to better understand the experimental results.

The test strategies for new technologies of very large-scale integration are studied. The influences of heavy ion parameters on devices are investigated, systematically. The results indicate that some important parameters for SEE testing, such as ion energy, ion range, beam flux, beam angle etc. have effects on the results. The angular dependence of multiple bit upset responses in a series of SRAM devices has been performed. We observed that the differences depend on the ion species and devices. Therefore it is important to select proper test conditions to ensure the experiment performed correctly.

We have done the computational simulation of single event upset (SEU) induced by the passage of heavy ions through the device with Geant4-tool based on Monte Carlo transport code. The key parameters affecting SEU occurrence are examined, and related geometrical construction and critical charge are all quantified. The multi-functional package for SEU analysis has been successfully programmed and applied for SEU occurrence after completion of device geometrical construction, critical charge and SEU cross section calculation.

Radiografted track-etched polymer membranes for research and application

CLOCHARD, Marie-Claude 1*

1 Laboratoire des Solides Irradiés, Palaiseau, France

The XPnano group at LSI (Ecole Polytechnique, France) synthesises nanoporous polymer membranes using ion track technology in collaboration with the CIMAP (GANIL). The zone of defects along the ion-trajectory, namely the latent track, is rich of radicals in numerous polymers and may be directly modified chemically by radio-induced grafting (lon-track grafting). Latent tracks may also be etched to obtain either cylindrical pores of monodisperse radii ranging from 10 nm to few microns or other geometries like biconical shapes with an aperture of only few nm. The remanence of radicals after etching in a semi-crystalline PVDF membrane was proven in our group by EPR for pore diameter inferior to 100 nm and the subsequent radiografting was localized by Confocal Laser Scanning Microscope. This property allows us to radiograft, very locally, a hydrophilic polymer in a hydrophobic matrice from nanopore walls. Using controlled radical polymerization (i.e. RAFT mechanism), the grafted layer can be tuned very accurately from nanometric coverage of nanopore walls to complete blockage of the pores and appearance of radiografted chain protusions at the membrane surface. lon-track grafting have permitted the fabrication of many devices in our group. Some achievements were obtained in proton-exchange membrane fuel cell (automotive application) and in water quality sensors for toxic metal ions at the trace level (sub-ppb sensitivity). Track-etched membranes are also routinely used as template to grow metallic nanowires (NWs) by electrodeposition. It opens the field of research to composite membranes. Non-conventionnal behaviour of embedded Ni NW magnetoresistance have been registered when biconical NWs are contacted. An experimental set-up at LSI allows contacting only one NW over billions. Combined to electroactive polymers such as piezoelectric β -PVDF, recent results have shown a giant magnetostrictive effect in a single Ni NW induced by mechanical stress.

AuAg alloy and porous Au nanowires and nanowire networks created by electrodeposition in ion-track etched polymer templates for plasmonic applications

SCHUBERT, Ina 1*; BURR, Loic 1; MARLENA, Dyzynski 1; TRAUTMANN, Christina 1; TOIMIL-MOLARES, Maria Eugenia 1

1 Materials Research Department, GSI, Darmstadt

Metallic nanowires have great potential for future plasmonic applications. By varying nanowire dimensions, composition, shape and morphology, their plasmonic resonance frequency and near field characteristics can be tuned for specific sensing functions in the infrared and visible light range. For their implementation as sensors, however, two main challenges are being tackled: (i) the nanostructures plasmonic performance must be understood and optimized and (ii) stable and complex assemblies of nanowires such as networks and arrays must be developed.

In this overview, we demonstrate how ion-track nanotechnology combined with electrochemical deposition allows the tailored synthesis of complex structures including three dimensional interconnected nanowires. Moreover, the deposition of special AuAg alloy wires is presented with Au:Ag concentrations tailored by varying the synthesis parameters. Chemical dissolution of the Ag content produces wires and mechanically stable networks of high porosity. The tremendously increased effective surface is of great interest for providing plasmonic hotspots. Compared to smooth nanowires, highly porous Au nanowires show a red-shift of their plasmon resonance frequency as demonstrated by electron energy-loss and infrared spectroscopy.

Giant rectification effect in PET suspended graphene nanopore

YAO, Huijun 1*; ZENG, Jian 1; ZHAI, Pengfei 1; LIU, Jie 1; SUN, Youmei 1; XIE, Lu 1

1 Institute of Modern Physics, Chinese Academy of Sciences

Graphene is an ultimate thin membrane with carbon atoms arranged in a honeycomb lattice and extra high mechanical property. Introduced nanopores in graphene can be used in water desalination technologies because of high efficiency in rejecting salt ions. Here, swift heavy ion was used to prepare single nanopore in monolayer graphene which was transferred to PET membrane. After asymmetric etching of irradiated PET membrane, the PET suspended graphene nanopore can be obtained and used to carry out the ionic transport study. In order to investigate the rectification effect of suspended graphene nanopore, three electrolytes with monovalent cations LiCl, NaCl and KCl are chose for current-voltage measurement, respectively. Obvious rectification effect was confirmed in the electrolytes of KCl and the rectification ratio can be adjusted by varying the concentration and pH value of KCl solutions. The giant rectification ratio of 190 was observed in 0.02 M KCl with the pH value of 2.

Modification of carbon nanomembranes and graphene with ions

H. Bukowska¹; F. Meinerzhagen¹; M. Karlusic²; O. Ochedowski¹; A. Turchanin³; M. Schleberger^{*1}

1 Universität Duisburg-Essen, Germany; 2 Ruđer Bošković Institute, Zagreb, Croatia; 3 Friedrich-Schiller-Universität Jena, Germany

Since two-dimensional materials with their unique physical properties have become accessible to experimental physics, the scientific interest in this material class has been very high as they promise a multitude of possible applications. In particular, it has been shown that ionizing particle irradiation allows structuring of these 2d materials [1- 4].

In addition to graphene, so-called carbon nanomembranes (CNMs) also belong to the class of the new two-dimensional materials. They offer the advantage that they can be produced and transferred by standard chemical and physical methods instead of mechanical exfoliation. For this experiment we have prepared single layer graphene as well as CNMs samples. The latter were prepared by electron induced crosslinking of aromatic self-assembled monolayers like biphenylthiol which was evaporated on copper [5,6]. Our samples have been irradiated with swift heavy ions under glancing angles of incidence. The samples were analysed by atomic force microscopy in ambient conditions and in ultrahigh vacuum. The latter measurements served as test measurements for our newly built setup at the M branch of the UNILAC beamline in GSI (Darmstadt, Germany) and were performed in-situ directly after irradiation.

The CNMs show modifications in form of extended pores with shapes different from those which we typically observe in graphene. Finally, experiments performed at different accelerator facilities (GSI, GANIL, and RBI) with different beams energies were used to determine the threshold for pore formation.

References:

- [1] S. Akcöltekin *et al.*, Appl. Phys. Lett. **98** (2011) 103103
- [2] O. Ochedowski *et al.*, Appl. Phys. Lett. **102**, 153103 (2013)
- [3] J. Hopster *et al.*, 2D Materials **1** (2014) 011011
- [4] R. Ritter *et al.*, Appl. Phys. Lett. **102**, (2013) 063112
- [5] A. Turchanin and A. Götzhäuser, Prog. Surf. Sci. **87**, 108 (2012),
- [6] D.G. Matei *et al.*, Adv. Mater. 2013, **25**, 4146–4151

56 Years of Ion Tracks: Where Do We Stand?

KLAUMÜNZER, Siegfried 1*

1 Helmholtz-Zentrum Berlin and GSI Darmstadt

After a brief historical and personal view on some highlights concerning ion tracks I will concentrate on the present state of understanding and modelling of track formation. The frequently used inelastic thermal spike model requires substantial modification with regard to two aspects. The first aspect concerns the assumption that the concentration of free carriers is independent of time and of the distance from the ion path. This assumption is only acceptable for metals but not for insulators and semiconductors. Several groups have now identified this deficiency and try to find solutions by following carrier production and subsequent processes in great detail. The progress made and the encountered difficulties will be outlined. The second aspect concerns the fact that the inelastic thermal spike model ignores thermal stresses. More precisely, the energy transferred from the electronic system to the atomic system appears not completely as heat as it is assumed in the inelastic thermal spike model, but is shared between heat and mechanical work (a generalization of the term $p\delta V$ in the first law of thermodynamics). The importance of this term for the energy balance will be demonstrated and the consequences with regard to melting and boiling will be discussed. It will turn out that, if the excitation in the track is sufficiently large, dislocation generation is much more probable than boiling. Experimental evidence for this process will be provided and its consequences for the radiation resistance of some non-amorphizable materials like NiO, MgO, and UO₂ will be demonstrated.

Atomic Physics, Plasma Physics, and Applied Science at the Future FAIR Facility

STÖHLKER, Thomas ^{1*}

¹ GSI, Darmstadt

FAIR with its intense beams of ions and antiprotons provides outstanding and worldwide unique experimental conditions for extreme matter research in atomic and plasma physics and for application oriented research in biophysics, medical physics and materials science. The associated research programs comprise interaction of matter with highest electromagnetic fields, properties of plasmas and of solid matter under extreme pressure, density, and temperature conditions, simulation of galactic cosmic radiation, research in nanoscience and charged particle radiotherapy. A broad variety of APPA-dedicated facilities including experimental stations, storage rings, and traps, equipped with most sophisticated instrumentation will allow the APPA community to tackle new challenges. The worldwide most intense source of slow antiprotons will expand the scope of APPA related research to the exciting field of antimatter.

Simulations of transient electronic and atomic kinetics: energy dissipation in highly excited dielectrics

MEDVEDEV, Nikita 1*

1 Center for Free Electron Laser Science, DESY

In this talk I will give an overview of the transient nonequilibrium electron and atomic kinetics after high-energy deposition in dielectric. An ultrafast energy deposition can be made by means of x-ray free-electron laser (FEL) irradiation or swift-heavy ion

(SHI) beams. The differences between the two methods will be discussed. In both cases, first, the electron subsystem of a dielectric is excited. Electrons are provided with energy up to a few tens of keV, which initiates nonequilibrium electron kinetics. High-energy electrons then perform secondary cascading and exchange energy with the lattice. The different channels of scattering and their simulation challenges will be addressed.

Dielectrics and semiconductors under irradiation with intense femtosecond laser pulses can undergo a phase transition via two different channels: thermal and nonthermal. Their difference will be discussed in detail. The first one occurs if the lattice is heated strongly enough by electron-ion (electron-phonon) coupling. The second one results from the modification of the atomic potential energy surface by excitation of electrons from the valence to the conduction band. I will present our developed approach to include both channels within a consistent framework.

The developed hybrid model consists of tight-binding molecular dynamics (TBMD) for modeling atomic system with the potential energy surface dependent on the state of electronic system [1]. Simultaneously, electronic state is traced with the Boltzmann equation for low-energy electrons, and with a Monte Carlo model for high-energy electrons. With this model it is possible to study different channels of energy dissipation in dielectrics. Examples of thermal and nonthermal melting and their interplay will be presented for silicon and diamond.

[1] N. Medvedev, H.O. Jeschke, B. Ziaja, New Journal of Physics 15, 015016 (2013)

SAXS and SANS characterization of ion irradiation in polymers

SCHAURIES, Daniel 1*; MOTA SANTIAGO, Pablo 1; TRAUTMANN, Christina 2; KIRBY, Nigel 3; GILBERT, Elliot 4; KLUTH, Patrick 1

1 Australian National University; 2 GSI Darmstadt; 3 Australian Synchrotron; 4 ANSTO Sydney

Organic polymers display some of the most prevalent applications in ion track technology. With the high susceptibility of ion tracks to chemical etching, track-etched polymers are commonly utilized for the production of nano-porous track-membranes and filters, embedding microelectronic devices such as micro-capacitors, diodes and nanowires as well as for in-vivo storage vessels and a large range of sensor applications.

We present our results on the investigation of un-etched ion tracks in polymers, such as polycarbonate and polyimide. The ion tracks were created by swift heavy ion irradiation at the Universal Linear Accelerator at GSI. We have previously demonstrated that synchrotron-based small angle x-ray scattering (SAXS) allows the detailed characterization of ion tracks in a number of materials [1]. Here, SAXS reveals a diameter of 5 nm for tracks in polycarbonate films. Complementary small angle neutron scattering (SANS) measurements reveal a similar value, yet the combination of both techniques allows an element-specific investigation in the change in density as a consequence of the ion irradiation. A significant hydrogen deficiency in the irradiation polymer areas is revealed that is independently confirmed by infrared spectroscopy (FTIR) on the same specimens.

Furthermore, the effect of energy deposition and irradiation fluence was studied systematically, both displaying a significant influence on the resulting track size. The stability of tracks was investigated by thermal annealing: For temperatures up to 200°C, the damage region was observed to recover gradually and a decreases in the difference in density to the undamaged region was measured. However, this process is accompanied by an increase in the track diameter, contrary to our previous results on tracks in inorganic materials, where the diameter displays a shrinkage. This suggests a fundamental different recovery mechanism for this class of materials.

[1] P. Kluth et al., Phys. Rev. Lett. 101 (2011) 175503.

Aliphatic polymers oxidative ageing under Swift Heavy Ion irradiation: LET, dose and dose rate effects

NGONO-RAVACHE, Yvette 1*; DANNOUX-PAPIN, Adeline 2; FERRY, Muriel 3; DAMAJ, Ziad 1; ESNOUF, Stéphane 4; COCHIN, Florence 5; BALANZAT, Emmanuel 1

1 CIMAP; 2 CEA/DEN/DTCD/SPDE/LCFI; 3 CEA Saclay; 4 CEA/DEN/DPC/SECR/LRMO; 5 AREVA NC DOR/RDP

Unlike beta- and gamma-rays irradiations that lead to quite homogeneous energy deposition, Swift Heavy Ions (SHI) induce an heterogeneous energy deposition at the nanoscale level. Due to their high LET and because SHI deposit their energy close to the ion path, in a track core of a few nanometers, the local dose nearby these track cores is huge; in between, the dose is very low. A great number of detailed studies were performed under inert environment to assess the influence of the high ionization and excitation densities induced by SHI on polymer ageing. It was shown that, the huge amount of energy deposited locally by SHI induces specific damage processes, which involve complex molecular rearrangements and collective atom motions. Contrary to what has been done under inert environment for assessing the specificity of SHI on polymers, only few detailed studies have been undertaken under oxidative environments. Thus, the aim of the present work is to understand how high ionization/excitation densities induced by SHI impact the mechanisms underlying polymer degradation in presence of oxygen.

Polymers submitted to ionising radiations are modified by the creation of macromolecular defects such as unsaturated bonds, chain scissions and crosslinks, or oxidative defects in presence of oxygen. The counterpart of these macromolecular defects is gas emission. We have examined both processes. In the course of the present work, we have studied the influence of the LET, the dose and the dose rate on different polymers. Additionally, we have considered the influence of the polymer chemical structure on its oxidative ageing, particularly as a function of the LET.

Effect of spatial confinement on the chemical damage induced by ion bombardment on ultrathin polymer films

THOMAZ, Raquel 1*; GUTIERRES, Leandro 1; MORAIS, Jonder 2; LOUETTE, Pierre 3; PIREAUX, Jean-Jacques 3; SEVERIN, Daniel 4; TRAUTMANN, Christina 4; PAPALÉO, Ricardo 1;

1 Pontifical Catholic University of Rio Grande do Sul (PUCRS); 2 Federal University of Rio Grande do Sul; 3 Université de Namur; 4 GSI, Darmstadt;

In this work, the influence of spatial confinement in one dimension on the chemical effects induced by 2.2 GeV Bi and 2 MeV H ions in ultrathin PMMA films was investigated, by quantifying bond breaking rates as a function of the thickness h of the polymer layers ($2 < h < 200$ nm). Our data indicate that for both beams damage cross-sections for carbon-oxygen bonds, do not show substantial difference down to the smallest thickness accessible to XPS analysis ($h \sim 5$ nm). The damage cross-sections estimated are

$\sim 1.5 \times 10^{-13} \text{ cm}^2$ (for O-C-O bonds) and $\sim 2.3 \times 10^{-13} \text{ cm}^2$ (for C=O bonds) for the Bi irradiation, whilst for proton irradiation the values are $\sim 2.7 \times 10^{-16} \text{ cm}^2$ and $\sim 4.4 \times 10^{-16} \text{ cm}^2$, for O-C-O and C=O bonds, respectively. Variation of the cross-sections among samples of different thicknesses were within error bars. Films thinner than ~ 5 nm become difficult to analyse, because of the non-negligible signal of the omnipresent carbon on the substrate and because of beam-induced surface roughening and sputtering.

The absence of a decrease in the damage cross section in ultrathin layers is surprising, considering the high velocity of the ions and the long range of the emitted secondary electrons, which may escape the sensitive volume before thermalization and thus lowering the effective dose. Our observations are also in contrast to recent findings of a strong thickness dependence of cratering and mass transport induced by swift heavy ions in ultrathin polymer layers, indicating that at least the chemistry probed by XPS is related to short-range events close to the track core, while in sputtering, long-range, cooperative effects along the track are of greater importance.

Swift Heavy Ion irradiation of III-N semiconductors: ion tracks and point defect formation

MONNET, Isabelle 1; SALL, Mamour 1*; MOISY, Florent 1; GRYGIEL, CLARA 1; BALANZAT, Emmanuel 1; TOULEMONDE, Marcel 1; LEBIUS, Henning 1; BAN D'ETAT, Brigitte 1; JUBLOT-LECLERC, Stéphanie 2

1 CIMAP, Caen, France; 2 CSNSM, Orsay, France

AlN, GaN and InN were irradiated at room temperature with monatomic Swift Heavy Ions and high energy fullerenes. Despite a common crystallographic structure, these compounds show much contrasted response towards the electronic energy deposition.

Transmission Electron Microscopy in both plane-view and cross-sectional modes is used to characterize ion tracks. AlN shows a remarkable resistance towards track formation. InN is the most sensitive and shows partial decomposition inside the tracks, likely into N₂ and In metallic clusters. In GaN tracks are observed, containing amorphous pockets, but high fluence irradiation does not give an amorphous layer because of recrystallization induced by track overlapping. In AlN, below the electronic stopping power threshold for tracks formation, optical absorption was studied in-situ at 15 K. Point defects inducing an absorption band at 4.7 eV are created. Detailed analysis of the influence of both electronic and nuclear stopping powers indicates a synergy between electronic excitations and elastic collisions. For the heaviest projectiles, the enhancement of the color center creation yield amounts to two orders of magnitude due to the electronic energy loss. An enhancement by electronic stopping power of point defect creation or of point defect mobility is also evidenced by TEM observations.

Local formation of nitrogen-vacancy centers in diamond by swift heavy ions

SCHENKEL, Thomas 1; SCHWARTZ, Julian 2*; SEVERIN, Daniel 3; BENDER, Markus 3; TRAUTMANN, Christina 3; TOMUT, Marilena 3; PERSAUD, A. 2;

1 Lawrence Berkeley National Laboratory; 2 Accelerator Technology and Applied Physics Division, Lawrence Berkeley National Laboratory, Berkeley, California 94720, USA; 3 GSI, Darmstadt;

We exposed nitrogen-implanted diamonds to beams of swift heavy ions (1 GeV, 4MeV/u) and find that these irradiations lead directly to the formation of nitrogen vacancy (NV) centers, without thermal annealing. We compare the photoluminescence intensities of swift heavy ion activated NV centers to those formed by irradiation with low-energy electrons and by thermal annealing. NV yields from irradiations with swift heavy ions are 0.1 of yields from low energy electrons and 0.02 of yields from thermal annealing. We discuss possible mechanisms of NV center formation by swift heavy ions such as electronic excitations and thermal spikes. While forming NV centers with low efficiency, swift heavy ions could enable the formation of three dimensional NV assemblies over relatively large distances of tens of micrometers. Further, our results show that NV center formation is a local probe of (partial) lattice damage relaxation by electronic excitations in diamond.

ACKNOWLEDGMENTS

This work was supported by the U.S. Department of Energy under Contract No. DE-AC02—05CH11231 and by the Laboratory Directed Research and Development Program.

[1] J. Schwartz, et al., J. Appl. Phys. 116, 214107 (2014)

Molecular dynamics simulations of swift heavy ion induced damage and recovery processes

PAKARINEN, Olli 1*; BACKMAN, Marie 1,2; DJURABEKOVA, Flyura 1; NORDLUND, Kai 1;
ZHANG, Yanwen 3; KLUTH, Patrick 4; RIDGWAY, Mark C. 2; WEBER, William 2

1 University of Helsinki; 2 University of Tennessee, USA; 3 Oak Ridge National Laboratory;
4 The Australian National University, Canberra ACT, Australia;

Swift heavy ion (SHI) irradiation leads to formation of narrow ion tracks in many materials, can be used in modifying nanomaterials, and in some materials with existing damage induces defect recovery. Molecular Dynamics (MD) simulations, which include the energy deposition from electronic stopping following the inelastic thermal spike calculation input, can show the time evolution of these processes, and reveal how differences in solid – liquid phase transitions and recrystallization lead to very different behavior in damage formation and recovery in different insulator and semiconductor materials, subjected to similar initial electronic excitation.

In silicon carbide (3C-SiC), MD simulations complement our recent ion-beam experiments and clearly show that the irradiation-induced defect recovery process in SiC is active from swift heavy ions to low values of electronic stopping, in a regime where electronic stopping is often considered negligible. In other materials like zircon, an opposite co-operative effect of nuclear and electronic stopping is observed. The competitive processes of damage production and defect recovery are relevant for understanding radiation damage production for many materials in nuclear energy applications and for investigating radiation damage in materials using ion irradiation methods.

In a-Ge, a-Si and their alloys, local melting around the swift heavy ion path leads to formation of nanometer scale voids and/or ion tracks, the latter observable in these amorphous materials only indirectly as localized density changes in SAXS experiments. MD simulations explain the formation of the density variations and the shape of voids, due to the volume contraction associated with the molten phase and the following radially progressing expansion of the resolidifying ion track.

Comprehensive analysis of the recrystallization effect induced by swift heavy ions in silicon carbide

BENYAGOUR, Abdenacer 1*

1 CIMAP-GANIL

This contribution discusses recent results on the recrystallization effect [1,2] induced by swift heavy ions (SHI) in pre-damaged silicon carbide. The recrystallization kinetics was followed by using increasing SHI fluences and by starting from different levels of initial damage within the SiC samples. The quantitative analysis of these data shows that the recrystallization rate depends drastically on the local amount of crystalline material: it is nil in fully amorphous regions and becomes more significant with increasing amount of crystalline material. For example, in samples initially nearly half-disordered, the recrystallization rate per incident ion is found to be 3 orders of magnitude higher than what it is observed with the well-known IBIEC process using low energy ions. This high rate can therefore not be accounted for by the existing IBIEC models. A comprehensive quantitative analysis of all the experimental results indicates that the SHI induced high recrystallization rate can only be explained by a mechanism based on the melting of the amorphous zones through a thermal spike process followed by an epitaxial recrystallization initiated from the neighboring crystalline regions if the size of the latter exceeds a certain critical value. Finally, this quantitative analysis also reveals that the molecular dynamic (MD) calculations [3,4] supposed to reproduce the recrystallization phenomenon are actually far from being realistic since they lead to a recrystallization rate per incident ion which is about 40 times higher than the experimental value [5].

[1] A. Benyagoub, A. Audren, L. Thomé, F. Garrido, Appl. Phys. Lett. 89, 241914 (2006).

[2] A. Benyagoub, A. Audren, J. Appl. Phys. 106, 083516 (2009).

[3] A. Debelle, M. Backman, L. Thomé, W. J. Weber, M. Toulemonde, S. Mylonas, A. Boule, O. H. Pakarinen, N. Juslin, F. Djurabekova, K. Nordlund, F. Garrido, D. Chaussende, Phys. Rev. B 86, 100102(R) (2012).

[4] M. Backman, M. Toulemonde, O. H. Pakarinen, N. Juslin, F. Djurabekova, K. Nordlund, A. Debelle, W. J. Weber, Comput. Mater. Sci. 67, 261 (2013).

[5] A. Benyagoub, arXiv:1402.3200 (2014).

From water radiolysis to hadrontherapy: Nanox a multi-scale model for biological effects

BEUVE, Michaël 1*; CUNHA, M. 1; MONINI, C. 1; TESTA, E. 1

1 IPNL, Université de Lyon 1, CNRS/IN2P3

Biological effects induced by ionization radiations is a complex function of many parameters. Some are related to the type of irradiated cells and their environment. Some others are related to the irradiation characteristics. While considering the specific case of swift ions, not only the dose of irradiation but also the ion charge, the ion energy, the irradiation temporal and spatial substructures need to be considered.

In 2008, at the shim conference [1], we presented the two track-structure models dedicated to the prediction of cell killing induced by ions and pointed out some of the conclusions we drew from a detailed analysis of these models. Based on these conclusions, we developed an alternative model: nanoxTM (NAdosimetry and Oxidative stress). The nanoxTM model takes as input dosimetry quantities at multi-scale, starting from nanoscale, but also the production of radicals induced by water radiolysis. The model will be presented along with first results.

[1] M. Beuve, A. Coliaux, D. Dabli, D. Dauvergne, B. Gervais, G. Montarou, E. Testa, Statistical effects of dose deposition in track-structure modelling of radiobiology efficiency, Nuclear Instruments and Methods in Physics Research Section B: Beam Interactions with Materials and Atoms, Volume 267, Issue 6, March 2009, Pages 983-988

High energy heavy ion microbeam for interdisciplinary research

DU, Guanghua 1*; GUO, Na 1; GUO, Jinlong 1; LIU, Wenjing 1; CHEN, Hao 1; WU, Ruqun 1

1 Institute of Modern Physics, CAS

Heavy ions possess much higher linear energy transfer and produce severe ionizing damage to DNA in biological sample or PN junction in microelectronics along the ion trajectory. Heavy ion microbeam and high energy microbeam is attracting more and more interests because of the clinical spread of high energy particle cancer therapy using protons and carbon beams and care of space radiation effect, especially from cosmic heavy ion rays, in spacecraft and astronauts. Such a microbeam is a powerful tool to study the spatial radiation response or the local radiation effect both in materials and biological samples to simulate the space radiation at ground, and the high energy and long penetration of hundred MeV/u beam may also expand the application of the above mentioned microbeam application to large samples. This work presents the development of the interdisciplinary experimental system at the high energy microbeam of IMP, and then shows the study of protein dynamics of DNA repair after single ion irradiations.

Spatiotemporal dynamics of repair proteins at DNA damage induced by particles of different energy and LET

JAKOB, Burkhard 1*; DURANTE, Marco 1; TAUCHER-SCHOLZ, Gisela 1

1 GSI, Darmstadt

Energetic charged particles (HZE) are encountered in spaceflight as part of the galactic cosmic rays, where they pose a health risk to astronauts. However their destructive potential can be used in heavy ion tumour therapy. The deposition of energy of these HZE particles occurs mostly along the trajectory of the particle itself, but depending on its energy, there is some probability for energy deposition relatively far from the nominal trajectory, due to long-ranged delta rays. These delta rays are considered to induce non correlated DNA damage similar to low-linear energy transfer (LET) radiation (like X-rays), whereas the dense ionizing track of HZE particles is assumed to produce more complex and clustered DNA damage, which is slowly repaired or is even irreparable. To study the spatiotemporal protein dynamics during charged particle irradiation, a remote controlled microscope was established at the accelerator facility of GSI. The system enables the acquisition of high-resolution fluorescence images of living cells during ion irradiation. The microscope allows studying early radiation effects without the time lag of minutes presently conditional on limitations of access to the irradiation devices. GFP-tagged repair proteins like NBS1 were used for the spatio-temporal characterization of DNA damage in respect to the particle trajectory in cell nuclei. To compare high LET (ions) and sparsely ionizing radiation (X-rays) induced DNA damage, the microscope can alternatively be equipped with a 35 kV x-ray tube operated at high dose rate (40 Gy/min).

Time-lapse series of repair proteins like XRCC1 proved accumulations within seconds along the ion tracks indicating a fast recognition of DNA damage in combination with a quite stable location of damage processing. In the study presented here, we used a spectrum of different particles over a broad range of LETs in addition to x-rays to address the dynamics of the early DNA damage response in regards to the damage density in living cells. The detailed analysis of NBS1-GFP revealed differences in the recruitment kinetics and retention at damage sites in connection to the LET and radial track structure of the particles.

The sound of protons - Ionoacoustics for ion range determination

ASSMANN, Walter 1*

1 LMU München

Ions offer a more advantageous dose distribution than photons for external beam radiotherapy, due to their inverse dose deposition and, in particular, a characteristic dose maximum at their end of range (Bragg peak). Therefore, a more conformal therapeutic dose can be applied to the tumor while sparing the surrounding healthy tissue, even if organs at risk are in striking distance. This makes, however, a precise positioning of the Bragg peak inside the tumor volume a challenging demand.

Range verification in ion beam therapy relies to date on nuclear imaging techniques which require complex and costly detector systems, and none has still reached clinical maturity. In this project, we make use of the pressure pulse and related acoustic wave induced by ions stopping in tissue (ionoacoustics) to measure the ion range with ultrasound methods. This technique could offer a simple and more direct possibility to correlate, in-vivo and in real-time, the conventional ultrasound echo of the tumor region with the position signal of the ion Bragg peak.

The idea of using acoustic signals in water for detection of high energy particles, in particular of neutrinos, has long been proposed and ultrasound signals have first been measured in 1979 with energetic protons. The first demonstration of an acoustic pulse generated in a patient during radiation treatment with a proton beam was performed in 1995, but the accuracy needed in radiation therapy could never be reached. However, to-day's more advanced irradiation schemes with active beam scanning and dose delivery with higher pulse intensities are in favor of a more accurate ionoacoustic approach. This presentation will address our experimental and simulation work investigating the potential of the ionoacoustic method to enable sub-mm imaging of the Bragg peak. The proof-of-principle experiments were performed at the Tandem accelerator of the LMU and TU Munich, using a 20 MeV proton beam and different focused US transducers.

Ultrafast temporal response of materials to proton irradiation

ZEPF, Matt 1,2*; DROMEY, B. 3; COUGHLAN, M. 3; SENJE, L. 4; TAYLOR, M. 3; KUSCHEL, S. 5; STEFANUIK, R. 5; NERSISYAN, G. 3; DUNNE, P. 5; BORGHESI, M. 3; CURRELL, F. 3; RIDLEY, D. 3; JUNG, D. 3; WAHLSTROM, C.-G. 4; LEWIS, C. L. S. 3

1 Queens University Belfast, UK; 2 Helmholtz Institut Jena, Germany; 3 Queens University Belfast, UK; 4 Lund University, Sweden; 5 University College Dublin, Ireland

Proton accelerators driven with ultra-intense short pulse lasers provide proton beams with extraordinary characteristics. The extreme acceleration fields (typically exceeding TV/m) allow very compact accelerators (acceleration lengths on the micrometer scale) to reach energies of 10s of MeV with up to $2 \cdot 10^{13}$ particles per bunch and excellent spatial beam quality (transverse emittance). The short duration of the acceleration fields excited by the laser provides the basis for proton bunches with ultrashort pulse duration. Such short proton pulses raise the possibility of investigating the temporal dynamics of the fundamental interaction of protons and ions with matter directly. Here we report on the temporal characterisation of few picosecond (ps, 10^{-12} s) laser driven proton bunches for this purpose. Prompt transient opacity for optical probe radiation from protons stopping in high purity fused silica (a-SiO₂) provides the basis for single-shot characterisation of laser-accelerated proton bunches. The rapid ionization dynamics allow the measurement of proton pulse durations as short as 3.5 ± 0.7 ps in a 0.4 ± 0.05 MeV bandwidth. This corresponds to an ultra-low longitudinal emittance of $(1.75 \pm 0.25) \times 10^{-6}$ eV s and is in excellent agreement with numerical modelling. These observations pave the way to generating seed pulses for proton-driven wakefield acceleration of electrons in advanced lepton collider concepts.

Ion-shaped Metallic Nanoparticles: Fundamental Aspects and Applications

COULON, Pierre-Eugene 1*; RIZZA, Giancarlo 1; FAFIN, Alexandre 2; KHOMENKOV, Vladimir 2; DUFOUR, Christian 2; KOCIK, Mathieu 3; LOSQUIN, Arthur 3; KOBYLKO, Mathias 1; PERRRUCHAS, Sandrine 4; GACON, Thierry 4; MAILLY, Dominique 5; LAFOSSE, Xavier 5; ULYSSE, Christian 5; MONNET, Isabelle 2; CARDIN, Julien 2;

1 Laboratoire des Solides Irradies, Ecole Polytechnique, 91128 Palaiseau, France; 2 Centre de Recherche sur les Ions, les Matériaux et la Photonique, 14070 Caen, France; 3 Laboratoire de Physique des Solides, Université Paris Sud XI, 91405 Orsay, France; 4 Laboratoire de Physique de la Matière Condensée, Ecole Polytechnique, 91128 Palaiseau, France; 5 Laboratoire de Photonique et de Nanostructures, 91460 Marcoussis, France;

In the last years, ion-shaping technique has been proposed as an innovative and powerful tool to manipulate matter at the nanometer scale. Deformation can be indirectly induced by embedding metallic NPs into an ion-deformable amorphous host matrix. With this technique, it is possible to transform nanospheres into nanorods, nanowires, faceted nanoparticles, or other original shapes. The aspect ratio and spatial orientation of these NPs can be tuned by varying the irradiation conditions (ion, ion-energy, irradiation angle, fluence). To understand the mechanisms of deformation, the evolution of the temperature profile during the ion impact within the nanoparticle is simulated by implementing the thermal-spike model for three-dimensional anisotropic and composite media. By this way, a straight correlation is found between the fraction of the nanoparticle that is molten (vaporized) and the deformation path followed by the nanoparticles during the irradiation. This allows to relate the initial nanoparticle to its final morphology, in order to generalize the ion-beam shaping process for all the nanoparticle shapes and dimensions.

Besides the fundamental aspects related to the ion-matter interaction, ion-shaping can also be used to give new insights into the plasmonic properties of metallic nanoparticles. Here, Electron Energy Loss Spectroscopy (EELS) is used to study Localized Surface Plasmon Resonances (LSPR) in ion-shaped metallic nanoparticles with a nanometer-scale spatial resolution. LSPR are generated through electron excitation in a Scanning Transmission Electron Microscope (STEM), equipped with a High Angle Annular Dark Field (HAADF) detector. These experimental results are simulated using a specifically developed Auxiliary Differential Equations-Finite Difference Time Domain (ADE-FTDT) code and the Metallic NanoParticles Boundary Element Method (MNPBEM) code.

Investigation of swift heavy ion induced modifications of size of embedded Au nanoparticles by atomistic simulations

KHAN, Saif 1*; AVASTHI, Devesh K. 1

1 Inter-University Accelerator Centre, New Delhi

Nanometer-sized noble metallic particles embedded in dielectric matrices have attracted a great deal of attention. They are used in many applications mostly due to surface plasmon resonance which has dependence on their size and shape. Therefore, efforts have been made to vary their size and shape by various methods during or after fabrication. Swift heavy ion irradiation has been found to be very useful in this objective [1-3]. It has been shown that the size and shape of nanoparticles can be varied depending on the particle size and the expected size of the ion tracks in the matrix [4]. In particular, swift heavy ion irradiation has been recommended as size filter to embedded noble nanoparticles [5]. Our group has proposed a model based on inter-particle separation to explain the swift heavy ion induced modification in the size of embedded nanoparticles smaller than the ion track size in matrix [4]. In the present work, we have tested this hypothesis by atomistic simulation and tried to gain a better understanding of nanoparticle size modification pathway. The size of nanoparticles and inter-particles separation, kept in the simulation, were taken from the experimental work [4]. Effect of ion irradiation was mimicked by considering local short-time heating effects. The results agree with the experimental results of growth or reduction of embedded nanoparticles depending on the inter-particle separation.

References:

- [1] Y.K. Mishra, D. Kabiraj, D.K. Avasthi, J.C. Pivin, *Radiat. Eff. Defects Solids*, 162, 207 (2007).
- [2] Y. K. Mishra, D. K. Avasthi, P. K. Kulriya, F. Singh, D. Kabiraj, A. Tripathi, J. C. Pivin, I. S. Bayer and A. Biswas, 90, 073110 (2007).
- [3] F. Singh, S. Mohapatra, J.P. Stolquert, D.K. Avasthi, J.C. Pivin, *Nucl. Instr. and Meth. B*, 267, 936 (2009).
- [4] D.K. Avasthi, Y.K. Mishra, F. Singh, J.P. Stoquert, *Nucl. Instr. and Meth. B*, 268, 3027 (2010).
- [5] Y. Yang, C. Zhang, Y. Song, J. Gou, L. Zhang, Y. Meng, H. Zhang, Y. Ma, *Nucl. Instr. and Meth. B*, 308, 24 (2013).

PW-LASER produced MeV PROTON BEAMS STOPPED in WDM PLASMAS (H, He, Ar, N, Xe)

DEUTSCH, Claude 1; CHEN, SOPHIA 2*; FUCHS, JULIEN 2

1 LPGP UParis-Sud; 2 LULI-PALaiseau FRANCE

Physical processes involved in the interaction of ion beams in Warm Dense Matter (WDM) (i.e. 1 - 100 eV, 0.01-100 g/cc) is fundamental to the understanding of condensed matter, solid-state physics, fusion sciences, and astrophysical phenomena. In particular, in the WDM regime the charge equilibrium and stopping power of ions differs significantly from that of both cold matter and ideal plasma due to free electron contributions, plasma correlation effects and electron degeneracy. Furthermore, experimental data is extremely scarce in this regime; the reason being that the creation a WDM state with a temporal duration consistent with the particles used to probe it has been extremely difficult to achieve experimentally. For the past couple of years, we have been developing an experimental platform using short pulse lasers that can produced relatively short bunches of protons (picosecond time scale) to study plasmas in the WDM regime. Earlier this year, using the Titan Laser at JLF, we used the CPA laser to create two identical proton beams in a gas jet. One was used as a reference, and the other beam was used to perform the stopping power measurement in a gas plasma that was heated by the long pulse beam. These measurements will allow for a first evaluation of semiempirical formulas that are being used to predict the stopping power of ions in numerical codes that are often used in ICF and astrophysics. The development of this short-pulse laser platform thus shows great promise to push further the investigation of ion interactions in the experimentally challenging conditions of WDM.

Ion-induced hillock formation: kinetic and potential energy contributions of highly charged ions and swift heavy ions

WANG, Yuyu 1*; GRYGIEL, Clara 2; DUFOUR, Christian 2; MONNET, Isabelle 2; BOUFFARD, Serge 2; TOULEMONDE, Marcel 2 GRUBER, Elisabeth 3; SUN, J.R. 1; WANG, Z.G. 1; ZHAO, Y.T. 1; XIAO, G.Q. 1; CASSIMI, Armin 2; AUMAYR, F. 3

1 Institute of Modern Physics, CAS, Lanzhou, China; 2 CIMAP-GANIL; 3 TU Wien, 1040 Vienna, Austria

The nature and intensity of ion-surface interactions are intimately connected to projectile energy deposition in the target and therefore depend both on the kinetic and the potential energies [1]. The energy losses of swift heavy ions (SHI, MeV to GeV) induce along the ion path intense electronic excitations in a small volume which spawn formation of surface modifications and latent tracks in depth. Beside it, highly charged ions (HCI) carry several tens of keV of potential energy which is delivered into only few atomic layers of the surface, resulting in many different phenomena that are significantly dependent on the potential energy deposition. Quite recently a coherent synergy of nuclear and electronic energy losses is suggested in ion-irradiation processes from the nuclear to the electronic energy regime [2] and the model developed for track formation was extended to explain the nuclear effect. In our recent work, a complementary study [1] has shown an additive effect between depositions of kinetic energy and potential energy in a medium energy range for surface nanostructure formation on CaF_2 . Based on suggestion of Aumayr et al. [3] and on knowledge of track formation at high energy, including experiments and model description [4], we will show the results of surface modifications on various insulating material surfaces (i.e. CaF_2 $E_g=12\text{eV}$ (done in [1]), c-SiO_2 $E_g=9\text{eV}$, Al_2O_3 $E_g=8\text{eV}$ and MgO $E_g=7.8\text{eV}$) induced by highly charged ions and swift heavy ions in a medium energy range.

[1] Y.Y. Wang et al, Sci. Reps. 4(2014)5742

[2] M.Toulemonde et al, PRB 83(2011)054106

[3] F. Aumayr et al, J. Phys. Cond. Matt. 23(2011)393001

[4] A. Meftah et al, NIMB 237(2005)563

Crystalline hillock formation of oxides irradiated with swift heavy ions -TEM study-

ISHIKAWA, Norito 1*; OKUBO, Nariaki 1; TAGUCHI, Tomitsugu 1

1 Japan Atomic Energy Agency

In this study, CeO_2 and NiO were irradiated with Au ions in the energy range of 200-340 MeV at oblique incidence. Observation of as-irradiated samples by transmission electron microscope (TEM) shows that hillocks are created not only at the wide faces but also at the crack faces of thin samples. Since the hillocks created at the crack faces can be imaged by TEM, their shape and crystallographic features can be revealed by TEM. From the images of hillocks created at the crack faces, many of the hillocks are found to be spherical for ion-irradiated CeO_2 . For ion-irradiated NiO , atomic-scale steps are found to be created at the top surface of the hillocks. We present an experimental evidence that hillocks created for both oxides irradiated with swift heavy ions have a crystal structure whose lattice spacing and orientation coincide with those of the matrix. The mechanism of hillocks formation will be discussed based on the present results, and the advantages of the novel observation technique used in the present study will be also discussed.

$\text{Y}_2\text{Ti}_2\text{O}_7$ and Me_{23}C_6 nanoparticles in swift heavy ion irradiated ODS alloys

SKURATOV, Vladimir 1*; SOHATSKY, Alexander 1; O'CONNELL, Jacques 2;
KORNIEIEVA, Kateryna 1; UGLOV, Vladimir 3; NEETHLING, Jan 2; NIKITINA, Anastasiya
4; AGEEV, Valery 4

1 FLNR, JINR, Dubna, Russia; 2 CHRTEM, NMMU, Port Elizabeth, South Africa; 3
Belarusian State University, Minsk, Belarus;
4 JSC VNIINM, Moscow, Russia

Y-Ti oxides and Me_{23}C_6 precipitates are typical representatives of nanoparticle population in ferritic oxide dispersion strengthened (ODS) steels. Their stability during dense ionization in the so-called swift heavy ion regime has received considerable attention in recent years because the change in nanoparticle morphology should inevitably affect the mechanical properties of the first few subsurface microns of cladding material that is in contact with fissionable fuel and exposed to fission fragments. In this report we present and discuss the results of a TEM study of structural changes induced by krypton and xenon ions of fission fragment energy (1.2 MeV/nucleon) in $\text{Y}_2\text{Ti}_2\text{O}_7$ and Me_{23}C_6 nanoparticles in EP450 ODS steel. It was found that swift heavy ion irradiation leads to formation of amorphous latent tracks in both materials. The electronic stopping power threshold for track formation in pyrochlore nanoparticles lies in the range 7.4– 9.7 keV/nm and the mean track diameter varies linearly with the electronic energy loss.

Swift Heavy Ion Irradiation of Dense GeO₂ Glass at Ultrahigh Pressure: Formation and Stabilization of a Disordered NiAs-Type Structure

PALOMARES, Raul 1*; LANG, Maik 1; TRAUTMANN, Christina 2; EWING, Rodney 3; ZHANG, Fuxiang 4

1 University of Tennessee; 2 GSI, Darmstadt; 3 Stanford University; 4 University of Michigan

Research on materials under coupled extreme conditions including pressure, temperature, and irradiation has become a new and vibrant area of investigation [1]. Incorporation of relativistic ion beams, in particular, has proven effective for synthesis and stabilization of novel phases far from thermodynamic equilibrium [2]. The technique couples static compression and high-density energy deposition via the bombardment of pressurized samples by relativistic heavy ions that are injected into a diamond-anvil cell [3]. Most recently, we applied this technique to amorphous germanium dioxide (GeO₂).

Germanium dioxide boasts a diverse array of polymorphs. One hexagonal polymorph, disordered niccolite (d-NiAs-type) GeO₂, is notably absent in nature. This d-NiAs-type structure forms exclusively from aperiodic starting materials during shockwave experiments, and static compression experiments in a limited temperature range (1000 – 1300 K) at pressures above 6 GPa [4]. Prior attempts to quench the high-pressure phase were unsuccessful —noting a gradual transformation to the stishovite structure within hours. Here, we report on the crystallization and permanent stabilization of the d-NiAs-type structure of GeO₂ formed by in situ irradiation of GeO₂ glass with 6 GeV 209Bi ions at 45 GPa in the absence of external heating. Synchrotron x-ray structural refinement of the quenched material suggests that the phase is stabilized by ion-induced cation vacancies that randomly occupy half of the octahedral sites.

References:

- [1] R.J. Hemley, G.W. Crabtree & M.V. Buchanan, *Physics Today* 62, 32-37 (2009)
- [2] M. Lang et al., *Nature Materials* 8, 793-797 (2009)
- [3] M. Lang et al., *J. Synchrotron Rad.* 16, 773–777 (2009)
- [4] V.B. Prakapenka et al., *J. of Phys. and Chem. of Solids* 65, 1537-1545 (2004)

Swift heavy ion modifications of astrophysical water ice

DARTOIS, Emmanuel 1*; AUGÉ, Basile 1,2; ROTHARD, Hermann 2; BODUCH, Philippe 2; BRUNETTO, Rosario 1; CHABOT, Marin 3; DOMARACKA, Alicija 2; DING, Jing Jie 2; KAMALOU, Omar 2; LV, Xue Yang 2; FROTA DA SILVEIRA, Enio 4; THOMAS, Jean-Charles 2; PINO, Thomas 5; MEJIAGUAMAN, Christian 4; GODARD, Marie 6; DE BARROS, Ana 7

1 Institut d'Astrophysique Spatiale-CNRS, Orsay France; 2 CIMAP-Ganil CNRS, Caen, France; 3 CNRS-IN2P3, IPNO, ORSAY, FRANCE; 4 Physics Department, Pontificia Universidade Catolica do Rio de Janeiro; 5 ISMO-CNRS, Orsay, France; 6 CSNSM-CNRS, Orsay, France; 7 Physics Department, Centro Federal de Educação Tecnológica Celso Suckow da Fonseca, Rio de Janeiro

In the relatively shielded environments provided by interstellar dense clouds in our Galaxy, infrared astronomical observations have early revealed the presence of low temperature (10-100 K) ice mantles covering tiny grain “cores” composed of more refractory material. These ices are of specific interest because they constitute an interface between a solid phase under complex evolution triggered by energetic processes and surface reactions, with the rich chemistry taking place in the gas phase. The interstellar ice mantles present in these environments are immersed in a flux of cosmic ray particles [1-3] that produces new species via radiolysis processes, but first affects their structure which may change and then induces desorption of molecules and radicals from these grains [4-6]. These cosmic rays can be simulated in the laboratory for a better understanding of astrophysical processes. The high-energy cosmic ray component (just below or above 100 MeV/u) was so far only scarcely simulated experimentally. Nevertheless, there is a clear need to study the interaction of high energy cosmic rays with ices, since the energy deposited on dust grains and ice mantles is expected to be important compared to protons and concomitant with UV photons. In particular, the physical state of the ice is extremely important in many respects for astrophysicists, to allow in particular surface physicist to perform experiments on realistic surfaces for a better understanding of interstellar chemistry. This talk will be dedicated to describe the evolution, in an astrophysical context and based on laboratory experiments, of the ice's physical state (amorphous, crystalline, metastable), including sputtering, resulting from the interactions with swift ions and photons.

[1] Shen et al. 2004, A&A, 415, 203; [2] de Nolfo et al. 2006, Adv. Space Res., 38, 1558; [3] George et al. 2009, ApJ, 698, 1666 ; [4] Fama et al. 2010, Icarus, 207, 314; [5] Dartois et al. 2013, A&A 557, A97; [6] Mejía et al. 2015, Icarus, 250, 222.

Time-of-flight Secondary Neutral & Ion Mass Spectrometry using swift Heavy Ions

WUCHER, Andreas 1; BREUER, Lars 1*; MEINERZHAGEN, Florian 1

1 Universität Duisburg-Essen

We report on a new time-of-flight (TOF) spectrometer designed to investigate sputtering phenomena induced by swift heavy ions in the electronic stopping regime. In this experiment, particular emphasis is put on the detection of secondary ions along with their emitted neutral counterparts in order to examine the ionization efficiency of the sputtered material. For the detection of neutral species, the system is equipped with a pulsed VUV laser for post-ionization of sputtered neutral atoms and molecules via single photon ionization at a wavelength of 157 nm (corresponding to 7.9 eV photon energy). For alignment purposes and in order to facilitate comparison to nuclear sputtering conditions, the system also includes a 5-keV Ar⁺ ion beam directed to the same sample area. The instrument has been added to the GSI M-branch beam line and was tested with 4.8 MeV/u Au²⁶⁺ ions impinging onto various samples including metals, salts and organic films. It is found that secondary ion and neutral spectra obtained under both bombardment conditions can be acquired in an interleaved manner throughout a single accelerator pulse, thus making efficient use of valuable beam time. In addition, the keV ion beam can be intermittently switched to dc mode between subsequent accelerator pulses in order to ensure reproducible surface conditions by dynamical sputter cleaning. For the case of a clean metal surface, comparison of secondary ion and neutral signals obtained under otherwise identical instrumental conditions reveal that the ionization probability of atoms emitted under electronic and nuclear sputtering conditions is similar.

Synergy effect between electronic and collisional sputtering: The case of amorphous silicon nitride irradiated with energetic C₆₀ ions

KIMURA, Kenji 1; KITAYAMA, Takumi 1*; MORITA, Yosuke 1; NAKAJIMA, Kaoru 1;
NARUMI, Kazumasa 2; SAITOH, Yuichi 2; MATSUDA, Makoto 2; SATAKA, Masao 2;
TOULEMONDE, Marcel 3

1 Kyoto University; 2 JAEA; 3 CIMAP, Caen (F)

Amorphous silicon nitride films (thickness 30 nm) deposited on Si(001) were irradiated with 30 – 1080 keV C₆₀ and 100 MeV Xe ions to fluences ranging from 2.5×10^{11} to 1×10^{14} ions/cm². The composition depth profiles of the irradiated samples were measured using high-resolution Rutherford backscattering spectrometry.

Both silicon and nitrogen signals in the film decrease with fluence. The sputtering yields were estimated from the observed RBS spectra. The observed total sputtering yield of C₆₀ increases from 1200 to 4600 when the energy increases from 30 to 1080 keV. The corresponding sputtering yields estimated using the SRIM code are less than 100, suggesting that the electronic sputtering is responsible for the observed large sputtering yields. On the other hand, the observed sputtering yield of 100 MeV Xe is about 500. Considering the fact that the electronic stopping power of 100 MeV Xe ion (16.6 keV/nm) is larger than those of 30 – 1080 keV C₆₀ ions (2 – 10 keV/nm), the large sputtering yields of C₆₀ ions are ascribed to the synergy effect between the electronic and collisional sputtering. In order to estimate such a synergy effect, calculations of the sputtering yield are now in progress using the inelastic thermal spike model taking account of the nuclear stopping power [1]. The result of the calculation will be presented at the conference.

[1] M. Toulemonde, W.J. Weber, G. Li, V. Shutthanandan, P. Kluth, T. Yang, Y. Wang and Y. Zhang, Phys. Rev. B **83** (2011) 054106.

Ion induced reactivity in systems of astrophysical interest

DOMARACKA, Alicia 1*; BODUCH, Philippe 1; ROTHARD, Hermann 1; PILLING, Sergio 2; DA SILVEIRA, Enio F. 3; STRAZZULLA, Giovanni 4

1 Centre de Recherche sur les Ions, les Matériaux et la Photonique (CEA/CNRS/ENSICAEN/Université de Caen-Basse Normandie); 2 Instituto de Pesquisa e Desenvolvimento (IP&D), Universidade do Vale do Paraíba (UNIVAP), São José dos Campos, SP 12244-000, Brazil; 3 Physics Department, Pontifícia Universidade Católica, Rua Marquês de S. Vicente 225, 22451-900 Rio de Janeiro, Brazil; 4 INAF-Osservatorio Astrofisico di Catania, 95123 Catania, Italy

Complex organic molecules are observed in many astrophysical objects, but little is known about their formation mechanism and survivability. In molecular clouds, atoms and molecules condense on dust particles leading to formation of icy mantles.

Astrophysical ices contain mainly H₂O, while CO, CO₂, NH₃, and CH₃OH are also commonly observed. These ices are exposed to energetic processing by ions, photons and electrons, and/or thermal processes that trigger the chemical evolution of the ice.

Laboratory simulations on interstellar ices and molecular clusters are therefore of paramount importance for understanding the origin of complex organic molecules (possibly relevant to the origin of life). Studying in-situ the chemical evolution of ices and of remaining refractory organic residues (after slow heating-up) provides relevant hints on the fundamental physical and chemical steps associated with the increase of the molecular complexity in space. Several experiments show that the basic building blocks of organic matter can be formed by interaction of UV photons, electrons and keV-MeV light ions with ices. The aim of the present work is to mimic the reactivity in ices and molecular clusters triggered by heavier ions, also being present in space. On the one hand, we will focus on the physical chemistry induced by heavy-ion cosmic rays inside ammonia-containing ices (e.g. H₂O:NH₃:CO) irradiated by Ni ions. The infrared spectra of the irradiated ice samples exhibit bands of several new species including HNCO, N₂O, OCN-, and NH₄+. After IR measurements the irradiated samples were slowly warmed up to room temperature. This IR spectrum contains bands that can be tentatively assigned to vibration modes of zwitterionic glycine and to hexamethylenetetramine. Moreover, we need to know the probability that such complex organic molecules survive when exposed to radiation. Therefore, we have also performed irradiations of adenine films with MeV ions.

On the other hand, it is believed that PAHs are omnipresent in the interstellar medium. We will also present very recent results on ion-induced reactivity in pyrene clusters and radiolysis of pyrene films.

Transmission Electron Microscopy Study on Ion Tracks in Ceria

YASUDA, Kazuhiro 1*; TAKAKI, Seiya 1; YAMAMOTO, Tomokazu 1; MATSUMURA, Syo 1; ISHKAWA, Norito 2

1 Kyushu University; 2 JAEA

High density electronic excitation caused by fission fragments (FFs) in nuclear fuels and transmission targets is known to induce of ion tracks along the penetration path of FFs. Understanding of the structure of ion tracks together with the overlapping effects is one of the essentials for the development and assessment of the fuel/target materials under the extreme radiation condition. This paper reports the structure and accumulation process of ion tracks in ceria through a variety of transmission electron microscopy (TEM) and scanning transmission electron microscopy (STEM) techniques.

Ion tracks in CeO₂ have been shown to retain the fluorite structure. Bright-field TEM and high-angle annular dark-field (HAADF) and annular bright-field (ABF) STEM techniques showed that the core region of ion tracks is 3-4 nm in diameter [1,2], and that the atomic density inside the ion tracks is decreased for about 10% [3]. Furthermore, ABF-STEM observation detected the preferential disorder of O-anion sublattice at the core region of the ion track [3]. On the other hand, analysis of the accumulation of ion tracks suggested the existence of an influence region, in which the formation and recovery of ion tracks are balanced [1]. The significantly large size of influence region (17 nm in diameter) than observable size is discussed that the core damage region detected by TEM and STEM is a vacancy-rich region formed after the recovery process of thermal spike [4]. Interstitial ions are considered to be generated during the recovery process within a rather wide region, to result in the development of dislocation structure at high fluence irradiation condition. It is also presented in this paper that the size of Fresnel contrast of ion tracks with bright-field TEM strongly depends on the defocused condition.

[1] K. Yasuda, et al., Nucl. Instr. Meth. B 314 (2013) 185

[2] K. Yasuda, et al., Proc. on 11th Int. Topical Meetings on Nuclear Applications of Accelerators (2013) 7.

[3] S. Takaki et al., Nucl. Instr. Meth. B, 326(2014) 140.

[4] S. Takaki et al., Prog. Nucl. Energy (2014) in press.

Recent advances in characterisation of ion tracks using small angle x-ray scattering measurements

KLUTH, Patrick 1*; SCHAURIES, Daniel 1; AFRA, Boshra 1; NADZRI, Allina 1; MOTA SANTIAGO, Pablo 1; PROFT, Max 1; NORDLUND, Kai 2; PAKARINEN, Olli 2; LEINO, Aleksi 2; DJURABEKOVA, Flyura 2; LANG, Maik 3; EWING, Rodney C. 4; TRAUTMANN, Christina 5; KIRBY, Nigel 6

1 The Australian National University; 2 University of Helsinki; 3 University of Tennessee; 4 Stanford University; 5 GSI, Darmstadt; 6 Australian Synchrotron

Small angle X-ray scattering (SAXS) provides an interesting tool to study the structure of etched and un-etched ion tracks. It is non-destructive and can yield high precision measurements of the track radii in bulk amorphous and crystalline materials. Short acquisition times associated with the high photon flux at 3rd generation synchrotron devices facilitate in situ studies to determine the annealing kinetics of ion tracks as well as the use of diamond anvil cells to investigate track stability under high pressure conditions. Monte Carlo calculations enable advanced SAXS data analysis using complex track shapes.

This presentation will give an overview of our recent advances in characterising ion tracks using SAXS and outline potential future directions. Examples include: In situ annealing experiments of ion tracks in quartz to study a complex elastic behaviour of the tracks [1] as well as their annealing kinetics; the composition dependent annealing behaviour of tracks in natural apatite; etching experiments in apatite which reveal hexagonally shaped etch pits depending on track orientation and apatite composition; ion track formation at elevated temperatures in apatite and quartz showing an increase in the track radii by approximately 1 Å/100°C as a consequence of an increased local temperature leading to a larger melting radius in the thermal spike [2]; the influence of pressure on the formation, stability and annealing behaviour of ion tracks. Increasing pressure during formation leads to increased track radii, while track recovery appears to be enhanced at elevated pressures. Experimental results were complemented by molecular dynamics simulations.

[1] B. Afra et al., Phys. Rev B 90 (2014) 224108

[2] D. Schauries et al., J. Appl. Cryst. 46 (2013) 1558

Structural modifications induced by swift heavy ions in Al_2O_3

GRYGIEL, Clara 1*; MOISY, Florent 1; SALL, Mamour 1; LEBIUS, Henning 1; BALANZAT, Emmanuel 1; MONNET, Isabelle 1

1 CIMAP-GANIL

Defects in oxide materials created by irradiation are often revealed by optical absorption for the formation of colour centres and by transmission electron microscopy (TEM) for the individual latent track and microstructure evolution observations. The characterizations by X-Ray diffraction of irradiated materials were lesser used but are since few years under investigation going with the development of versatile laboratory diffractometers allowing good resolution and grazing geometry (GIXRD) required to probe the upper irradiated part of samples.

In this work a detailed study on the structural modifications of Al_2O_3 compound induced by swift heavy ion irradiation is presented by an original combination of the three techniques, previously mentioned, in-situ GIXRD, TEM and in-situ UV-Vis absorption. The irradiation experiments have been performed at IRRSUD beamline of GANIL where the energy range, i.e. 0.3-1 MeV/A, implies a mean projected range in solid matter around only a few micrometers and a decrease with depth of the electronic stopping power (Se). Depth profile by GIXRD is thus topical to get structural parameters at different Se values.

In the communication the study of $\alpha\text{-Al}_2\text{O}_3$ polycrystals and single crystals irradiated by 92 MeV Xe and 74 MeV Kr will be shown. Contributions from point defects and extended defects induced by irradiation to structural modifications will be discussed.

An amorphization of the material is observed and its kinetics of ion track overlapping will be shown. This amorphization is associated in the crystalline part to tensile strain, unit cell swelling, microstrain, grain subdivision and a variable damaging sensitivity of the anionic and cationic sublattices. Our results are consistent with the previous reports found in literature and are in agreement with the given Se threshold for amorphization. These results will be fully described and illustrated during the communication.

Systematic study of the phase behavior of f-block oxides irradiated with swift heavy ions

TRACY, Cameron 1*; LANG, Maik 2; ZHANG, Fuxiang 1; TRAUTMANN, Christina 3; EWING, Rodney 4

1 University of Michigan; 2 University of Tennessee; 3 GSI, Darmstadt; 4 Stanford University

The localized nature of f-electrons results in systematic variation in the structures and electronic configurations accessible to oxides across the lanthanide and actinide series, with some exceptions due to partial f-electron itinerancy in the light actinides. To study the influence of the resulting variation in f-block oxide phase space on the response of these materials to highly-ionizing radiation, various lanthanide and actinide oxides were irradiated with swift heavy ions possessing energies ranging from 167 MeV to 2.2 GeV. Modifications to the materials were characterized using x-ray diffraction, x-ray absorption spectroscopy, and Raman spectroscopy. Sesquioxides (A_2O_3), with the bixbyite structure and minimal redox activity, exhibited radiation-induced phase transformations to high temperature polymorphs, with the final phase and the transformation rate showing dependence on the cation ionic radius. In contrast, fluorite-structured dioxides (AO_2) retained their initial structure, but underwent partial cation valence reduction to the trivalent state, causing unit cell expansion and microstrain commensurate with the propensity of their cations to accommodate these valence changes. Finally, uranium trioxide (UO_3) showed extensive cation reduction to the tetravalent state, decomposing to a UO_{2+x} phase with the fluorite structure. From these results, the effects of swift heavy ion irradiation on the f-block oxides can be understood in terms of coupled modifications to their atomic and electronic structures. These effects are constrained by the stabilities of structures and electronic configurations, governed by variations in ionic radius and f-electron itinerancy characteristic of the f-block oxides.

Commissioning of the PRIOR prototype at GSI

VARENTOV, Dmitry 1*

1 GSI, Darmstadt

High energy proton microscopy (HEPM) or radiography is a novel technique for probing the interior of dense objects in static or dynamic experiments by mono-energetic beams of GeV-energy protons. A special system of magnetic lenses is employed for imaging and aberrations correction. Using this technique, one can measure the areal density distribution of a thick sample with sub percent accuracy, micrometer-scale spatial and nanosecond-scale temporal resolutions. HEPM is of considerable interest for materials research, plasma physics, biophysics and medicine.

The future PRIOR (Proton Microscope for FAIR) facility will use 1 - 10 GeV intense proton beams and will allow for a significant step forward in spatial ($\sim 10\text{-}15\text{ }\mu\text{m}$) and temporal ($\sim 5\text{-}10\text{ ns}$) resolution. A PRIOR prototype has been constructed and successfully commissioned at GSI in 2014 using 3.5 - 4.5 GeV intense proton beams from the SIS-18 synchrotron. The status of the PRIOR project and the first results obtained in static and dynamic experiments with the PRIOR prototype are presented.

Resonant coherent excitation under swift heavy ion channeling

AZUMA, Toshiyuki 1*

1 RIKEN AMO Physics laboratory

For decades we have been involved in the selective excitation of the heavy atomic ions from Ar to U in the x-ray energy domain making use of a thin single crystal. The swift ions accelerated to ~70 % of the speed of light using the heavy ion synchrotron facility are guided in the silicon single crystal, and excited by a temporally oscillating strong Coulomb field arising from the periodical atomic arrangement. When one of the frequencies corresponds to the transition energy of the ion, the oscillating field has a chance to resonantly excite the internal atomic states of the ion. This process is called “resonant coherent excitation” (RCE). Starting from the resonance by periodic field due to the arrays of the atomic strings in the crystal (2D-RCE) under the planar channeling condition, we developed the resonance technique by the periodical field by an array of the atomic planes (3D-RCE) under the non-channeling condition.

Making use of the 3D-RCE, we have made a significant progress in the selective excitation of heavy atomic ions like Ar and Fe ions accompanying one or a few electrons. Control of magnetic substate population i.e., ion alignment has been achieved by selecting polarization of the periodic field. The use of double resonance technique offered a variety of population control and probing scheme in three-level configurations, that enabled observation of 1) quantum optical phenomena like dressed atoms even in the x-ray energy domain, 2) double excitation to make two K-shell holes in an heavy ion, and 3) sequential excitation to the higher electronic states.

We also have succeeded in observing the 2s-2p transitions of Li-like U ions, which offers us a future possibility of the precision atomic spectroscopy.

Determination of electronic stopping powers of 0.05-1 MeV/u ^{131}Xe -ions in C-, Ni- and Au-absorbers with calorimetric low temperature detectors

ECHLER, Artur 1*; EGELHOF, Peter 2; GRABITZ, Patrick 2; KETTUNEN, Heikki 3; KRAFT-BERMUTH, Saskia 1; LAITINEN, Mikko 3; MÜLLER, Katrin 1; ROSSI, Mikko 3; TRZASKA, Wladyslaw 3; VIRTANEN, Ari 3

1 IAMP, University of Giessen; 2 GSI, Darmstadt; 3 JYFL, University of Jyväskylä

Precise data on electronic stopping powers for heavy ions are of high interest in various fields of research. Since more than one decade a new technique, which uses a combination of time-of-flight and energy detectors to collect continuous dE/dx data over a wide range of energies in a single measurement [1], has been successfully applied in different experiments. However, for high ion masses and low energies, where dE/dx data are nowadays still scarce, ionization based energy detectors suffer from incomplete energy detection, resulting in pulse height defect and a relatively poor energy resolution. As calorimetric low temperature detectors (CLTD's) provide substantially better energy resolution and linearity (with the absence of any pulse height defect) for heavy ion detection [2], this type of energy detectors has the potential to increase sensitivity and accuracy for dE/dx measurements and to extend the accessible energy range towards lower energies. For that purpose a CLTD array has been used to replace the Si-detector in an established setup for dE/dx measurements at the K-130 cyclotron at the University of Jyväskylä, and to perform measurements with 0.05–1 MeV/u ^{131}Xe -ions in carbon, nickel and gold absorbers [3]. In addition to the determination of new stopping power data for low energy heavy ions, the excellent energy resolution of CLTD's allowed to resolve unexpectedly strong channeling effects for thin polycrystalline absorbers in the transmission type energy loss measurement, and therefore also to obtain data for channeling energy loss of 0.1–0.5 MeV/u ^{131}Xe ions in nickel and gold absorbers. This contribution will present the detector concept of CLTD's as well as the results of this recent application for stopping power measurements.

References

- [1] W.H. Trzaska et al., Nucl. Instr. Meth. B (2002) 195, 147.
- [2] P. Egelhof and S. Kraft-Bermuth, Top. App. Phys. (2005) 99, 469.
- [3] A. Echler et al., J. Low Temp. Phys. (2014) 176, 5, 1033.

Design and fabrication of waveguides and optical gratings in crystals and glasses via swift ion irradiation

BANYASZ, Istvan 1*; OLIVARES VILLEGAS, José 2; BERNESCHI, Simone 3; PELLI, Stefano 4; NUNZI CONTI, Gualtiero 3; RIGHINI, Giancarlo 5; PEÑA RODRIGUEZ, Ovidio 6; RAJTA, István 7; NAGY, Gyula 7; HAVRANEK, Vladimir 8; VOSECEK, Vaclav 8; ZOLNAI, Zsolt 9; VERES, Miklos 1; HIMICS, Laszlo 1

1 Wigner Research Centre for Physics, Budapest, Hungary; 2 Instituto de Óptica 'Daza de Valdés', CSIC, Madrid, Spain; 3 Instituto di Fisica Applicata "Nello Carrara", Sesto Fiorentino, Italy; 4 Instituto di Fisica "Nello Carrara", Sesto Fiorentino, Italy; 5 "Enrico Fermi" Center for Study and Research; 6 Institute of Nuclear Fusión, Universidad Politécnica de Madrid, Spain; 7 Institute of Nuclear Research of the Hungarian Academy of Sciences, Debrecen, Hungary; 8 Nuclear Physics Institute of the ASCR, Rez, Czech Republic; 9 Centre for Energy Research of the Hungarian Academy of Sciences, Budapest, Hungary

Active and passive optical waveguides are fundamental elements in modern telecommunications systems. A great number of optical crystals and glasses were identified and are used as good optoelectronic materials. However, fabrication of waveguides in some of those materials remains still a challenging task due to their susceptibility to mechanical or chemical damages during processing. Researches were initiated on ion beam fabrication of optical waveguides in tellurite glasses. Channel waveguides were written in Er: $\text{TeO}_2\text{--WO}_3$ glass through a special silicon mask using 1.5 MeV N^+ irradiation. This method was improved by increasing N^+ energy to 3.5 MeV to achieve confinement at the 1550 nm wavelength, too. An alternative method, direct writing of the channel waveguides in the tellurite glass using focussed beams of 6–11 MeV C^{3+} and C^{5+} and 5 and 10 MeV N^{3+} , has also been developed. Channel waveguides were fabricated in undoped eulytine- ($\text{Bi}_4\text{Ge}_3\text{O}_{12}$) and sillenite type ($\text{Bi}_{12}\text{GeO}_{20}$) bismuth germanate crystals using both a special silicon mask and a thick SU8 photoresist mask and 3.5 MeV N^+ irradiation. By using even higher energy irradiation, 25 MeV C^{5+} at low doses, planar optical waveguides were fabricated in sillenite-type BGO crystal.

Focussed ion beam (11 MeV C^{3+} , 10 MeV N^{3+}) irradiation was also used to fabricate transmission optical gratings in Pyrex and Er:

$\text{TeO}_2\text{--WO}_3$ glasses, sillenite type BGO and LiNbO_3 crystals. The waveguides were studied by phase contrast and interference microscopy and micro Raman spectroscopy. Guiding properties were checked by using m-line spectroscopy and the end fire method.

In-Situ SEM-Investigation of SHI induced Modification of Surfaces and Thin Films

BOLSE, Wolfgang 1*; AMIRTHAPANDIAN, Sankarakumar 2; FERHATI, Redi 1;
GARMATTER, Daniel 1; HAAG, Michael 1; DAUTEL, Knut 1; ASDI, Mazhar 1;
SRIVASTAVA, Neelabh 1; WIDMANN, Barbara 1; BAUER, Martin 1

1 Institut für Halbleiteroptik und Funktionelle Grenzflächen, Universität Stuttgart, Germany; 2
Materials Physics Division, Indira Gandhi Centre for Atomic Research, Kalpakkam, India

We are running a High Resolution Scanning Electron Microscope in the beam line of the UNILAC ion accelerator at the GSI Helmholtz Centre for Heavy Ion Research in Darmstadt, Germany, which has recently been extended also with an EDX-system and two micro-manipulators. This instrument allows us to in-situ investigate the structural and compositional development of individual objects and structures in the um- and nm-range under swift heavy ion bombardment, from the very first ion impact up to high fluences of the order of several $10^{15} / \text{cm}^2$. The sample under investigation is irradiated in small fluence steps and in between

SEM-images (and EDX-scans) of one and the same surface area are taken. The irradiation can be carried out at any incidence angle between 0 and 90 degree and also under stepwise or continuous azimuthal rotation of the sample. The micro-manipulator system allows us to perform additional analysis like electrical and mechanical characterization as well as substrate-free EDX at sub-um objects. We are now also able to irradiate almost free standing sub-um structures (pasted on a nanoscale tip or held in micro-tweezers). In this report an overview over this unique instrument and its capabilities and advantages will be given, illustrated by the results of our recent in-situ studies on ion induced modification of thin films (dewetting and self-organisation) and on shaping of sub-um objects with swift heavy ions (by taking advantage of ion sputtering, ion hammering and ion induced visco-elastic flow).

POSTERS

Session A

Monday, 4.30 – 6 pm

*** Primary author**
Presenting author

Observation of ejected electron-target core interaction in He^{2+} -argon collisions

MA, Xinwen 1; GAO, Yong 1*; GUO, Dalong 1; QIAN, Dongbin 1; ZHU, Xiaolong 1; FENG, Wentian 2; ZHANG, Ruitian 1; LI, Bin 1; YAN, Shuncheng 1; XU, Shengyue 1; ZHANG, Pengju 1;

1 Institute of Modern Physics, Chinese Academy of Sciences

We have investigated the single ionization with simultaneous single and double capture in He^{2+} collisions with argon by means of reaction microscopes [1,2]. Here, we report the dependence of the azimuth angle of the ejected electron on the transversal recoil momentum in single capture with double ionization process for 30 keV/u He^{2+} collisions with Ar. The azimuth angle is defined by the transversal momentum of the recoil ion and the emitted electron. In the present work, we focus on the azimuth angle distributions of the ejected electrons in the transverse recoil momentum ranges of 0–4, 4–8, 8–15, 15–30 a.u., respectively. It is found that the relative intensity of the peak at 0 degree decreases rapidly with transversal recoil momentum increasing, however, the one at 180 degree strongly increases. The phenomenon may be the result of ejected electron-target core interaction. At small transverse recoil momentum, the trajectories of most of the ejected electrons are far away from the target cores, and the interactions of the ejected electrons with the target cores are weak. As a result, the motions of the ejected electrons are hardly changed by the field of target cores. In contrast, at large transverse recoil momentum, the ejected electrons are strongly attracted by the target cores and their moving directions are dramatically deviated. In consequence, parts of the electrons ejected at azimuth angle of 0 degree initially are directed to 180 degree.

This work was partially supported by the Major State Basic Research Development Program of China (973 Program, Grant No. 2010CB832902) and the National Natural Science Foundation of China under Grants Nos. 10979007, 10974207 and 11274317.

References

- [1] X. Ma, R. T. Zhang, S. F. Zhang et al., Phys. Rev. A 83, 052707 (2011)
- [2] R. T. Zhang, X. Ma, S. F. Zhang et al., Phys. Rev. A 89, 032708 (2014)

Vicinage Effect on the Generation Mechanism of ConvoY Electrons

TOMITA, Shigeo 1*; KINOSHITA, Ryo 1; SHIINA, Yoko 1; IMAI, Makoto 2; KAWATSURA, Kiyoshi 3; MATSUDA, Makoto 4; SASA, Kimikazu 5; SATAKA, Masao 5

1 Institute of Applied Physics, University of Tsukuba; 2 Dep. Nuclear Engineering, Kyoto Univ.; 3 Kansai Gaidai University; 4 Japan Atomic Energy Agency; 5 Tandem Accelerator Complex, University of Tsukuba

It is known that the yield of secondary electron for fast molecular ion injection is reduced strongly comparing the vicinage effect on the electronic stopping power. Thus, the reduction induces the strong violation of the relation, $Y_e = \lambda S_e$, where Y_e is secondary electron yield, S_e is electronic stopping power, and the parameter λ is material parameter. We think that the

behavior of scattered electron produced by projectile ion inside material must be crucial to understand the special cluster effect. Zero degree electron spectroscopy is employed in the present study to investigate the behavior of the electrons inside material produced by the transmission of swift molecular ions. The experiments were conducted on the tandem accelerator at the Japan Atomic Energy Research Institute of Tokai. The carbon molecule ions, C_n^+ were produced from benzene in the ECR ion source located on the high voltage platform of the accelerator. The ions were mass selected and accelerated to the velocity of 3.5 MeV/atom. The ions were injected on thin carbon foils and the electrons emitted towards beam direction were analyzed using electrostatic energy analyzer. The yield of convoy electron was normalized with emerging beam current and measured as a function of target thickness.

The normalized convoy electron yield of C_n^+ decreases with target thickness and becomes almost n times of that of atomic ion injection. Since the yield normalized with emerging beam current, convoy electron with enough thick target shows vicinage effect. In addition, the attenuation length of the convoy electron by molecular ion is found to be longer than the case of atomic ion. The longer attenuation length indicates higher capture cross section by the projectile atoms. The higher cross section for molecular ions also induce higher yield of convoy electron for C_n^+ .

01 - Atomic physics + Electronic excitation

Mo-PA3

Coincidence measurements between multiple ionization and fragmentation of acetylenemolecules induced by fast heavy ions

YOSHIDA, Shintaro 1*; MAJIMA, Takuya 1; ASAI, Tatsuya 1; MATSUBARA, Masaya 1; TSUCHIDA, Hidetsugu 1; ITOH, Akio 1

1 Kyoto University

Fast ion collisions with polyatomic molecules generate multiply charged and highly excited states, which initiate bond bending, stretching and breaking. Since a collision of a MeV energy ion with a molecule finishes less than a femtosecond including ionization processes, we can consider that multiply charged states are transiently produced as an intermediate state before fragmentation. To understand the fragmentation mechanism, it is important to know the charge state of the intermediate ions. In this work, we performed coincidence measurements between the number of ionized electrons and product ions from acetylene (C_2H_2) molecules in charge-changing collisions.

A beam of 0.8 MeV C^+ ions from the 1.7 MV tandem accelerator facility of QSEC, Kyoto University was crossed with a C_2H_2 molecular target. Three dimensional momentum vectors and mass-to-charge ratios of product ions were obtained by time-of-flight (TOF) measurements with a position-sensitive detector. Secondary electrons were detected with a semiconductor detector (SSD) on a potential at +25 kV. The number of electrons were deduced from a pulse height analysis of SSD signals. Coincidence measurements between the TOF and secondary electrons were performed under single electron capture and loss conditions. Degrees of multiple ionization are directly obtained from the number of emitted electrons and charge difference between projectile ions before and after collisions. We found that higher degrees of multiple ionization are involved at electron loss collisions compared with electron capture collisions, due to interaction in smaller impact parameters. In addition, slightly higher degrees of fragmentation and higher kinetic energy releases in electron loss collisions are observed even at the same intermediate charge state. These are consistent

with previous results for other molecules, i.e. C₆₀ and ethane [1]. The amount of excitation has a good correlation with the number of direct ionization, while electron capture processes themselves do not accompany greatly the extra excitation.

Reference:

[1] Majima et al, Phys. Rev. A 69, 031202(R) (2004), Phys. Rev. A 90 (2014) 062711.

01 - Atomic physics + Electronic excitation

Mo-PA4

Stopping of hundreds keV Proton/Helium Ion in Plasma

ZHAO, Yongtao 1*; WANG, Yuyu 1; REN, Jieru 2; XU, Ge 3; HOFFMANN, Dieter H.H. 2; CHENG, Rui 1; ZHOU, Xianming 1; LEI, Yu 1; DENG, Jiachuan 1; MA, Lidong 1; XIAO, Guoqing 1; ALEXANDER, Golubev 4;

1 Institute of Modern Physics, CAS, Lanzhou, China; 2 Technische Universität Darmstadt; 3 IAP, Goethe University Frankfurt am Main; 4 ITEP, Moscow

Investigation of the interaction processes of ion beams with plasma has attracted a lot of attention during the last decades. Due to the strong non-linear effects and the special importance in ICF research, more and more emphasis has been given to the investigations for ion beam in low energy range and/or for plasma with high intensity. Herein we address the recent progress on the energy loss measurement in case of hundreds keV proton/helium ions passing a gas-discharged plasma. The experiments were carried out at the HV-ECR (High Voltage Electronic Cyclotron Resonance ion source) platform at IMP, where both proton and heavy ion beams with energy up to 320*q keV (q is the charge state of the ions) can be provided. After passing through the plasma target, the ion beam is analyzed by a bending magnet and reaches a fast-gated position-sensitive detector with minimum gate of 10ns (in experiments the gate was set as 100-1000ns to ensure sufficient statistics). The energy resolution of the setup is around 1%, depending on the beam size and the beam divergence (see details in ref [1, 2]).

We found that, the measurements of energy loss in plasma fit very well with the theoretical predicts after the discharging reaching the maximum, during this period the plasma condition is somehow more stable. However, the measurements were far below the predicted value at the very beginning of the discharging, the reason is still unclear, so far we consider that, the electrons in the target will absorb most part of the discharging power at the beginning so that the electron temperature (or the average velocity of the electrons) will be very high, this may cause a remarkable degradation of the dominating Se (electron stopping power). Suppresingly, we also found that, a part of the proton beam was strongly focused and passed through the plasma without any energy loss, this phenomina might be reated to the wakefield addressed in the plasma.

References:

[1] Zhao Y. et al. 2012 Laser and Particle Beams 30 679–706

[2] Cheng R. et al. 2013 Phys. Scr. T156 014074

Energy deposition and charge state evolution of heavy ions traveling through hydrogen plasma

MORALES, Roberto 1*; BARRIGA-CARRASCO, Manuel D. 1*; CASAS, David 1, BOINE-FRANKENHEIM, Oliver 2; JACOBY, Joachim 3

1 E.T.S.I. Industriales, Universidad de Castilla-La Mancha; 2 Institut für Theorie Elektromagnetischer Felder (TEMF), Technische Universität Darmstadt; 3 Institut für Angewandte Physik, J. W. Goethe-Universität Frankfurt

In this work, the charge state evolution and the possible primordial role of her initial charge state in the energy deposition into the target has been analyzed for Uranium ions traveling through fully ionized hydrogen plasma. According to dielectric formalism, the energy loss of the heavy ion depends on its velocity and on its charge density. Also, it depends on the target through its dielectric function; here the random phase approximation (RPA) model is used because of its simplicity and the excellent results in the previous works in the description of the fully ionized plasmas. Mean charge state has been also calculated by two methods: by the stripping criterion of Kreussler et al. adapted to the plasma conditions, and by cross section. In the Kreussler et al. criterion, the Brandt-Kitagawa (BK) model has been employed to depict the projectile charge space distribution. The charge state evolution and the time (or length) to reach the equilibrium charge state when the ion is traveling through the plasma is calculated and analyzed for different initial charge states. This calculation allows us to evaluate the energy loss as a function of the initial charge state and to notice the role of the initial charge state in the energy loss. Finally, the energy loss has been calculated by the mean charge state and by the charge state evolution to assess the difference between both results.

In conclusion, it has established two models to calculate the mean charge state of heavy ions traveling through fully ionized plasma and one method to calculate the charge state evolution of the ion inside the plasma. Furthermore, it has proved the differences in the time necessary to reach the equilibrium charge state for different initial charge states. It has also observed differences in the two methods to calculate the mean charge state, where the Kreussler criterion establishes a smaller charge state than the cross sections. Finally, comparing our estimations with experimental data from the literature, it is found that our theoretical predictions are in good agreement with the experimental results.

Electronic sputtering of thin Au films: Experimental results and its thermal spike simulations

SINGH, Udai Bhan 1; AVASTHI, D. K. 1*; PANNU, Compesh 1; KHAN, Saif Ahmad 1; AGARWAL, Dinesh Chandra 1; OJHA, Sunil 1

1 Inter-University Accelerator Centre, New Delhi

Thin films have transport properties different from corresponding bulk material. Therefore, a modified thermal spike (TS) calculation should be taken for systematic and thorough investigation to improve the understanding of the mechanism behind electronic sputtering

taking simulation parameters of thin film. When thickness of metallic thin film is equal to or less than the mean free path (MFP) of electron in bulk, the electrical and thermal transport properties are completely changed from that of bulk. Therefore, in present study, a detailed experimental study on electronic sputtering and its thermal spike simulation for Au thin film has been performed under ion irradiation. For this purpose, thin films of different thicknesses (5-200 nm) were deposited on quartz substrates by electron beam evaporation technique. These films were irradiated with 100 MeV Ag ions to a fluence of 1×10^{13} ions/cm². The surface microscopy reveals that the grain size in Au films (5-200nm) varies from 15 ± 2 to 44 ± 3 nm. The RBS spectra of pristine and irradiated thin films show that sputtering yield of Au film from thickness of 5 nm [917 ± 11 atoms/ion] to thickness of 50 nm [171 ± 41 atoms/ion] is higher than that expected for bulk. The large sputtering of Au from thin films is attributed to the enhancement of electron phonon coupling and decrease in thermal conductivity due to reduction in MFP of electron. In an inelastic TS simulation, the variation of thermal conductivity (K) and electron phonon coupling factor (g) have been included to demonstrate the importance of new TS simulation for sputtering in thin film. The new TS simulation with the modified K and g shows higher increase in lattice temperature (up to the sublimation temperature for thin film up to thickness of 50 nm) as compared to previously reported values in bulk Au which is responsible for higher sputtering rate for thinner films.

02 - Sputtering + Desorption

Mo-PA7

Irradiation of nitrogen rich ices by swift heavy ions, clues to the origin of ultracarbonaceous micrometeorites

AUGÉ, Basile 1*; DARTOIS, Emmanuel 1; BODUCH, Philippe 1; DOMARACKA, Alicja 1; ROTHARD, Hermann 1; BRUNETTO, Rosario 1; ENGRAND, Cécile 1; BARDIN, Noémie 1; DELAUCHE, Lucie 1; DUPRAT, Jean 1; SILVA VIGNOLI MUNIZ, Gabriel 1; MEJÍA, Christian 2,1; MARTINEZ, Rafael 3,1

1 CIMAP-GANIL 2 PUC-Rio; 3 UNIFAP, Brazil

Micrometeorites recovered from Antarctica snow are very well preserved interplanetary dust particles. The CONCORDIA collection of Antarctica micrometeorites (AMMs) contains primitive micrometeorites including fine-grained fluffy particles and Ultra Carbonaceous AMMs, hereafter referred as UCAMMs [1]. The UCAMMs exhibit much higher carbon content than other classes of AMMs (typically >50wt%). This carbonaceous compound is a primitive organic material (OM) characterized by extreme D/H ratio up to 30 times the terrestrial reference (SMOW). This OM also contains minerals, including a substantial proportion of crystalline phases [2]. OM also presents large nitrogen concentration up to 10 times higher than observed in OM from meteorites [3]. All together the mineralogical, chemical and isotopic data obtained on UCAMMs indicate that they most probably originate from the surfaces of trans-Neptunian large icy parent bodies, where the temperature stays low enough (<35 K) to retain N₂ ices together with a carbonaceous precursor. They can be processed by energetic cosmic rays over very long time scale (billions of years). We irradiated a mixture of frozen N₂/CH₄ (90:10 and 98:2) at GANIL (Caen, France) [4] with swift heavy ions to simulate cosmic rays in the outer Solar System, representative of the surfaces of trans-Neptunian objects. The structural and chemical evolution was monitored by infrared absorption spectroscopy during irradiation and subsequently during annealing to room temperature [4]. The IR spectra of the residues exhibit striking similarities with that of UCAMMs taken at SOLEIL synchrotron facility [3]. The comparison with an IR spectrum of

HCN indicates an effective production of a HCN-polymer during irradiation. Ex-situ electron microprobe analysis of refractory residues was performed at Camparis. The measured atomic N/C ratios of about 1 confirm the formation of a poly-HCN-like residue.

References

- [1] Duprat, J. et al., 2010. Science 328, 742-745.
- [2] Dobrica, E. et al., 2008. Meteoritics & Planetary Science 43, A38
- [3] Dartois, E. et al., 2013. Icarus 224, 243–252.
- [4] Munoz, G et al., 2014. Astronomy & Astrophysics 566, A93.

Sputtering of Silicon Oxide by Swift Heavy Ions: Dependence on Charge State and Angle of Incidence

BOLSE, Wolfgang 1; WIDMANN, Barbara 1*; ASDI, Mazhar 1

1 Institute for Semiconductor Optics and Functional Interfaces , Stuttgart University

When irradiating a SiO₂ layer on Si with SHI under oblique ion incidence we observed that in the beam-shadow of micron- and sub-micron scaled Si particles on the film surface significantly enhanced sputtering occurs. This effect can be attributed to a transition of the initial (low) charge state of the ion to the (high) equilibrium charge state in matter and the respective increase of the electronic stopping power when passing through the particle. This effect has some importance for 3D-structuring of surfaces and thin films by oblique SHI irradiation. We have therefore investigated the charge state and angle dependence of sputtering and related changes in the surface morphology of thin SiO₂ films, from the very first single ion impacts over partially overlapping tracks up to "high" fluences of 10¹⁴ /cm². Total sputtering yields were determined by measuring the change in film thickness by RBS, while differential sputtering yields as a function of the emission direction of the sputtered particles were determined by catching the sputtered material on arc-shaped C-foils and their subsequent RBS investigation. The modification of the surface morphology was monitored by means of SEM and AFM. At normal ion incidence a big difference of the sputtering yields for low and high ion charges was observed, while only small deviations of the sputtering yields of low and highly charged ions was visible at grazing incidence. The latter indicates charge equilibration in the first few nm of the ion trajectory inside the film. In fact, at grazing incidence open surface tracks (from which the material is removed by sputtering) of up to 100 nm length became visible along the beam direction, which is by far long enough for charge equilibration. From the length of these tracks we can further conclude that sputtering only occurs within a surface layer of typically 5 nm thickness. Detailed results and conclusions will be presented in the report.

Experimental measurements of sputtering yield for pure metal Mo, W and ternary TiNbN compound by RBS method

KISLITSIN, Sergey 1*; GORLACHEV, Igor 1; IVANOV, Igor 1; ZDOROVETS, Maxim 1

1 Radiation Solid State Physics Department

Experimental measurements of the sputtering yield (Ks) are a subject of attention of researchers during long time, and for Ks measurement various methods and equipment are used [1]. We have selected following procedure for experimental measurements of Ks. The sputtered layer thickness was measured by means of Rutherford backscattering (RBS) method. For experiments the samples representing 20 mm × 20 mm substrates from aluminum with Mo (W) coating, deposited by the magnetron sputtering were prepared. This was done to increase the accuracy of determining the thickness of the sputtered layer by RBS method as the atomic weight of the materials of substrate (Al) and coating (Mo, W) are significantly different. Respectively RBS spectra of backscattered ions from substrate and coating well splits up and coating thickness is possible to measure with rather high accuracy. In case of ternary TiNbN compound the two-layer samples – stainless steel substrate with TiNbN layer deposited by the magnetron sputtering from two magnetrons with cathodes from Ti and Nb were prepared for experiments. Sputtering of the surface was carried out by heavy ions ($^{40}\text{Ar}^{5+}$ for Mo, W and $^4\text{He}^{2+}$, $^{84}\text{Kr}^{14+}$, $^{132}\text{Xe}^{18+}$ for TiNbN) on low-energy channel of the heavy ions cyclotron DC-60 of Astana branch of INP. Energy of bombarding particles constitutes 20 keV per charge, ion fluencies was 10^{16} cm^{-2} - 10^{18} cm^{-2} . Sputtered layer thickness was measured by RBS method on proton at the accelerator UKP-2-1 of INP in Almaty and on the nitrogen ions on high energy channel of accelerator DC-6 in Astana. Results of experimental determination of the sputtering yield, changes of surface structure and element composition for TiNbN coating compared with the SRIM calculations and experimental data of other authors [1].

References:

[1] Sputtering by Particle bombardment I. Physical Sputtering of Single-Element Solids. Eds. R. Behrisch, Springer-Verlag 1984: 336

Ethane ices in the outer Solar System: Spectroscopy and Physicochemical Effects

MEJÍA, Christian 1*; DE BARROS, Ana L. F. 2*; DA SILVEIRA, Enio 1; DOMARACKA, Alicja 3; ROTHARD, Hermann 3; BODUCH, Philippe 3

1 PUC-Rio, Brazil; 2 CEFET-RJ, Brazil; 3 CIMAP GANIL, France

The atmosphere of Titan, one of Saturn's moons, is rich in water and hydrocarbon molecules such as ethane (C_2H_6). At low temperature these molecules condensate into ice grains which may be traversed by cosmic rays. The passage of energetic ions through the grain causes ionization which triggers chemical reactions that can be studied in laboratory by

bombarding ice analogues with MeV ion beams. The radiolysis of a C₂H₆:H₂O ice mixture was induced by 40 MeV ⁵⁸Ni¹¹⁺ ion beam delivered by the GANIL accelerator in Caen, France and its chemical evolution monitored by infrared spectroscopy (FTIR) [1]. The sample was prepared by directing a vapor jet towards a CsI substrate at 15 K (thickness: ~ 0.77 µm). Infrared absorption spectroscopy FTIR analysis of ethane, water and molecular products was performed. The ice thickness was thin enough that the projectiles kept a constant velocity close to the equilibrium charge state. The induced C₂H₆ + H₂O reaction produces the daughter species: CH₄, C₂H₄, C₂H₂, C₃H₈, C₄H₈, C₅H₁₀, CO, CO₂, HCOH, CH₂OH, CH₃OH and C₂H₄ (OH)₂. Their formation and dissociation cross sections are determined. The destruction cross section for C₂H₆ obtained is $(2.3 \pm 0.5) \times 10^{-13} \text{ cm}^2$, and that for H₂O is $(3.6 \pm 0.3) \times 10^{-13} \text{ cm}^2$. The carbon, oxygen and hydrogen budget analyses show that the total column density of the atomic species contained in the irradiated mixture is 30 - 50% larger than the sum of the column densities corresponding to the newly formed species. As an astrophysical application, the C₂H₆ + H₂O dissociation cross-sections due to other ion beam projectiles and energies are determined, assuming validity of the sd µ Se3/2 power law. As a consequence, the predicted values of the integrated dissociation rates confirm the importance of nickel and other heavy ion constituents of cosmic rays in astrochemistry.

References:

[1] C. F. Mejía, A. L. F. de Barros, V. Bordalo, E. F. da Silveira, P. Boduch, A. Domaracka, H. Rothard, Monthly Notices of the Royal Astronomical Society , 2013, 433, 2368-2379.

02 - Sputtering + Desorption

Mo-PA11

Time-of-flight SIMS/SNMS of Molecular Samples using swift Heavy Ions

HERDER, Matthias 1*; Wucher, Andreas 1; Meinerzhagen, Florian 1; Breuer, Lars 1

1 University Duisburg-Essen

We report on the application of a new time-of-flight Secondary Ion and Neutral mass spectrometer (TOF-SIMS/SNMS) to the analysis of molecular samples under bombardment with swift heavy ions. In this technique, use is made of the fact that mass spectrometric analysis of the flux of material sputtered from the bombarded surface delivers molecular information in addition to simply stoichiometric element analysis. As a special feature of the system set up at the GSI M-branch beam line, particular emphasis is put on the detection of secondary ions along with their emitted neutral counterparts in order to examine the ionization efficiency of the sputtered material. For that purpose, secondary neutral molecules are detected by means of single photon post-ionization using an intense pulsed VUV laser beam (wavelength 157 nm corresponding to 7.9 eV photon energy) intersecting the plume of sputtered material closely above the bombarded surface. In a series of first test measurements using 4.8 MeV/u Au26+ ions irradiating a number of thin molecular films deposited on a silicon substrate, we show that (quasi-) molecular secondary ions of the type [M+H]⁺ or [M-H]⁻ can be detected along with post-ionized neutral molecules delivering a molecular ion signal of the type [M]⁺, which represent the chemical structure of the

unfragmented target molecule M. In contrast, these signals are either absent or much weaker if the sample is irradiated with a 5 keV Ar⁺ ion beam and the acquired TOF-SIMS/SNMS spectra are clearly dominated by rather unspecific fragment ions.

Depth distribution of Frank loop defects formed in ion-irradiated stainless steel and its dependence on Si addition

CHEN, Dongyue 1*; MURAKAMI, Kenta 1; DOHI, Kenji 2; NISHIDA, Kenji 2; SONEDA, Naoki 2; LI, Zhengcao 3; SEKIMURA, Naoto 1;

1 The University of Tokyo, Department of Nuclear Engineering and Management, Japan; 2 Central Research Institute of Electric Power Industry, Japan; 3 Tsinghua University, School of Materials Science and Engineering, Beijing, China;

Unlike neutron irradiation, displacement damage rate in heavy ion irradiation could differ a lot at different depths, which may result in different microstructure evolution. Such depth distribution of radiation defects needs to be understood, especially when ion-irradiation is used as a tool to simulate material behavior under neutron irradiation. In this work, stainless steel, the structural material applied in light water reactor core, is analyzed for defect depth distribution after 3MeV Fe ion irradiation at 400°C to 3dpa. Si is a typical alloying element in stainless steel and is believed to change point defect diffusivity, so its influence is also studied by using stainless steel model alloys with three different Si contents (~0%, 0.42wt.%, and 0.95wt.% Si).

Transmission electron microscopy (TEM) images show that the major defect formed after irradiation is Frank loop. Loop density reaches maximum at the depth of 800~900nm, and decrease distinctly in near-surface region and beyond 1.1μm depth, which is consist with SRIM calculation. Average size of Frank loop also reaches peak at the same depth, but its change at different depths is much smaller compared to loop density. When Si is added, both loop density and average size are reduced at all depths. Especially for sample with 0.95wt.% Si, loop density is almost zero in near-surface region (200~600nm). This should be attributed to the surface sink effect. In near-surface region, fast-diffusing interstitials are easily trapped by surface sink. Si promotes diffusivity for both interstitials and vacancies, so in high Si sample, interstitial Frank loop can hardly form in near-surface region as surface trapping and recombination are both enhanced by Si. Nano-hardness is tested and correlated with loop formation by the Orowan model. By considering loop depth distribution, α factor is calculated to be around 0.30, which matches α value previously drawn from neutron irradiation.

Temperature-dependent conductive AFM measurements of single conducting ion tracks formed by swift heavy ion irradiation of tetrahedral amorphous carbon

AMANI, Julian Alexander 1*; SCHMIDT, Hendrik 1; KRAUSER, Johann 2; ROTHARD, Hermann 3; KOPPE, Tristan 1; VETTER, Ulrich 1; HOFSSÄSS, Hans 1; DELLA-NEGRA, Serge 4; TRAUTMANN, Christina 5

1 Georg-August-Universität Göttingen; 2 Department of Automation and Computer Sciences, Harz University of Applied Sciences, Wernigerode; 3 CIMAP-Ganil CNRS; 4 Matière Nucléaire, Institut de Physique Nucléaire, Orsay; 5 GSI, Darmstadt;

Passing of a swift heavy ion through a thin film of tetrahedral amorphous carbon, where around 80% of the bonds between carbon atoms are σ -bonds, leaves behind a track with a higher conductivity than the unirradiated matrix and a characteristic nanometer-sized hillock, visible in the surface topography measured with atomic force microscopy (AFM). Up to now, the electrical characteristics of such single ion tracks were studied at room temperature only. Using a conductive atomic force microscope that allows to set and hold different temperatures of the samples while measuring the current-voltage curve of a track allows to look at the temperature-dependent current-voltage curve of single ion tracks for the first time. This enables us to find the characteristic activation energies that dominate the conductivity in the track. The around 80nm thick layer of tetrahedral amorphous carbon was grown on highly-conductive silicon substrates using mass selective ion beam deposition. The tracks were formed by irradiation with 30MeV C^{2+}_{60} fullerenes which leads to very narrow distributions of track conductivities for comparable regions of a sample.

Radiation Damage and Annealing in Graphite: Ways to Improve the Lifetime of Targets

PELLEMOINE, Frederique 1*; BECEIRO NOVO, Saul 2; JAGGI, Vinder 3; KUMAR, Nalin 4; MITTIG, Wolfgang 2; STODEL, Christelle 5;

1 Michigan State University - Facility for Rare Isotope Beams; 2 Michigan State University - National Superconducting Cyclotron Laboratory; 3 Micromatter; 4 UHV Technologies, Inc.; 5 Grand Accélérateur National d'Ions Lourds GANIL

The Facility for Rare Isotope Beams FRIB (USA) under construction at Michigan State University is based on a 400 kW heavy ion accelerator to generate rare isotope beams. In the context of a new generation of high-energy high-intensity heavy ion beam facilities and recent development in the ion source, production targets and stripper foils are a major challenge due to unprecedented power densities. Presently graphite presents the most promising material.

In addition to extreme thermal conditions, continuous irradiation with swift heavy ions will result in radiation damage to the graphite materials, leading to changes in structure and thermo-mechanical properties and limiting target and stripper lifetime. Therefore, durable graphite target and carbon stripper foils are essential for efficient accelerator operations. As part of the development work for the FRIB project, thin carbon foils were irradiated at

different temperature at National Superconducting Cyclotron Laboratory (NSCL) and at Grand Accélérateur National d'Ions Lourds (GANIL) with swift heavy ion beams. In addition, foils produced by making multi-layers of carbon and boron were tested. Annealing was evidenced by two different effects: -Previous studies [1] showed effects of annealing with increasing temperature. Annealing at high temperature was also observed with these strippers. -Development of new multi-layer nano-crystalline thin foil produced by different methods showed a significant improvement in the stripper lifetime. We will present and discuss results from tests performed with graphite and nanostructured carbon foils. The material presented is partially based upon work supported by the U.S. Department of Energy Office of Science under Cooperative Agreement DE-SC0000661, the State of Michigan and Michigan State University and the Small Business Innovation Research – Phase I project “Low Z Thin Films for Stripper Foils, Targets and X-Ray Windows” between National Superconducting Cyclotron Laboratory and UHV Technologies, Inc. under DE-SC0011287.

References:

[1] S. Fernandes et al., Nucl. Instrum. Methods Phys. Res. B 314 (20013) 125-129.

03 - Metals + Carbon-based materials

Mo-PA15

Swift Heavy Ion irradiation induced interface mixing of Co/Sb bilayer thin films

BALA, Manju 1*; AVASTHI, Devesh 1; ASOKAN, K 1; TRIPATHI, T.S. 2; GUPTA, Srashti 1; TRIPATHI, S.K. 3;

1 IUAC; 2 Aalto University; 3 Panjab University;

In the present work, the synthesis of Co-Sb alloys using swift heavy ion beam induced mixing of bilayer Co/Sb system is investigated. Co-Sb alloys are known to be good thermoelectric material in mid temperature range (400-700K). The bilayers of Co (~50 nm)/Sb (~100 nm) thin films were prepared by successive thermal evaporation of Co and Sb respectively over quartz substrate. Mixing of bilayer were studied by (i) annealing in temperature range 200oC to 400oC in the presence of atmosphere of Ar+2%H₂ for 1 hour, and (ii) irradiating with 100 MeV Ag ions with 1×10^{14} ions/cm² fluence and post irradiation annealing in the temperature range 200oC to 400oC in the atmosphere of Ar+2%H₂ for 1 hour. All the samples were characterized by Rutherford Backscattering Spectrometry (RBS) and High Resolution X-ray diffraction (HRXRD). In case of annealed films, mixing of bilayer Co/Sb thin film is observed at 400oC while for high energy post irradiated annealed samples mixing take place at 200oC and at 400oC complete mixing is observed forming CoSb₂ and CoSb₃ phases. Therefore, thermodynamical growth of Co-Sb alloys are modified in irradiated samples at much lower post irradiation annealing temperatures than that observed for just annealed samples. The mechanism governing the formation of Co-Sb alloy in post irradiated annealed samples may be attributed to 'radiation enhanced diffusion'. To study the effect of interface mixing on thermoelectric properties Co-Sb system resistivity and thermopower measurement were also done using four probe and bridge method, respectively. Thermoelectric Power of 100MeV Ag ion irradiated samples annealed at 400oC, was found to be higher than pristine and just annealed samples.

Conducting ion tracks in amorphous carbon generated with swift heavy ions of selected charge state

HOFSÄSS, Hans 1*; TRAUTMANN, Christina 2; KRAUSER, Johann 3; SEVERIN, Daniel 2; BENDER, Markus 2; GUPTA, Srashti 1;

1 Georg-August-Universität Göttingen; 2 GSI, Darmstadt; 3 University of Applied Sciences, Harz, Werningerode;

Tetrahedral amorphous carbon (ta-C) thin films exhibit diamond-like properties, including high hardness and high electrical resistivity. Upon irradiation with swift heavy ions, highly conducting ion tracks are formed. For 1 GeV U irradiation with maximum electronic energy loss in ta-C of about 40 keV/nm, track conductivities of the same sample vary by an order of magnitude due to incomplete track formation. To achieve higher and more uniform conductivities, we performed irradiations with charge state selected swift heavy ions at the M-branch of the GSI. It is expected that ions with highest charge state will produce the highest electronic energy loss. Previously, the effect of charge state selected ion irradiation on conducting ion tracks in ta-C was studied at GANIL using 4.57 MeV/u Pb ions with charge states 53+, 56+ and 60+. Here we present experiments carried out at GSI using 4.77 MeV/u Bi and 4.8 MeV/u Au ions with charge states from 50+ to 61+ and fluences of 5×10^9 - 5×10^{10} ions/cm². 26+ ions from the LINAC were stripped using an Al foil at the beginning of the M-branch beam line. The following defection magnets of the M-branch were then used for charge state selection. We found Gaussian charge state distributions with maximum at 54+ and width of 2-3 charge states. The intensities of 47+ and 60+ beams was 10^7 ions/cm²/s. ta-C film were synthesized on highly conducting Si wafers by mass selected ion beam deposition. After irradiation, ion tracks were identified using atomic force microscopy (AFM) by characteristic hillocks at the surface. Topography and conductivity of ion tracks were measured by conductive AFM measurements. We find that the hillock height increases with increasing charge state from 1.5 nm to 3 nm. Compared to the very low track conductivities for 50+ ions, the track conductivities for 60+ and 61+ ions are about an order of magnitude higher, however, we still observe non-uniform track conductivities for different tracks on the same sample.

Reversibility of heavy-ion-induced deformation of metallic foils

MINAGAWA, Hideaki 1; TSUCHIDA, Hidetsugu 1; ITOH, Akio 1; MURASE, Ryu 1

1 Kyoto University

Swift heavy-ion irradiation of materials causes deformation of materials by electronic and nuclear energy deposition. We have studied deformation phenomena of free-standing metallic foils induced by MeV-energy heavy-ions by a shape measurement method using a laser displacement meter [1]. The deformation appears just like a metal spring under non-irradiation and irradiation conditions. To obtain information about a microstructural change in the reversible deformation, in this work we investigate the lattice constant during foil-

deformation by X-ray diffraction methods. A driving factor of reversible deformation is discussed.

The experiments were conducted using our specially developed apparatus, which enables us to perform in situ X-ray diffraction measurements for targets under ion irradiation. A well-annealed aluminum foil having a purity of 99.999% and a thickness of 3 or 4 μm was used as a target specimen. The target was irradiated by three different projectiles of C, O, and Si ions with MeV energies. Foil-deformation that occurred during irradiation was measured by using X-ray diffractometer. We investigated a change in the diffraction spectra under non-irradiation and irradiation conditions, as a function of beam flux. We considered the following conditions for defining the reversible deformation. In comparison between the diffraction spectra measured under non-irradiation and irradiation, those peak positions, peak intensities, and peak widths accord within experimental errors. It was found that in the reversible deformation phenomena a change in the lattice constant is due to beam heating effects. We will discuss the flux dependence on the reversible deformation in more detail.

[1] H. Tsuchida et al., Phys. Rev. B (2004) 70, 054112.

03 - Metals + Carbon-based materials

Mo-PA18

Phase transition and change in mechanical properties of Ni-based intermetallic compounds induced by energetic ion beam

KOJIMA, Hiroshi 1; YOSHIZAKI, Hiroaki 1; HASHIMOTO, Akihiro 1; KANENO, Yasuyuki 1; HORI, Fuminobu 1; SENBOSHI, Satoshi 2; SAITO, Yuichi 3; ISHIKAWA, Norito 4; OKAMOTO, Yoshihiro 5; IWASE, Akihiro 1

1 Osaka Prefecture University; 2 Tohoku University Materials Research Institute (Kansai Center); 3 Takasaki Advanced Radiation Research Institute, Japan Atomic Energy Agency; 4 Tokai Research and Development Center, Japan Atomic Energy Agency; 5 Quantum Beam Science Center, Japan Atomic Energy Agency

In this presentation, we will show the effect of energetic ion irradiation on the transformation of lattice structures and mechanical properties for several Ni-based intermetallic compounds. Bulk specimens used in the present experiment were Ni-25at%V, Ni-25at%Al, Ni-25at%Nb and Ni-50at%Al alloys. They were irradiated with 4-200 MeV heavy ions at room temperature. After the irradiation, the lattice structures of the specimens were investigated by using an X-ray diffraction measurement (XRD). The local atomic arrangements around selective atoms (V and Nb) were examined by means of EXAFS at a synchrotron facility. The change in surface hardness was measured by Vickers hardness tester. The microstructure observation was carried out by means of transmission electron microscope (TEM). The thermal annealing effect was also investigated after the irradiation. Ni_3V , Ni_3Al and Ni_3Nb intermetallic compounds show D022, L12 and D0a lattice structures at room temperature, respectively. In the ion-irradiated Ni_3V , we observed the disordered A1 structure which is intrinsically the high temperature structure in the phase diagram. In the ion-irradiated Ni_3Al , we also observed the A1 structure which is not found in the thermal-equilibrium phase diagram. In the ion-irradiated Ni_3Nb , we observed the amorphous state. The hardness of Ni_3V and Ni_3Al were decreased by the ion irradiation. On the other hand, the hardness of Ni_3Nb was increased. In the symposium, the ion beam induced phase transition will be discussed in terms of collective atomic displacements such as elastic thermal spike and sequential replacements of atoms. The recoveries of the irradiation-

induced lattice structures and the mechanical properties by the thermal treatments will also be discussed.

Effects of ion irradiation on optical property of silicon films

ZHU, Yabin 1; YAO, Cunfeng 1; SUN, Jianrong 1; WANG, Zhiguang 1

1 Institute of Modern Physics, Chinese Academy of Sciences

As one of the most important semiconductor materials, silicon films have been considered as the most promising candidates for the fabrication of large area and low cost solar cells. Since the optical property of silicon films has great effects on the performance of the solar cells, modification of silicon films on optical property has attracted much attentions. In this work, amorphous and nano-crystalline silicon films have been irradiated at room temperature by Kr and Xe ions with the energies from several to hundreds MeV. The effects of ion irradiation on the optical property of silicon films have been studied. The obtained results show that the optical band-gap decreases at an exponentially rate as ion fluence increases. Combining the analysis of structural results, it has been considered that the irradiation induced reduction in optical band-gap of the samples is related with several aspects, including defect generation, amorphization and hydrogen release of the samples. The defects induced by the irradiation produce the defect energy levels in the forbidden band. These energy levels lead to the broadening of the valence and conduction band tails as well as the decrease of the optical band-gap. The amorphization of the nano-crystalline silicon films weakens the quantum size effect of the nano-sized crystallites and results in the decrease of the optical band-gap. Moreover, comparison of the results of hydrogenated and unhydrogenated silicon films indicates that the hydrogen release results in the decrease of short-range structural order, which also plays an important role on the reduction in optical band-gap.

Self-assembling of nanovoids in irradiated strained Sn nanodots

GAIDUK, Peter 1; SKURATOV, Vladimir 2; NYLANDSTED LARSEN, Arne 3

1 Belarusian State University; 2 FLNR JINR; 3 Aarhus University, Denmark

Self-assembling of nanovoids in thin strained layers and dots is interesting for both fundamental and practical reasons ranging from physical and technical to medical applications. Evolution of point defects and dopants in strained layers is important for defect engineering and controllable phase transformation in low-dimensional structures as well. In

this talk we will briefly review own studies of vacancy accumulation into self-assembled voids and cavities in Si/SiGe and Si/SiSn- heterostructures. An impact of slow light (He, 30 – 250 keV) and swift heavy (Xe, 167 MeV) ions at different irradiation temperatures (RT to 400 °C) will be compared in terms of point defect generation, diffusion and evolution. Self-assembling of spherically shaped voids in nanometer size strained Sn precipitates after ion irradiation in different conditions will be reported. The concept of void formation will be discussed which utilize the ability of compressively strained Si/SiGe and Si/SiSn layers to collect vacancies, initially produced in the trails of swift heavy ions. Possible practical implementations of void-containing structures will be discussed. A special attention will be devoted to formation of plasmonic core-shell structures to enhance the efficiency of light absorption in Si layers and devices.

04 - Semiconductors

Mo-PA21

Effect of swift heavy ions irradiation at 500 °C on polycrystalline silicon carbide implanted at room temperature

HLATSHWAYO, Thulani 1

1 University of Pretoria

The effect of swift heavy ion (Xe 167 MeV) irradiation on polycrystalline SiC, individually implanted with 360 keV Kr, I and Xe ions at room temperature, was investigated using Raman spectroscopy, Scanning electron microscopy (SEM) and Rutherford Backscattering Spectrometry (RBS). The samples were irradiated with 167 MeV Xe⁺²⁶ ions to fluences of $5 \times 10^{13} \text{ cm}^{-2}$ at 500 °C. Irradiation of the initially amorphised layer (due to the implantation of the 360 keV ions) caused recrystallization. More recrystallization took place on I implanted samples as compared to Kr and Xe implanted samples. Annealing at 500 °C caused more recrystallisation as compared to swift heavy ions irradiation at 500 °C for all the samples. No diffusion of the implanted fission product elements was observed on both annealed and irradiated samples.

04 - Semiconductors

Mo-PA22

Investigation on the Dielectric response of NdMnO₃/LSAT thin films: Effect of 200 MeV Ag⁺¹⁵ ion irradiation

KUBERKAR, DEELIP 1; UDESHI, Malay 1; VYAS, Brinda 1; TRIVEDI, Priyanka 1; KATBA, Savan 1; SOLANKI, P.S. 1; SHAH, N.A. 1; RAVALIA, Ashish 2; ASOKAN, K. 3; OJHA, Sunil 3

1 Department of Physics, Saurashtra University, Rajkot, India; 2 Shantilal Shah College of Engineering Bhavnagar Gujarat India; 3 Inter University Accelerator Center, New Delhi, India

We report the results of the 200 MeV Ag⁺¹⁵ ion irradiation on the modifications in structural and dielectric behavior of PLD grown NdMnO₃ (NMO) manganite thin films on (100) single crystalline (LaAlO₃)_{0.3} (Sr₂AlTaO₆)_{0.7} (LSAT) substrate. Irradiation of films with different ion

fluences (5×10^{10} , 5×10^{11} , 5×10^{12} ions/cm²) results in modifying the structure and dielectric response of the films. Structural strain was quantified using XRD while Rutherford backscattering (RBS) measurements were performed on pristine NMO film to conform the elemental composition, thickness and oxygen content. Dielectric measurements performed on all the irradiated NMO/LSAT films show that dielectric constant decreases with increase in fluence which has been correlated with the irradiation induced increase in strain at the interface and oxygen vacancies. Various models have been used to fit the data for understanding the relaxation behavior of irradiated films.

The resistance anisotropic of high energy Ne ion deposition on 6H-SiC crystals

GOU, Jie 1; ZHANG, Chonghong 1

1 Institute of Modern Physics, Chinese Academy of Sciences

In the present work, the Ne ion irradiation induced the resistivity anisotropy of the 6H-SiC is published. A Ni/Mo/Au electrode was prepared on the 6H-SiC specimen before irradiation. The 6H-SiC was irradiated by the 196 MeV Ne ion in different fluences with a reducing energy installation at liquid nitrogen cooled temperature. The resistivity of the pristine 6H-SiC is 0.02~0.2 $\Omega \cdot \text{cm}$. The irradiation of 196 MeV $^{20}\text{Ne}^{9.5+}$ (9.8 MeV/u) ions was performed in a terminal chamber of the Sector-focused cyclotron (SFC) in the National Laboratory of Heavy-ion Accelerators in Lanzhou. Fluences of ions were in the range of 1×10^{12} ions/cm² to 1×10^{15} ions/cm². This experiment minimized the temperature effects of the disorder accumulation and achieved a relative uniform distribution region for the Ne ion implantation and damage. The currents at different fluences tested at 1V in different directions were published and the ratio of the two currents along two directions was also calculated. One direction is along the opposite angles and the other is along the opposite sides. The resistivity increases with the fluence and increases sharply when the fluence reached 1×10^{14} ions/cm². The resistivity increases with the fluence more quickly along the direction of opposite angle than that along the direction of opposite side. The ratio of the two currents reaches the biggest (50.3) when fluence reached 1×10^{14} ions/cm² and decreases (12.8) when the fluence reached 1×10^{15} ions/cm². It means the implantation of the Ne ion in SiC induced the resistance anisotropy of the SiC material, and the extent of the anisotropy of the Ne ion reached maximum value when the fluence reached 1×10^{14} ions/cm². From the figure showed below, we can get that the irradiation introduce the resistance anisotropy in the 6H-SiC specimen. It may be related to the anisotropy of disorder.

In situ Raman measurements of Calcite and Malachite during the irradiation with swift heavy ions

DEDERA, Sebastian 1; GLASMACHER, Ulrich A. 1; BURCHARD, Michael 1; SEVERIN, Daniel 2; TRAUTMANN, Christina 2

1 University of Heidelberg; 2 GSI, Darmstadt

Raman spectroscopy is widely used in geosciences and materials research to characterize radiation damage caused by accelerated heavy ions or by fission fragments from natural radioactive decay processes. Ion beam induced modifications are typically analysed long after the irradiation and outside of the irradiation chamber. To study the evolution of the material change with increasing fluence, the irradiation of a series of sample with swift heavy ions was necessary in the past. Here we present a project designed to monitor online and in-situ Raman spectra prior, during, and shortly after ion irradiation. This approach has the advantage that the same sample location is analyzed for all fluences and thus a fluence series becomes independent of sample inhomogeneities and crystallographic orientation effects. A confocal Raman spectroscopic setup was developed and installed at the experimental irradiation chamber of the M3-beamline (UNILAC, GSI, Darmstadt). The system was tested by irradiating trigonal calcite (CaCO_3) with 4.8 MeV/u Au ions, (2 Hz, 1.2 ms pulse length) and monoclinic malachite ($\text{Cu}_2(\text{CO}_3)(\text{OH})_2$) with 4.8 MeV/u Xe ions (5 Hz, 1.2 ms pulse length). The in-situ recorded Raman spectra indicate an increase of defect bands with increasing fluence and a significant change in amplitude and shape of the malachite Raman bands. We demonstrate that the new confocal Raman system is a powerful tool, to investigate changes of matter prior, during, and shortly after irradiation with swift heavy ions.

Formation of dislocations along tracks of swift heavy ions in LiF crystals

ZABELS, Roberts 1; MANIKA, Ilze 1; SCHWARTZ, Kurt 2; MANIKS, Janis 1; GRANTS, Rolands 1; TAMANIS, Edmunds 3

1 University of Latvia, Institute of Solid State Physics; 2 GSI Helmholtzzentrum für Schwerionenforschung Darmstadt; 3 Daugavpils University

As extension of our recent investigation [1], dislocation structures in LiF crystals created by irradiation with GeV-energy Bi, U and Au ions, which produce complex tracks exhibiting core damage have been studied. Chemical etching combined with AFM, High resolution XRD and nanoindentation have been used as investigation methods. Irradiations were performed at normal and oblique incidences of the ion beam (from 90 deg to 30 deg in respect to the

irradiated surface) at fluences ranging $10^9 - 10^{12}$ ions/cm² ensuring formation of separate as well as overlapping tracks. For all investigated ion species and beam incidence angles results show rows of dislocation loops along individual ion tracks. Formation of interstitial type prismatic dislocations is suggested. At the stage of track overlapping the density of ion-induced dislocations increases and their structure becomes self-ordered due to interaction of the stress fields of dislocations and tracks. At fluences $>10^{12}$ ions/cm² the high resolution XRD indicates the presence of a mosaic-type nanostructure with low angle boundaries between domains. Both, the dislocation-rich structure and mosaic-type nanostructure exhibit substantial hardening that confirms accumulation of ion-induced dislocations. In summary, the results allow us to conclude that creation of dislocations along ion path is an essential feature of the track damage.

References

[1] R. Zabels, I. Manika, K. Schwartz, J. Maniks, R. Grants, Nucl. Inst. Meth.B 326 (2014) 318-321

The work has been supported by ESF project Nr.:
2013/0015/1DP/1.1.1.2.0/13/APIA/VIAA/010

Non-destructive visualization of ion tracks in colored calcites (CaCO₃) by Raman spectroscopy

SCHÖPPNER, Nicole ¹; GLASMACHER, Ulrich A. ¹; TRAUTMANN, Christina ²;
BURCHARD, Michael ¹

¹ Institut für Geowissenschaften, Universität Heidelberg; ² GSI, Darmstadt

Calcite bearing sedimentary rocks host large oil and natural gas deposits in the world. To understand the formation of the oil and gas deposits, the formation and temperature history of calcite cements is of high importance. Calcite has uranium concentrations in the range of < 120 µg/g. Therefore, a possible technique to date the formation and temperature history of calcite would be the quantitative analysis of fission tracks. Natural fissioning of ²³⁸U causes the accumulation of fission tracks with time. The determination of the ²³⁸U content and the volume density of fission tracks in calcite would allow calculating a thermochronological age. To quantify the amount of fission tracks in calcite etching and counting the etch pits by optical microscopy is presently common practice. However, non-destructive techniques such as Raman spectroscopy would allow the determination of higher track densities than those accessible by track etching. To test this approach, we exposed calcite samples to swift heavy ions under controlled irradiation conditions. Six different colored calcites (CaCO₃) were irradiated with fluences between $1 \cdot 10^6$ and $2 \cdot 10^{12}$ ²⁰⁹Bi-ions/cm² at the UNILAC (GSI, Darmstadt). Raman measurements were performed before and after the irradiation. The spectra of the investigated samples show decreasing Raman band intensities with

increasing fluences. New bands are identified at wave number 430 cm^{-1} and 860 cm^{-1} . The appearance of these bands occurs at different fluences, depending on the color of the calcite. We assume that the bands are assigned to the Ca-CO vibrational mode, which suggests that the irradiation with ions liberates O_2 from the crystal lattice. The spectra of all yellow calcites show an extraordinary band at $\sim 1017\text{ cm}^{-1}$ regardless of applied fluence. We assume that the band is related to the ν_1 (SO_4) vibrational mode because chemical analysis of the yellow calcite indicates a content of 0.38 wt. % of sulfur.

Ion induced nanostructures by swift heavy ion irradiation under grazing incidence

GRUBER, Elisabeth 1*; LATTOUF, Elie 2; BERGEN, Lorenz 1; LEBIUS, Henning 2; GRYGIEL, Clara 3; WANG, Yuyu 4; BENYAGHUB, Abdenacer 2; LEVAVASSEUR, Delphine 2; RANGAMA, Jimmy 2; OCHEDOWSKI, Oliver 5; BAN D'ETAT, Brigitte 2; SCHLEBERGER, Marika 5; AUMAYR, Friedrich 1;

1 Institute of Applied Physics, TU Wien, 1040 Vienna, Austria, EU; 2 CIMAP, Blvd. Henri Becquerel, 14070 Caen Cedex 5, France, EU; 3 CIMAP, Blvd. Henri Becquerel, 14070 Caen Cedex 5, France,; 4 Institute of Applied Physics, TU Wien, 1040 Vienna, Austria, EU; Institute of Modern Physics, Chinese Academy of Sciences, 730000 Lanzhou, China; 5 Experimentelle Physik und CENIDE, Universität Duisburg-Essen, 47048 Duisburg, Germany, EU;

The irradiation of solid targets with swift heavy ions (SHI) can lead to permanent structural modifications in the bulk and at the surface (see [1-3] and refs. therein). In most studies the irradiation is performed under normal incidence with respect to the surface plane. The impact of each individual projectile induces a long, straight nanometric track consisting of amorphous or otherwise modified target material. At the impact site of the ion usually a hillock- or crater-type nanostructure can be observed.

In this contribution we present new experimental results for SHI irradiation under grazing incidence, a geometry which offers new possibilities for the modification of surface and bulk properties on the nanometer scale. This particular collision geometry forces the track formation to a region close to the surface sometimes visible as a chain of individual nanodots, whose length can be controlled by the angle of incidence [1,3]. So far, the formation of these chain-nanostructures have been observed for insulating materials like polymers, oxides and ionic crystals and their formation has been linked to a critical electronic energy loss dE/dx of the incident projectiles [1,3].

By using high resolution atomic force microscopy, comparative studies of the chain formation for different materials, i.e. SrTiO_3 , TiO_2 , CaF_2 and mica, have been performed. These targets have been irradiated with Xe and Pb ions at kinetic energies between 90 and 100 MeV under small grazing incidence angles (0.2° - 2°). Imaged under AFM the track structures observed are strongly material dependent. For mica, e.g. surprisingly “double tracks” seem to be formed which eventually combine to a single track. The experiments were supported by the French-Austrian collaboration SIISU, co-financed by ANR (France) and FWF (Austria).

[1] E. Akcöltekin, et al., Nature Nanotechnology 2, 290 (2007)

[2] N. Khalfaoui, et al., NIMB 240, 819 (2005)

[3] F. Aumayr, et al., J. Phys.: Cond.Mat. 23, 393001 (2011)

Characterization of swift heavy ion induced effects in complex oxides with neutron and synchrotron radiation

SHAMBLIN, Jacob 1; TRACY, Cameron 2; ZHANG, Fuxiang 2; PALOMARES, Raul 1; PERLOV, Brandon 1; TRAUTMANN, Christina 3; EWING, Rodney 4; LANG, Maik 1

1 University of Tennessee; 2 University of Michigan; 3 GSI, Darmstadt; 4 Stanford University

Structural and chemical modifications in complex oxides (e.g., $\text{Dy}_2\text{Ti}_2\text{O}_7$, Dy_2TiO_5 , $\text{Dy}_2\text{Sn}_2\text{O}_7$) induced by high energy ion irradiation were characterized using pair distribution function analysis (PDF) from total neutron scattering experiments at the Nanoscale Ordered Materials Diffractometer (NOMAD) beamline at the Spallation Neutron Source at Oak Ridge National Laboratory. Key to the experimental procedure is the use of GeV ions to produce sufficient sample material irradiated with a near uniform electronic energy loss. Such experiments required a new strategy to facilitate the preparation of ~150 mg homogeneously irradiated powder sample required to conduct neutron characterization experiments. Samples were irradiated at the GSI Helmholtz Center in Darmstadt, Germany at room temperature with swift heavy ions (e.g., Au ions, 2.2 GeV) to fluences up to 8×10^{12} ions/cm². Ion-beam induced structural modifications including defect formation, amorphization and crystalline-to-crystalline phase transformations were studied for the first time in terms of both the average and local sample structure. Unlike X-rays, neutrons scatter strongly from low Z elements, permitting a detailed analysis on both the cation and oxygen-anion sublattices. This information is crucial to better understand sublattice-specific disordering which swift heavy ions induce in many complex oxides. PDF analysis provides data on the local defect structure, including changes in site occupation, coordination, bond distance and bond angle. These results are compared to complimentary synchrotron powder XRD performed at the Advanced Photon Source at Argonne National Laboratory.

TEM and MD study of latent track interference in SHI irradiated Al_2O_3 Latent track interference in SHI irradiated Al_2O_3

O'CONNELL, Jacques 1*; RYMZHANOV, Ruslan 2; SKURATOV, Vladimir 3; VOLKOV, Alexander 4; NEETHLING, Johannes 1;

1 CHRTEM; 2 Joint Institute for Nuclear Research; 3 FLNR JINR; 4 NRC Kurchatov Institute;

Swift heavy Xe and Bi ions were implanted into c oriented Al_2O_3 single crystals to varying fluences. After irradiation, plan view TEM specimens were prepared and imaged. It was noted that the ion track density saturates and tracks range from highly contrasting to barely visible indicating some level of in-situ recovery of the track cores. Through focal series HRTEM images were recorded on a Cs corrected JEOL ARM 200F. The complex electron exit wave was reconstructed from the focal series and geometric phase analysis was

performed on the phase images in order to map residual strain around individual track cores. In addition to the experiments, the material excitation in a SHI track was simulated with the help of classical molecular dynamics. The velocity distribution of the Al and O atoms in proximity to a 167 MeV Xe ion trajectory was obtained from a Monte-Carlo model describing the excitation of the electron subsystem of a target inside SHI tracks. It is demonstrated that the relaxation of the excess lattice energy result in the formation of a cylinder-like disordered region of about 2 nm in diameter.

Modeling of the passage of the second ion in the vicinity of this disordered region revealed that this damaged area can be restored to near-crystalline state. The estimation of a maximal effective distance of recrystallization between the ion trajectories gives the value about 7 nm. This distance corresponds to the maximal density of ion track, that can be observed on the experiment, of approximately $2.0 \times 10^{12} \text{ cm}^{-2}$.

Swift Heavy Ion Irradiation of Silicon Oxynitrides

MOTA-SANTIAGO, Pablo 1*; SCHAURIES, Daniel 1; NADZRI, Allina 1; RIDGWAY, Mark Cameron 1; KLUTH, Patrick 1;

1 Australian National University;

We present direct evidence for the formation of ion tracks in 1-micron-thick silicon oxynitrides of different stoichiometry grown by plasma enhanced chemical vapour deposition. The samples were irradiated with 185 MeV Au^{13+} ions to fluences up to $1 \times 10^{13} \text{ ions/cm}^2$. At such energies, the incident ion interacts predominantly with the system in the electronic regime with approximately constant energy loss throughout the thin layer. The subsequent transfer of energy to the lattice can yield melting along the ion path after which rapid quenching freezes in structural disorder resulting in an ion track [1]. The stoichiometry of the samples was determined using spectral reflectometry and Rutherford backscattering (RBS), the track radius and was measured by means of small angle X-ray scattering (SAXS) and Fourier transform infrared spectroscopy (FTIR).

SAXS measurements reveal a core-shell structure for the ion tracks similar to that previously observed for thermally grown SiO_2 , with a typical radius between 3-6 nm. FTIR measurements demonstrate a modification of the structure of the oxynitrides showing a decrease in N concentration with increasing ion fluence. In the case of Si_3N_4 , we observe a decrease in the SiN absorption peak as a function of the irradiation fluence, a small shift was also observed only at higher fluences, which can be understood as a change in the bond angle.

Such structural modification of amorphous silicon oxynitrides (SiO_xN_y) is reflected in their mechanical and optical properties, increasing their applicability as barrier material in the semiconductor industry or as gradient-index materials for optoelectronic devices, making them also suitable candidates for the synthesis of nanostructures [2].

[1] Kluth, P. et al., Fine Structure in Swift Heavy Ion Tracks in Amorphous SiO_2 , Phys. Rev. Lett. 101 175503 (2008)

[2] Baak, T., Silicon Oxynitride; a material for GRIN optics, Appl. Opt. 21 6 1069 (1982)

Defect Driven Modifications in the Ferroelectric Behavior of BiFeO₃ Films

KUBERKAR, Deelip 1; RAVALIA, Ashish 2*; VAGADIA, Megha 3; TRIVEDI, Priyanka 1; KATBA, Savan 1; ASOKAN, K 4; GAUTAM, S 5; CHAE, K.H. 5;

1 Department of Physics, Saurashtra University, Rajkot – 360 005 (India).; 2 Shantilal Shah Engineering College, Bhavnagar – 364 060 (India) and Department of Physics, Saurashtra University, Rajkot – 360 005 (India).; 3 Tata Institute of Fundamental Research, Homi Bhabha Road, Mumbai – 400 005 (India).; 4 Inter University Accelerator Center, Aruna Asaf Ali Marg, New Delhi – 110 067 (India).; 5 Nano Material Analysis Centre, Korean Institute of Science & Technology, Seoul 136-79 (South Korea).;

In this communication, we report the results of the studies on Swift Heavy Ion (SHI) induced modifications in the polarization of 200nm BiFeO₃ (BFO) multiferroic films grown on SrTi_{0.998}O_{0.002}TiO₃ (SNT0) substrate. BFO/SNT0 films, irradiated with 200MeV Ag⁺15 ions with $5 \cdot 10^{10} - 5 \cdot 10^{12}$ ions/cm² fluencies, were characterized using X-ray diffraction (XRD), atomic force microscopy (AFM), magnetization (M–H), polarization (P–E) and near edge X-ray absorption fine structure (NEXAFS) measurements. Modifications in the ferroelectric polarization of BFO films have been discussed in the light of formation of structural defects and oxygen vacancies due to SHI irradiation. Structural defects induced enhancement in the structural strain and reduction in mobility of charge carriers may lead to the improvement in ferroelectric behaviour of BFO films. In addition, the modifications in local electronic structure have been understood using NEXAFS studies revealing the significant change in spectral feature suggesting its role in the ferroelectric behaviour.

Characterization of Ion Tracks in Oxides using Advanced Scanning Transmission Electron Microscopy

WEBER, William 1*; SACHAN, Ritesh 2; CHISHOLM, Matthew 2; ZHANG, Yanwen 2;

1 The University of Tennessee; 2 Oak Ridge National Laboratory;

The irradiation of complex oxides with swift heavy ions often results in the creation of amorphous ion tracks with complex interfacial structures. We have used state-of-the-art scanning transmission electron microscopy (STEM) techniques to provide detailed characterization of the structure and electronic properties of ion tracks in perovskite and pyrochlore structures. High resolution STEM is used to determine track radii, and we have confirmed the increase in diameter with increasing electronic energy loss along the ion path. High angle annular dark field (HAADF) imaging and annular bright field (ABF) imaging provide details of cation and anion positions, respectively. Using HAADF and ABF imaging, we have mapped the local strain across the core-shell interface structure in Gd₂Ti₂O₇, and investigated the cation and anion disordering across the track core and interfaces in Sm₂Ti₂O₇ and SrTiO₃. Using HAADF imaging, we have characterized the kinetics of electron-beam-induced crystallization of the amorphous track core to the defect-fluorite

structure in Yb₂Ti₂O₇. Using low-loss EELS, we have measured a decrease in optical band gap of the amorphous track core structure relative to the crystalline matrix in LiNbO₃, and measure the change in electronic structure in the amorphous core, across the defect-fluorite core-shell structure, and in the pyrochlore matrix in Gd₂Ti₂O₇. These experimental results can be directly compared to the results from density functional theory and atomistic simulations.

Parameters of 1.2 MeV/amu Latent Xe Ion Tracks in YAlO₃ and Y₃Al₅O₁₂

JANSE VAN VUUREN, Arno 1*; SKURATOV, Vladimir 2; O'CONNELL, Jacques 1;
SAIFULIN, Maxim 2;

1 Nelson Mandela Metropolitan University; 2 Joint Institute for Nuclear Research;

Oxide dispersion strengthened (ODS) steels are novel materials consisting of nano-sized oxide particles dispersed throughout a steel matrix. The oxide particles may consist of oxides having different compositions. However oxide particles containing yttrium have been shown to be more stable at elevated temperatures. ODS steels are expected to have superior radiation resistance, superior strength and good creep resistance due to dislocation pinning. However, there is uncertainty concerning the overall irradiation performance of ODS steels, specifically the effect of radiation on the oxide particles. It is envisioned that ODS steels will be used in both fission and fusion reactors as structural materials in the reactor core and will therefore be subject to large irradiation doses of different types. The radiation stability of these particles is one of the determining factors in the selection of the oxide which is most suitable. The aim of this investigation is to assess the effects of swift heavy ion (SHI) irradiation on the microstructure of single crystalline YAP (Y-Al-perovskite, YAlO₃) and YAG (Y-Al-garnet, Y₃Al₅O₁₂). The samples used in this investigation were irradiated with 167 MeV Xe ions to fluences up to $3 \times 10^{12} \text{ cm}^{-2}$. TEM results show that swift Xe ions produce discontinuous latent tracks in both YAP and YAG. The threshold electronic stopping powers for track formation estimated from ion range measurements are $\sim 8.4 \text{ keV/nm}$ for YAP and $\sim 6.7 \text{ keV/nm}$ for YAG. Selected area diffraction and high resolution TEM indicate that some tracks in YAP are amorphous whereas most tracks in YAG are crystalline with some degree of disorder. The threshold values and track morphology in these materials were assessed within the framework of the thermal spike model and show some notable discrepancies when compared to predicted values.

On the Self-organization of Barium Fluoride Thin Films Surfaces under SHI Irradiation

KUMAR, Manvendra 1; PANDEY, Ratnesh 1*; KHAN, Saif 2; AVASTHI, Devesh 2;
TRIPATHI, Ambuj 2; YADAV, Avinash 3; PANDEY, Avinash 3;

1 University of Allahabad; 2 Inter University Accelerator Centre, New Delhi; 3
Nanotechnology Application Centre, University of Allahabad;

In the present work, we report self-organisation phenomenon in nano-granular barium fluoride thin films deposited on glass substrate due to 100 MeV Au ions irradiation at liquid nitrogen temperature and at a grazing angle incidence of 15°. Cracking of the surface, perpendicular to the beam direction, started at lower fluence and shrinking of the materials is observed at higher fluence. After application of further high fluences up to 3×10^{14} ions/cm², the surface layer was reorganised in 1.25 μm thick and 450 nm high lamellae of the separation distance 2–3 μm and orientation as found for the cracks and normal to the beam direction. With increasing the ion fluence the width of the lamellae structures decreases and the separation between the adjacent structures increases. Energy dispersive X-ray emission (EDAX) coupled with SEM was performed to get the information of the constituents of the lamellae walls. EDAX results showed that the walls are made of Ba and F, while the gaps between the lamellae are showing Si signal. The self-organization phenomenon is explained on the basis of grain rotation during irradiation.

Color center creation in LiF crystals irradiated with heavy ions: dependence on energy loss and fluence

SCHWARTZ, Kurt 1*; SOROKIN, Michael 2

1 GSI Helmholtzzentrum für Schwerionenforschung Darmstadt; 2 National Research Centre
'Kurchatov Institute'

Color center creation in LiF crystals irradiated with ¹²C, ¹⁴N, ⁴⁰Ar, ⁸⁴Kr and ¹³⁰Xe ions (energy: 5 - 225 MeV) was studied as a function of energy loss and fluence (absorbed energy). Irradiation experiments were completed at the cyclotron DC60 in Astana, Kazakhstan. This study focused on high absorbed energies, where the energy per ion exceeds the binding energy [1, 2]. For light ions (¹²C, ¹⁴N) the saturation of single F centers takes place at a higher absorbed energy ($\sim 5 \times 10^{23}$ eV/cm³) as compared with ⁴⁰Ar, ⁸⁴Kr and ¹³⁰Xe ions ($\sim 8 \times 10^{22}$ eV/cm³). The saturation concentration of F centers (NF_{sat} = 2×10^{19} cm⁻³) is for ¹²C and ¹⁴N ions two times larger. After saturation of single F centers, at higher absorbed energies, the concentration of single F- and F_n-centers decreases in LiF for light ions due to the formation of larger aggregates [3]. This is in contrast to heavier ions, for which the single F center concentration remains constant up to absorbed energy of 10^{25} eV/cm³. The properties of F₂ and F₃⁺ centers were studied by means of luminescence

spectroscopy before and after annealing. It was evident that anion vacancies V_{a} play an important role in the formation and transformation of these color centers [4]. Core damage was only observed for irradiation experiments with ^{84}Kr and ^{130}Xe ions. Experimental results were compared to a developed model which takes into account the color center distribution within a single ion track [5].

- [1] N. Itoh, D.M. Duffy, S. Khakshouri, A. M. Stoneham, J.Phys: Condens.Matter.21 (2009) 474205.
- [2] A. Rusakova, M.V. Sorokin, K. Schwartz, A. Dauletbekova, A. Akilbekov, M. Baizhumanov, M. Zdorovets, M. Koloberdin, Nucl. Instr. Meth. B 313 (2013) 21.
- [3] R. Zabels, I. Manika, K. Schwartz, J. Maniks, R. Grants, Nucl. Instr. Meth. B 326 (2014) 318.
- [4] A. Dauletbekova, et. al., Nucl. Instr. Meth. B 295 (2013) 89.
- [5] M. V. Sorokin, et.al., Nucl. Instr. Meth. B 326 (2014) 307.

06 - Optical properties of insulators

Mo-PA36

Color centers and nanostructures in LiF irradiated with 150-MeV Kr ions

DAULETBEKOVA, Alma 1*; SCHWARTZ, Kurt 2; SOROKIN, Michael 3; MANIKS, Janis 4; AKILBEKOV, Abdirash 1; BAIZHUMANOV, Muratbek 1; ASYLBAJEV, Ruslan 1;

1 L.N. Gumilyov Eurasian National University, Astana, Kazakhstan; 2 GSI Helmholtzzentrum für Schwerionenforschung Darmstadt; 3 National Research Centre 'Kurchatov Institute, Moscow, Russia'; 4 Institute of Solid State Physics, University of Latvia, Riga, Latvia;

Swift heavy ions in dielectric materials can produce color centers and aggregates in nanometric vicinities around their trajectories [1]. The damage structure turns out to be different at low fluence (in the single tracks) and at high fluences, where ion tracks overlap. The radiation damage in LiF crystals irradiated with 150-MeV and 50-MeV Kr ions was studied by optical spectroscopy, chemical etching and scanning electron microscopy (SEM) in the fluence range of 3×10^{10} - 10^{14} ions/cm². The irradiations were performed at the cyclotron DC60 (Astana, Kazakhstan) [2, 3].

Irradiation of LiF with MeV krypton ions leads to saturation of the average volume concentration of single F centers at the absorbed energy of $\sim 8 \times 10^{22}$ eV/cm³, and at higher absorbed energy (fluence) up to 10^{25} eV/cm³ the concentration remains constant $\sim 8 \times 10^{18}$ cm⁻³. Such behavior differs from the case of irradiation with light ions (^{12}C , ^{14}N), where the concentration reaches a maximum value, higher than the saturation level for krypton [2, 3]. The ion track morphology was investigated along the ion path using short-term chemical etching and SEM [4]. In the initial part of the ion track, where 140-MeV Kr ions deposit more than 10 keV/nm, a regular structure of dislocation loops was observed, whereas in the deeper layers, where the energy loss is below the threshold, the dislocation loops are unordered, and their density is noticeably lower.

- [1] N. Itoh, D. M. Duffy, S. Khakshouri et al., J. Phys.: Condens. Matter 21 (2009) 474205.
- [2] A. Russakova, M.V. Sorokin, K. Schwartz et al., Nucl. Instr. Meth. B 313 (2013) 21.
- [3] M.V. Sorokin et al., Nucl. Instr. Meth. B 326 (2014) 307.
- [4] J. Maniks, I. Manika, R. Zabels et al., Nucl. Instr. Meth. B 282 (2012) 81.

Track overlapping in LiF crystals: effect of energy loss

SOROKIN, Michael 1*; BENHACINE, Hamdani 2; SCHWARTZ, Kurt 3; DAULETBEKOVA, Alma 4;

1 National Research Centre 'Kurchatov Institute', Moscow, Russia; 2 LRPCSI, University of 20 Août 1955 Skikda, Algeria; 3 GSI Helmholtzzentrum für Schwerionenforschung, Darmstadt, Germany; 4 L.N. Gumilyov Eurasian National University, Astana, Kazakhstan;

Irradiation of lithium fluoride crystals with swift ions leads to accumulation of color centers, depending particularly on the projectile kind and energy. Optical absorption spectroscopy allows quantitative analysis of their average concentrations; however the local distribution of radiation defects around the projectile trajectories remains a subject of modelling.

For all kinds of projectiles one can observe saturation of the F-center concentration with fluence increase, following the growth of the absorption in the wavelength range of 300-700 nm, corresponding to formation of complex centers. However for light ions the saturation can be assigned with ubiquitous growth of the F-center concentration during the manifold track overlapping, which increases the recombination losses and stimulates the aggregation processes as well. Note, that for the light ions the concentration of F centers reaches a maximum and then decreases similarly it would be in the case of uniform irradiation [1, 2]. At the same time, defect haloes of heavy projectiles are almost saturated with F centers within individual tracks, and the average F-center concentration grows close to the exponential distribution of the track overlapping [3, 4].

Consideration of experimental data obtained with various ions from ^{12}C to ^{208}Pb motivated improvement of the defect accumulation model [2] to take into account the recombination processes and provide a seamless description for the wide range of projectile energy losses.

[1] A. Russakova, M.V. Sorokin, K. Schwartz, A. Dauletbekova, A. Akilbekov, M. Baizhumanov, M. Zdorovets, M. Koloberdin, Nucl. Instr. Meth. B 313 (2013) 21.

[2] M.V. Sorokin, K. Schwartz, C. Trautmann, A. Dauletbekova, A.S. El-Said, Nucl. Instr. Meth. B 326 (2014) 307.

[3] P. Thevenard, G. Guiraud, C.H.S. Dupuy, Radiat. Eff. 32 (1977) 83.

[4] K. Schwartz, C. Trautmann, A.S. El-Said, R. Neumann, M. Toulemonde, W. Knolle, Phys. Rev. B 70 (2004) 184104.

Thickness dependence of the evolution of microstructure, surface morphology and optical band gap of NiO thin films under 200 MeV Ag ion irradiation

MALLICK, Pravanjan 1*; KANJILAL, D 2; MISHRA, N.C. 3; PRAKASH, Jai 2; CHOUDHARY, R.J. 4; AVASTHI, D.K. 2;

1 North Orissa University; 2 Inter University Accelerator Center; 3 Utkal University; 4 UGC-DAE Consortium for Scientific Research;

The evolution of microstructure, surface morphology and optical band gap of NiO films of different thicknesses (75, 150 and 300 nm) grown on Si(100) under the impact of 200 MeV Ag ion irradiation is reported. Ion irradiation led to increase of the size of the crystallites for the thinnest film. For thicker films (150 and 300 nm), the crystallite size did not change on irradiation. The evolution of the surface of the films with irradiation also showed thickness dependence behavior. Irradiation smoothen the surface in case of 75 nm thick NiO films, but does not affect the surface roughness in case of thicker films. A detailed power spectral density analysis of the surface features indicated that the surface morphology of the pristine NiO films of all thicknesses is governed by the combined effect of volume diffusion and surface diffusion processes. Irradiation by 200 MeV Ag ions does not affect the surface evolution processes for thicker films, whereas the evolution of the surface morphology of 75 nm thick films under ion irradiation is found to be governed mainly by the surface diffusion processes. The optical band gap also shows similar thickness dependence. Narrowing of the band gap is observed on irradiation of the thinnest film. There was no noticeable change in the band gap of the thicker films on irradiation. Our observation points to the confinement of the thermal spike induced by the 200 MeV Ag ions in thin films of NiO.

Swift heavy ion induced decomposition of AuFe alloy nanoparticles embedded in silica matrix

PANNU, Compesh 1*; SINGH, Udai Bhan 1; SRIVASTAVA, Sanjeev Kumar 2; KABIRAJ, Debdulal 1; AVASTHI, Devesh Kumar 1;

1 Inter University Accelerator Centre, New Delhi; 2 Department of Physics Indian Institute of Technology Kharagpur, India;

In the present work, the stability of Au/Fe alloy nanoparticles embedded in silica matrix is investigated under thermal spike generated by swift heavy ions. Thin films of silica containing Au-Fe alloy nanoparticles were prepared by atom beam cosputtering technique. The contents of Au and Fe, and the thicknesses of nanocomposite thin films, were determined by Rutherford backscattering spectrometry. These films were subjected to 100 MeV Au ions irradiation at different fluences varying from 1×10^{13} ions/cm² to 1×10^{14} ions/cm². X ray diffraction, X ray photoelectron spectroscopy, optical absorption spectroscopy and transmission electron spectroscopy were used to characterize the as deposited and irradiated nanocomposite thin films.

A detailed study of the results suggests the decomposition of alloy nanoparticles and reprecipitation of constituent metals to form individual nanoparticles of elemental Au and Fe. This is further corroborated by the appearance of surface plasmon resonance peak of Au in optical absorption spectra of the irradiated films. The decomposition and reprecipitation of constituent metals after irradiation is explained on the basis of inelastic thermal spike model. It is proposed that a transient temperature rise within the ion track in silica is created for picoseconds and temperature of silica raises above its melting point. The molten silica feeds heat to the alloy nanoparticle and raises the temperature above its melting point. The dissolution of the alloy nanoparticle takes place as a consequence, and the constituent metal atoms diffuse within the ion track resulting in the reprecipitation of individual metal nanoparticles.

Fast luminescence in vacuum ultraviolet in heavy-ion-irradiated α - Al_2O_3

KOSHIMIZU, Masanori 1*; FUJIMOTO, Yutaka 1; ASAI, Keisuke 1; KIMURA, Kazuie 2;

1 Tohoku University; 2 RIKEN;

Dense electronic excitation along the heavy ion trajectory in solids has attracted considerable attention from the viewpoints of basic science of radiation-matter interaction and applications for materials modification. To reveal the relaxation process of the dense electronic excitation and its relation to track formation, extensive research has been performed experimentally and using modeling. Among this research, time-resolved luminescence measurements have been a powerful tool for analyzing the dynamics of the high-density excited states. One of the authors (K.K.) has performed pioneering time-resolved luminescence measurements with a time resolution of less than 100 ps and revealed fast and peculiar scintillation in alkali halides. In this work, we analyzed the time-resolved luminescence of α - Al_2O_3 .

We measured the time-resolved luminescence in the vacuum ultraviolet (VUV) wavelength region using a MgF_2 lens, a VUV monochromator, and an eight-channel photomultiplier tube with a MgF_2 window. The temporal profile of the luminescence was obtained by time-correlated single-photon counting, in which the arrival times of single ions were determined by a multichannel plate-based secondary ion detector. The sample crystal was irradiated in a cryostat with N, Ar, and Xe having an energy of 2.0 MeV/nucleon. We found a luminescence band at approximately 170 nm, which is quite similar to the band ascribed to self-shrunk excitons (SSEs). The initial intensity of the band increased with the excitation density or linear energy transfer. In addition, radiative decay was enhanced at high excitation densities, as in the case of an electron-hole plasma (EHP) in semiconductors. These results indicate that the dense electronic excitation in α - Al_2O_3 is characterized by a fast radiative decay analogous to EHP and a lattice relaxation analogous to SSEs.

Ion Beam Induced Damage in Aliphatic Polymers

HOSSAIN, Umme Habiba 1*; ENSINGER, Wolfgang 2;

1 Technische Universität Darmstadt, Department of Materials Sciences, Materials Analysis, Alarich-Weiss-Str. 2, 64287 Darmstadt, Germany; 2 GSI Helmholtz Centre for Heavy Ion Research, Materials Research, Planckstr.1, 64291 Darmstadt, Germany

The interaction between swift heavy ions and materials, including polymers, is dominated by their inelastic collisions with the target electrons. The intense electronic excitation leads to polymer damage by the formation of ion tracks in which bonds are broken and molecular fragments are formed [1, 2].

In this work, radiation damage of aliphatic polymers induced by highly energetic heavy ions was investigated. Structure changes of the materials produced by ion irradiation were studied as a function of ion fluence and type of polymers. Therefore, polymer foils were irradiated with heavy ions having kinetic energies up to 0.9 GeV (e.g. U and Au) applying fluences ranging from 1×10^9 to 1×10^{12} ions / cm². Structure changes of the polymer foils were characterized by in-situ Fourier-transform-infrared (FT-IR) Spectroscopy and Mass Spectrometry, as well as by Raman spectroscopy. Both bond scission and formation of new bonds is spectroscopically shown. The resulting volatile fragments lead to a considerable mass loss of the polymer. The structural changes resulted in a reduction in the thermal stability of the residual polymer.

[1] Hossain UH, Seidl T, and Ensinger W., Polymer Chemistry 2014;5(3):1001-1012.

[2] Hossain UH, Lima V, Baake O, Severin D, Bender M, and Ensinger W., Nuclear Instruments and Methods in Physics Research Section B: Beam Interactions with Materials and Atoms 2014;326:135-139.

Effect of heavy ion irradiation on optical property of radiation-crosslinked hydroxypropyl cellulose gel containing methacrylate monomers

HIROKI, Akihiro 1*; YAMASHITA, Shinichi 2; KIMURA, Atsushi 3; NAGASAWA, Naotsugu 3; TAGUCHI, Mitsumasa 3;

1 Japan Atomic Energy Agency; 2 The University of Tokyo; 3 JAEA;

Polymer gel dosimeters utilizing radiation-induced polymerization of vinyl monomers are expected as a useful dosimeter for the dose distribution in heavy ion radiotherapy. Dose response of the dosimeters is evaluated by optical analysis as well as magnetic resonance imaging. Recently, we proposed a novel polymer gel dosimeter containing of 2-hydroxyethyl methacrylate (HEMA), nonaethylene glycol dimethacrylate (9G), and tetrakis (hydroxymethyl) phosphonium chloride (THPC) with radiation-crosslinked hydroxypropyl cellulose (HPC) gel, showing linear increase in absorbance with gamma-irradiation. In this work, effects of liner energy transfer (LET) and dose rate on the optical property of the dosimeters irradiated with He, C, Fe ions was investigated. HPC gels prepared by using radiation-crosslinking technique were immersed into aqueous monomer solution comprising

2 wt% HEMA, 3 wt% 9G, and 0.16 wt% THPC. The swollen gels were vacuum-packed to obtain sheet-type polymer gel dosimeters. Heavy ion irradiation was carried out using HIMAC at NIRS. The dosimeters irradiated with He ions (150 MeV/u), C ions (290 MeV/u), and Fe ions (500 MeV/u) were optically analyzed by a UV-Vis spectrophotometer.

The absorbance of the polymer gel dosimeters at 660 nm increased approximately linearly with increasing dose up to 10 Gy. Dose sensitivities estimated from the increment in absorbance per unit dose decreased in order of He, C, Fe ions irradiation. Radiation chemical yield, G value, of OH radical and hydrated electron decreases with LET because of the overlap of spurs. The increase in LET affected the decrease in the number of polymerization initiator, resulting in the reduction of dose response of the dosimeters. At the same total dose, the absorbance of the dosimeters decreased with increasing dose rate in the range of 0.1 to 6.8 Gy/min. This would be due to the decline in the degree of polymerization with increasing termination reaction.

Swift Heavy Ion induced Radiolysis of Adenine

MUNIZ, Gabriel 1*; DOMARACKA, Alicja 1; AUGÉ, Basile 1; MEJIA, Christian 2;
ROTHARD, Hermann 3; PHILIPPE, Boduch 1;

1 CIMAP; 2 PUC-Rio, CIMAP; 3 CIMAP-Ganil CNRS;

Adenine is a purine nucleobase and an integral part of biomolecules of unique importance such as DNA, RNA, FAD, ATP, etc. Several theories claim that possibly adenine or its precursors may have reached the early Earth via comets and meteorites [1]. There is indisputable evidence that comets and meteorites carry organic molecules such as amino acids and nucleobases or their precursors [2]. In the literature, there are studies showing the destruction by or resistance to of adenine in condensed phase by irradiation with UV photons [3], and electrons [4]. Data on alpha particles, protons and heavy ions at low energy exist for gas phase adenine. However, there are no data about the effects of heavy ions at high energy. It is important to note that although only a small part of the galactic cosmic rays (~ 1%) consists of heavy ions at high energy, it has been shown that their effect on the destruction and formation of new molecules cannot be neglected [5].

The aim of this work is to study the irradiation of adenine by heavy ions at high energies, simulating the effects of the corresponding part of galactic cosmic rays. The structural and molecular modifications are monitored via infrared absorption spectroscopy (FTIR). Furthermore, we intend to compare the irradiation of pure adenine and adenine covered with a thin water ice layer. Water is extremely abundant in outer space and furthermore because that molecule contains oxygen. It would enable a formation of more complex organic molecules, which is important to evolutionary biochemistry and astrophysical chemistry.

[1] Cooper et al. Nature 414 (2001)879

[2] Martins et al. Earth and Planetary Science Letters 270 (2008) 130

[3] Peeters et al. The Astrophysical Journal Letters 593 (2003)L129

[4] Evans et al. The Astrophysical Journal 730 (2011)69

[5]. De Barros et al. Monthly Notices of the Royal Astronomical Society 418 (2011)1363

Effect of the initial thickness dependence on the thinning rate of PMMA films induced by ion irradiation

THOMAZ, Raquel 1*; FRIEDRICH, Bárbara 2; GUTIERRES, Leandro 2; TEIXEIRA, Diego 2; PAPALÉO, Ricardo 2;

1 Pontifical Catholic University of Rio Grande do Sul (PUCRS); 2 Pontifical Catholic University of Rio Grande do Sul;

We report on the thickness decrease of poly(methyl methacrylate) thin and ultrathin layers after ion bombardment with 300 keV H⁺, 2 MeV H⁺, 18 MeV Au⁷⁺ and 2.2 GeV Bi^{eq+} ions. Thin films with initial thickness h_0 from 2 up to 200 nm were spun onto Si wafers with a native oxide layer. The thickness of the layers after ion beam irradiation with a fluence Φ , $h(\Phi)$, was measured by scanning force microscope and ellipsometry. For the proton and 18 MeV Au beams, we observe a clear thickness dependent thinning rate of the irradiated polymer films, which becomes progressively slower the smaller the initial thickness. However, for the H⁺ beams the thinning tends to saturate with increasing fluence, what was not observed for the 18 MeV Au beam at least in the fluence range investigated. On the contrary, irradiation with 2.2 GeV Bi ions results in a thickness independent thinning rate down to $h_0 \sim 20$ nm. Such differences are attributed to the different contributions of compaction, outgassing and sputtering to the overall thinning rate for the different types of beams.

Simulation study of radial dose due to the irradiation of a swift heavy ion aiming to advance the treatment planning system for heavy particle cancer therapy

MORIBAYASHI, Kengo 1*

1 Japan Atomic Energy Agency

Aiming to advance the treatment planning system for heavy particle cancer therapy, we have been developing a model for radial dose simulations due to the irradiation of heavy ions [1]. Here, radial dose is the dose due to the irradiation of this ion as a function of distances from the trajectory of this ion (r). The estimation functions of cell survival due to heavy ion irradiation have been has been incorporated into this treatment planning system at GSI and NIRS [2]. For these functions, radial dose is indispensable and two types of radial dose distributions have been available. However, these distributions had been developed without the detailed examinations of phenomena that occur near the trajectory of an incident ion, though this region is important to estimate cell survival. The progress of computers may allow us to execute such detailed examinations through simulations [3] and to obtain radial dose closer to reality [1]. Important features of our model are as follows. After an incident ion enters a target, molecules in this target are ionized and secondary electrons are emitted due to the incident ion impact ionization. For the movement of secondary electrons, we consider electric field formed from these molecular ions. This electric field traps some secondary electrons near the trajectory of this incident ion and these trapped electrons enhance radial dose [1, 3]. We compare radial dose distribution obtained from our simulation with the

conventional distributions and we suggest which conventional ones should be selected according to r and incident ion energies from this comparison. Our simulation model, which has become possible in this century, is the only way to examine phenomena that occur near the trajectory of an incident ion now as far as we know.

[1] K. Moribayashi, Rad. Phys. Chem. 96, 211 (2014)

[2] Y. Kase, et al., Phys. Med. Biol. 53, 37 (2008)

[3] K. Moribayashi, Phys. Rev. A. 84, 012702 (2011), Rad. Phys. Chem. 85, 36 (2013)

08 - Biology + Ion-Therapy

Mo-PA46

Studies of endothelial monolayer formation on irradiated Poly-L-lactide acid with differentiation energy densities.

GARCIA BERMUDEZ, Gerardo 1; ARBEITMAN, Claudia 2*; DEL GROSSO, Mariela 3; IBÁÑEZ, Irene 4; BEHAR, Moni 5

1 Gerencia de Investigación y Aplicaciones, TANDAR-CNEA, Buenos Aires, Argentina; 2 CONICET, Argentina - Gerencia de Investigación y Aplicaciones, TANDAR-CNEA, Buenos Aires, Argentina; 3 CONICET, Argentina - Gerencia de Investigación y Aplicaciones, TANDAR-CNEA, Buenos Aires, Argentina.; 4 CONICET, Argentina; 5 UFRGDS, Porto Alegre, Brazil

In this work we study cell adhesion, proliferation and cell morphology of bovine aortic endothelial cells cultured on poly-L-lactide acid (PLLA) modified by heavy ion irradiation. Previous work [1] compares the results of two beams with about the same stopping power and different ion velocities, therefore with different deposited energy density. They found, that at lower deposited energy density, 20 % increase of cell density and a general better cell morphology. The purpose of the present work is to continue this study and modify the chemically inert PLLA surface with ions with different deposited energy densities. To this end thin films of 50 μm thickness were irradiated with ^{12}C , ^{16}O , ^{28}Si , ^{32}S (2 MeV/amu) and ^{16}O , ^{63}Cu (0.05 up to 0.15 MeV/amu) ion-beams provided by the Tandem (Buenos Aires, Argentina) and Tandemtron (Porto Alegre, Brazil) accelerators, respectively. We analyzed the correlation between the stopping power and energy density, with cell metabolism and monolayer formation.

[1] C. Arbeitman, M. F. del Grosso, M. Behar, G. García Bermúdez. NIM B 314(2013)86-89.

08 - Biology + Ion-Therapy

Mo-PA47

Heavy-ion irradiation effects in aqueous solutions of radical scavengers

NOMURA, Shinji 1*; FURUYA, Ryosuke 1; MIYAHARA, Kento 1; MAJIMA, Takuya 1; TSUCHIDA, Hidetsugu 1; ITOH, Akio 1

1 Kyoto University

Irradiation of aqueous solutions with ionizing radiation produces free radicals via ionization and excitation of water molecules. Investigation of physicochemical processes of the production of free radicals is important for understanding of radiolysis of liquid materials. In

order to understand the role of free radicals in liquids, we performed direct measurements of reaction products emitted from aqueous solutions of radical scavengers by high-energy ion irradiation. We used L-ascorbic acid ($C_6H_8O_6$) that acts as a scavenger of superoxide radicals in liquids. By using a liquid microjet technique, a liquid target of ascorbic acid solution was introduced into a collision chamber in vacuum. The target was irradiated by a microbeam of swift heavy ions (4.0 MeV C^{2+}) produced by a capillary microbeam method. Secondary ions emitted from the liquid surfaces were mass-to-charge analyzed with a time-of-flight spectrometer. For pure water targets, the main secondary ions were hydronium ions and protonated water cluster ions, where the former were produced via ionization of water molecules and the latter was formed by clusterization of water molecules having a nucleus of a hydronium ion. We investigated a variation of these ion yields as a function of the ascorbic acid concentration. It was found that the yields of the hydronium ions decrease with increasing the ascorbic acid concentration, and then increase at above approximately 100 $\mu\text{mol \%}$ concentrations. Similarly, the yields of the protonated water cluster ions decrease with increasing the ascorbic acid concentration, but non-cluster formation was observed at above approximately 100 $\mu\text{mol \%}$ concentrations. This result implies that ascorbic acid molecules act as the prevention against coordination of water molecules to a hydronium ion. In this presentation, we will discuss the influence of radical scavengers in production of secondary ions from aqueous solutions.

Estimation method of micro-beam divergence from glass capillaries for biological use

BERECZKY, Réka Judit 1*; IKEDA, Tokihiro 1; KOBAYASHI, Tomohiro 2; UTSUGI, Megumi 3; IZUMI, Masako 1; HIRANO, Tomonari 4; SAKAI, Yasuhiro 5; ABE, Tomoko 1

1 RIKEN Nishina Center; 2 Atomic Physics Laboratory, RIKEN; 3 Toho University/RIKEN Nishina Center; 4 RIKEN Nishina Center/University of Miyazaki; 5 Toho University

When ions with energy of MeV are transmitted through a tapered glass micro-capillary, the extracted ions can be used as a micro ion beam for cell irradiation. Our purpose is the development of micro-beam irradiation of biological cells. In the case of thinner capillaries, i.e. order of one micron, the divergence of the transmitted beam has been investigated by many groups, but for larger outlet no study has been done yet. We will report about the estimation of the probability of mishitting of neighboring cells by the investigation of the beam divergence inside the glass capillary. These investigations were performed both experimentally and theoretically. In the experiment He ions with the energy of 4.5 MeV were used which were transmitted through capillaries with different outlet diameters of the order of 10 micron. The beam profile of the extracted beam was detected with CR-39. The measured beam profile was compared with simulation, based on energy loss and scatterings. As a result the probability of mishitting and the energy of these ions can be predicted in advance. Further systematic studies will be performed in the near future which will contribute to the development of micro-beam irradiation of biological cells.

Giant stress field induced in a single Ni nanowire by the mechanical strain of an active polymer matrix

MELILLI, Giuseppe 1*; WEGROWE, Jean-Eric 2; CLOCHARD, Marie-Claude 3;

The effects of thermoelastic and piezoelectric strain of an active track-etched b-PVDF polymer matrix on an electrodeposited single-contacted Ni nanowire (NW) are investigated at the nanoscale by measuring the change of magnetization (i.e. using the inverse magnetostriction effect). The magnetization state is measured locally by anisotropic magnetoresistance (AMR). The ferromagnetic NW plays thus the role of a mechanical probe that allows the effects of mechanical strain to be characterized and described qualitatively and quantitatively. The inverse magnetostriction was found to be responsible for a quasi-disappearance of the AMR signal for a variation of the order of $\Delta T \approx 10$ K. In other terms, the variation of the magnetization due to the stress compensates the effect of external magnetic field applied on the NW resistance. The induced stress field in a single Ni NW was found 1000 time higher than the bulk stress field (due to thermal expansion measured on the PVDF). This amplification could be attributed to three nanoscopic effects: (1) a stress mismatch between the Ni NW and the membrane, (2) a non-negligible role of the surface tension on Ni NW Young modulus, and (3) the possibility of non-linear stress-strain law. We investigate here the role of these different contributions using various types of track-etched polymer membranes leading, after electrodeposition, to embedded Ni NWs of different diameters and orientations.

A study of the composition of galactic cosmic rays based on meteorite olivine data

POLUKHINA, Natalia 1; VOLKOV, Alexander 2; SHCHEDRINA, Tatyana 3; STARKOV, Nikolai 3; SOE, Tan Naing 3; VLADYMYROV, Mikhailo 3; BAGULYA, Alexander 3; CHERNYAVSKI, Mikhail 3; GONCHAROVA, Lyudmila 3; GORBUNOV, Sergei 3*; KALININA, Galina 4; KONOVALOVA, Nina 3; OKATEVA, Natalia 3; PAVLOVA, Tatyana 4

1 Lebedev Physical Institute of RAS; 2 GSI, Darmstadt; 3 LPI; 4 Institute of Geochemistry and Analytical Chemistry

Research into galactic cosmic rays (GCR) is one of the main ways to study the charge composition and abundance of nuclei in nature. We report on the results of measuring the parameters of over 9000 relic tracks of GCR with charges greater than 55 detected in crystals of olivine from meteorites with age of 200 and 300 million years. The measurements have been conducted at the Lebedev Physical Institute (LPI) at the PAVICOM fully automated facility using unique software based on a special (etching–searching–measuring–grinding) technique of work with meteorite crystals developed by the LPI and IGAC (Institute of Geochemistry and Analytical Chemistry) authors. Identification of nuclear charges can be possible taking into account the results of irradiation of olivine crystals by swift heavy ions in accelerators. The charges of three detected nuclei have been found to be within the range of $105 < Z < 130$. Regression analysis enables amending the charge of one of these nuclei up

to the value of 119×10^{-6} with the probability of 95%. The minimal lifetime estimated for these nuclei is more than 3000 years. The fact of detecting and identifying such superheavy nuclei in nature supports the existence of theoretically predicted stability islands of nuclei and justifies efforts undertaken for the synthesis of similar nuclei under the Earth conditions.

Heavy ion tracks in fluoropolymer film: Recent developments and future prospects

YAMAKI, Tetsuya 1*; NURYANTHI, Nunung 2; TRAUTMANN, Christina 3; KOSHIKAWA, Hiroshi 1; ASANO, Masaharu 1; SAWADA, Shin-ichi 1; KITAMURA, Akane 1; MAEKAWA, Yasunari 1; VOSS, Kay-Obbe 3; SEVERIN, Daniel 3; SEIDL, Tim 3

1 Japan Atomic Energy Agency; 2 The University of Tokyo; 3 GSI, Darmstadt

Ion-track membranes of the fluoropolymers have been considered for applications to next-generation electro-chemical devices as well as the conventional microporous membranes for filtration. In the recent past, we developed polymer electrolyte membranes for fuel cells by filling the pores in the polyvinylidene fluoride (PVDF)-based ion-track membranes with proton-conductive polymer chains by gamma-ray-induced graft polymerization. The etched pores of a few hundred nanometers or less were preferable for modifying it with the graft chains at as high a density as possible. Thus, there must be an interest in controlling the pore diameter within the nanometer to submicrometer range. Practically, PVDF has been said to be the only fluoropolymer in which ion tracks can be developed by chemical etching. However, the etching condition was too severe to give ion-track membranes endowed with sufficient mechanical strength; there have never been their optimized preparation methods yet. We thus investigated the possibility of varying the beam parameters and applying the effect of a pre-etching treatment for PVDF ion-track membranes with the goal of achieving enhanced track etching for effective control of the pore size and shape. Our activities cover all types of fluoropolymers including PVDF. Compared to PVDF, poly(ethylene tetrafluoroethylene) and a series of perfluoropolymers (such as PTFE, PFA, and FEP) are known to be very stable in highly-concentrated acid or alkaline solutions or at higher temperatures. Although this property might make their ion-track etching very challenging, the ongoing research is expected to allow one to accumulate know-how on methods of chemical etching, which can be generalized for the chemical structures. These will give feedback to a guiding principle for effective ion-track etching in fluoropolymers.

Production of multi-, oligo- and single-pore membranes using continuous ion beam

APEL, Pavel 1,2*; MAMONOVA, Tamara 1; NECHAEV, Alexandr 1; OLEJNICZAK, Katarzyna 1,3; DMITRIEV, Sergey 1; VACIK, J. 4; IVANOV, Oleg 1; LIZUNOV, Nikolay 1

1 Joint Institute for Nuclear Research, Joliot-Curie str. 6, 141980 Dubna, Russia; 2 Dubna International University, Universitetskaya str. 19, 141980 Dubna, Russia; 3 Nicolaus Copernicus University, Gagarina str. 7, 87-100 Torun, Poland; 4 Nuclear Physics Institute ASCR, v.v.i., 25068 Rez, Czech Republic;

Ion track membranes (ITM) have attracted significant interest in the past two decades due to their numerous applications in physical, biological, chemical, biochemical and medical experimental works. A particular feature of ITM technology is the possibility to fabricate samples with a predetermined number of pores, including single-pore membranes [1]. The present report describes the procedure that allowed production of multi-, oligo- and single-pore membranes using a continuous ion beam from the IC-100 cyclotron. The beam was scanned over a set of small diaphragms, from 20 to 1000 μm in diameter. Ions passed through the apertures and impinged two sandwiched polymer foils, with the total thickness close to the ion range in the polymer. The foils were transported across the ion beam at a constant speed. The ratio between the transport speed and the scanning frequency determined the distance between irradiation spots. The beam intensity and the aperture diameters were adjusted such that either several, one or no ions passed through the diaphragms during one half-period of scanning. Poisson statistics was applied to predict the distribution of events in the irradiation spots. After irradiation, the lower foil was separated from the upper one and etched to obtain pores 6-8 μm in diameter. The pores were found using colour chemical reaction between two reagents placed on opposite sides of the foil. Using the obtained pattern as template, the tracks in the upper foil were located. Samples with single or few tracks were cut out and employed to study fine phenomena in ion track nanopores [2].

[1] R. Spohr, C. Zet, B.E. Fischer, H. Kiesewetter, P. Apel, I. Gunko, T. Ohgai, L. Westerberg, Controlled fabrication of ion track nanowires and channels. Nucl. Instrum. Meth. in Phys. Res. B 268 (2010) 676.

[2] P.Y. Apel, P. Ramirez, I.V. Blonskaya, O.L. Orelovitch, B.A. Sartowska, Accurate characterization of track-etched, conical nanopores. Phys. Chem. Chem. Phys. 16 (2014) 15214.

Visualization of ion tracks created by swift heavy ions in Dolomite ((Ca, Mg) CO₃) using etching techniques

KNÖRR, Baldur 1*; DEDERA, Sebastian 1; GLASMACHER, Ulrich A. 1; TRAUTMANN, Christina 2

1 University of Heidelberg; 2 GSI, Darmstadt

Dolomite bearing natural carbonate rocks host a large number of Oil and Gas deposits in the world. To understand the formation of Oil and Gas deposits the formation and temperature history of dolomite is of high importance. Unfortunately, the formation and temperature history of dolomite cannot be dated so far. Dolomite has uranium concentrations in the range of up to 30 ppm. Therefore, a possible technique to date the formation or the temperature history of dolomite would be the fission-track system. Natural fissioning of ²³⁸U causes the accumulation of fission-tracks with time. The determination of the ²³⁸U content and the volume density of fission tracks in dolomite would allow calculating a thermochronological age. To quantify the amount of fission tracks in dolomite etching and counting the etch pits would be one of the possible tools. The important step further is to establish an etching recipe that allows to visualize and count the etch pits by optical microscopy technique. As the ²³⁸U content varies in natural dolomite we chose to create a relative uniform distribution of ion tracks in dolomite by irradiation with swift heavy ions. Dolomite crystals were irradiated at GSI, Darmstadt by ¹⁹⁷Au ions (106 ions/cm²) at the UNILAC. The crystals were covered with a hexagonal mask during irradiation, creating irradiated and non-irradiated areas on the crystal surface. Tested etching agents are lactic acid (C₃H₆O₃) and hydrochloric acid (HCl), the latter showing best results so far. After 150 minutes of exposure to HCl solution (0.001 mol/l, 50°C), roughly triangular etch pits appeared, which are about 8 µm long and 6 µm wide. The amount of etch pits is in good agreement with the applied fluence, showing a high efficiency of the etching process. Each ion track is converted into an etch pit, so track dating of natural dolomite is possible. Etching experiments of dolomite that host artificial ion track with an energy loss similar to fission fragments are in progress.

Synthesis of photocatalytic p- and n-type Cu₂O nanostructures by ion-track technology

MAIJENBURG, Albert Wouter 1*; MOVSESYAN, Liana 1,2; TOIMIL-MOLARES, Maria Eugenia 1; TRAUTMANN, Christina 1; TEN ELSHOF, Johan E. 3

1 GSI Helmholtz Center for Heavy Ion Research, Darmstadt; 2 Technische Universität Darmstadt; 3 University of Twente

Fossil fuels are being depleted rapidly and solar energy conversion is a very promising path to fill the energy gap. For increasing the solar energy conversion efficiency, one-dimensional nanostructures are expected to exhibit high photoactivity due to their large surface-to-volume ratio. In addition, specific physical properties of most semiconductors, such as absorption depth and charge carrier diffusion length, demand the use of one-dimensional nanostructures to improve the transport of photogenerated charge carriers to the nanowire

surface while maintaining a sufficient “film” thickness for optimal photon absorption. For making these one-dimensional nanostructures, polycarbonate ion-track membranes were made using the GSI linear accelerator (UNILAC). The use of ion-track technology in combination with electrodeposition is highly advantageous, because the length and diameter of the desired nanostructures can be tailored during template synthesis. In addition, interconnected nanowire network structures can be made by irradiating the template from different angles. On the search for more efficient photocatalysts and photoelectrodes, we present the development and photocatalytic/photoelectrochemical characterization of several Cu₂O nanowire-based systems: (1) axially segmented p/n-Cu₂O nanowires dispersed in an aqueous solution for autonomous photocatalytic water splitting, and (2) interconnected p-Cu₂O nanowire networks for photoelectrochemical water splitting. In the former configuration, the formation of H₂ gas is demonstrated without the application of an external bias due to the combination of p- and n-type Cu₂O along the nanowire length. In the latter configuration, electrodeposition is performed inside templates with interconnected tilted pores leading to photocathodes consisting of three-dimensional nanowire network structures. By tuning the nanowire density and their dimensions, high mechanical stability and large surface-to-volume ratio can be achieved.

09 - Ion-track technology

Mo-PA55

Facile green route to improve water permeability of PET track etched membranes

ZDOROVETS, Maxim 1*, MASHENTSEVA, Anastassiya 2; GÜVEN, Olgun 3; KOROLKOV, Ilya 2

1 Institute of Nuclear Physics Republic of Kazakhstan, The L.N.Gumilyov Eurasian National University, Astana, Kazakhstan; 2 The L.N.Gumilyov Eurasian National University, Astana, Kazakhstan, Institute of Nuclear Physics, Astana, Kazakhstan; 3 Department of Chemistry, Hacettepe University, Ankara, Turkey

The mechanical strength, good heat and chemical resistance, dimensional stability and optical clarity of poly(ethylene terephthalate) PET, makes it one of the most important polymers for various industrial applications. High hydrophobicity and low functionality of PET however limits its use for certain applications. Track-etched membranes (TeMs) prepared from PET therefore need to be modified to overcome this problem to increase its use from health-care to energy and from electronics to water treatment. Nowadays PET TeMs have been utilized in a great number of specialty applications such as microfluidic devices, fuel cell membranes, biological sensors and in nanocatalysis. Despite all these developments the problem on improvement of hydrophilicity as well as water permeability of PET TeMs remains to be solved. A number of different techniques to improve hydrophilic properties of PET were described in the literature with limitations and restrictions (instability of hydrophilic layers, alterations in the pore size and distribution, etc.) inherent with the technique considered. In our recent publication [1] the effectiveness of H₂O₂/UV based oxidation system as compared to the use of “classical” oxidants was demonstrated. The carboxylic group functionality of the walls of PET TeMs were enriched by successive hydrolysis and oxidation. In this study we present results on application of advanced oxidation systems based on green oxidant - hydrogen peroxide for effective and non-toxic oxidation to improve the wettability and water transport properties of PET TeMs. Finally the water flow tests were carried out and PET TeMs treated with H₂O₂/UV showed improved water permeability parameter by 16% compared with only etched membrane, the same parameter was found to

increase by 21% in the case of Fenton/H₂O₂/Vis treatment. The proposed oxidation technique is very simple, environment friendly and not requiring special equipment or expensive chemicals. The hydrophilic properties of hydrolyzed/oxidized PET TeMs were found to be stable for a long period of time.

[1] Korolkov I. et al. (2014); Polym. Degr. Stab. 107, 150.

09 - Ion-track technology

Mo-PA56

Characterisation and electrodeposition of Bi_{1-x}Sb_x nanowire- networks in etched ion-track membranes for thermoelectric applications

WAGNER, Michael 1-3*; TRAUTMANN, Christina 2,3; TOIMIL-MOLARES, Maria Eugenia 3; VÖLKLEIN, Friedemann 1

1 Institute of Microtechnologies, Hochschule RheinMain, Am Brückweg 26, 65428 Rüsselsheim, Germany; 2 Technische Universität Darmstadt, Petersenstraße 23, 64287 Darmstadt, Germany; 3 Materials Research Department, GSI Helmholtz Centre for Heavy Ion Research, Planckstr. 1, 64291 Darmstadt, Germany

The application of ion-track etched polymer membranes for the electrodeposition of large area thermoelectric nanowire-networks is presented. Membranes with a large number of interconnected nanochannels are fabricated by sequentially irradiating 30 µm thin polycarbonate foils with GeV heavy ions under 45° angles between beam and sample surface, and turning the foils around the foil normal by 90° after each irradiation step. This way the foils are irradiated from four different directions. Subsequent chemical etching in 6M NaOH solution at 50°C selectively dissolves the tilted ion tracks and converts them into open nanochannels. Bi_{1-x}Sb_x nanowire-networks are prepared by filling the interconnected nanochannels by pulsed electrodeposition using an electrolyte based on hydrochloric acid, Bi(III)-, and Sb(III)-chloride and a three electrode setup. Pulsed deposition results in a very homogeneous growth, which is important for future device integration as well as for the mechanical stability of the network after dissolution of the polymer template. The influence of wire diameter and density on the mechanical stability and interconnectivity of the obtained nanowire networks is visualized by scanning electron microscopy. First measurements of the Seebeck coefficient, and electrical- and thermal conductivity of the networks will be discussed.

[1] M. Rauber, I. Alber, S. Müller, R. Neumann, O. Picht, C. Roth, A. Schökel, M. E. Toimil-Molares, and W. Ensinger; Highly-ordered supportless 3-D nanowire networks with tunable complexity and interwire connectivity for device integration; Nano Letters; 2011; 11(6)

[2] F. Völklein, H. Reith, and A. Meier; Measuring methods for the investigation of in-plane and cross-plane thermal conductivity of thin films; physica status solidi (a); 2013; 210(1)

[3] M. Wagner; Fabrication of antimony 3D nanowire-networks for thermoelectric applications; diploma thesis; Technische Universität Darmstadt; 2012

Study of the Ni/Fe nanotubes properties

ZHANBOTIN, Arman 1*; KOZLOVSKIY, Artem 2; KADYRZHANOV, Kairat 2; RUSAKOV, Vyacheslav 3; MANAKOVA, Irina 1; OZERNOY, Alexey 1; ZDOROVETS, Maxim 4

1 Institute of Nuclear Physics, 1 Ibragimov St., Almaty, 050032, Republic of Kazakhstan; 2 L.N. Gumilyov Eurasian National University, 2 Mirzoyana Str., Astana, 010008, Republic of Kazakhstan; 3 Lomonosov Moscow State University, Leninskie Gory, Moscow, 119991, Russian Federation; 4 Institute of Nuclear Physics Republic of Kazakhstan

In recent years, 1D nanostructures are actively studied in the field of nanoscience and technology due to their unique properties, which are different from crystalline powders. There are a lot of methods to obtain nanostructures. This work considers the process of Ni/Fe nanotubes obtaining by template synthesis method; magnetic properties were evaluated by Mössbauer spectroscopy. The track membranes (TM) based on the Hostaphan® type polyethylene-terephthalate (PET) with a pores density $1,0 \cdot 10^9 \text{ cm}^{-2}$ and a diameter $110 \pm 5 \text{ nm}$ were used as templates for Ni/Fe nanotubes template synthesis. The electrolyte composition is $\text{NiSO}_4 \times 7\text{H}_2\text{O}$ (110 g/l), $\text{FeSO}_4 \times 7\text{H}_2\text{O}$ (110 g/l), $\text{NiCl}_2 \times 6\text{H}_2\text{O}$ (5 g/l), H_3BO_3 (25 g/l) $\text{C}_6\text{H}_8\text{O}_6$ (3 g/l). The template synthesis was carried out in a potentiostatic mode at a voltage of 2V at room temperature for 210 seconds. Constant pH = 3 acidity level was controlled by ascorbic acid loading which prevents Fe^{2+} to Fe^{3+} oxidation. The deposition process control was carried out by chronoamperometry using the Agilent 34410A multimeter. According to the X-ray diffraction results, the Fe-Ni doublet was observed: FCC nickel with the lattice parameter of 3,540 Å and BCC iron with a lattice parameter of 2,866 Å. Mössbauer studies were carried out using the MS1104Em spectrometer. The values of hyperfine magnetic field localized in the field range from 280 to 360 kOe. This means that magnetically ordered iron oxides ($\alpha\text{-Fe}_2\text{O}_3$, $\text{g-Fe}_2\text{O}_3$, Fe_3O_4) cannot be detected in the nanotubes composition. In this case, typical local maxima were observed in the hyperfine field distribution $p(\text{Hn})$ due to different local environments of Mössbauer Fe - atom. Formed magnetic domains have sizes close to the nanotubes thickness with their magnetization vector is oriented at an angle of $36.330 \pm 0.9^\circ$ to the axis of the nanotubes. Overall, the research demonstrates promising Ni/Fe nanostructures application in the development of nano-electronics.

Dispersion of heavy ion deposited energy in thin layer electronic devices: experimental evidence and simulation possibilities

RAINE, Melanie 1*; GAILLARDIN, Marc 1; PAILLET, Philippe 1; DUHAMEL, Olivier 1; MARTINEZ, Martial 1; BERNARD, Helene 1

1 CEA, DAM, DIF

When studying heavy ion induced Single-Event Effects (SEE) in electronic devices, the Linear Energy Transfer (LET) is generally used as the main parameter to characterize the incident beam. The sensitivity of a particular device is then determined using an LET threshold criterion for the triggering of a given type of effect. Yet, this average metric does

not reflect the stochastic nature of particle-matter interaction, and the resulting intrinsic dispersion of energy deposited by direct ionization events. With technology scaling, active silicon layers are getting thinner, thus more and more sensitive to the scattering mechanisms of ion-matter interactions. There is then a need to quantify the variability of this deposited energy as a function of active layer thickness and beam characteristics, in order to evaluate its potential impact on SEE device testing. The following issue lies in the possibility to take into account this deposited energy dispersion in simulation studies. While Monte Carlo codes are by definition well suited to address the statistical nature of interaction mechanisms of ions in matter, most of them actually present some limitations when dealing with thin layers of material. They indeed often use simplifications or condensed approaches to optimize the calculations, thus limiting the simulation accuracy for small dimension geometries, and averaging in particular the energy loss dispersions. This could become a crucial issue at the nanometer scale involved in modern devices. This work will first propose to experimentally quantify the amount of these dispersions for advanced devices, with active layers as thin as 10 nm. Geant4 Monte Carlo simulation of deposited energy dispersion will then be presented, exploring the possibilities of recently implemented discrete energy loss models, called MicroElec, in comparison with traditional condensed history approaches.

10 - Others

Mo-PA59

With LIGHT to highest ion beam intensities and shortest ion beam pulses

SCHUMACHER, Dennis 1; ROTH, Markus 2; BLAZEVIC, Abel 1*; BUSOLD, Simon 1; DEPPERT, Oliver 2; BRABETZ, Christian 1; JAHN, Diana 1; BAGNOUD, Vincent 1;

1 GSI, Darmstadt; 2 TU Darmstadt

One objective of the LIGHT collaboration is the generation of short high-intensity ion bunches. Therefore a laser accelerated ion bunch is compressed by an rf cavity. With this technique bunch lengths below 500 ps have been reached in recent experiments.

This short ion pulses can be used for example to heat a target or to investigate energy loss in environments with a fast dynamic behavior. This talk gives an overview over the development of the LIGHT project over the last years and how these short pulses have been generated.

10 - Others

Mo-PA60

In situ ion beam analysis for swift heavy ion track characterisation

KARLUŠIĆ, Marko 1*; ŠANTIĆ, Branko 1; FAZINIĆ, Stjepko 1; SCHLEBERGER, Marika 2; JAKŠIĆ, Milko 1; SIKETIĆ, Zdravko 1; BULJAN, Maja 1

1 Ruđer Bošković Institute, Zagreb, Croatia; 2 Universität Duisburg-Essen, Duisburg, Germany

The damage which is produced when a swift heavy ion passes through solid material is called an ion track. Its cylindrical shape originates from the long range of the penetrating ion while at the same time the ion induced damage remains localized close to the ion trajectory.

Such nanoscale damage can be observed directly by means of TEM and AFM, but there are also number of other techniques that can be used to characterize ion tracks indirectly.

One of the most utilised techniques for indirect measurement of ion tracks is RBS/channelling. However, this ion beam analysis (IBA) technique is not available at large ion accelerator facilities where ion track studies are mostly done. Recent commissioning of the dual ion beam chamber at the RBI, Zagreb opens up an opportunity to study kinetics of ion track formation using in-situ RBS/c.

Ion track formation is accomplished using swift heavy ions delivered by the 6 MV EN Tandem Van de Graaff accelerator, while simultaneously RBS/c measurement is done using proton beams delivered from the 1 MV Tandetron. This approach is especially important for studies close to the ion track formation threshold, where deviations from simple overlap track models are expected.

To accomplish this, a substantial amount of experimental data is needed for reliable analysis (1) and this novel approach provides adequate solution to this challenge.

Another approach for in-situ IBA is to use swift heavy ions for simultaneous material modification and monitoring using ERDA. As shown recently (2) monitoring elemental changes in the sample, ion track characterisation can be accomplished. We present two applications of ERDA: a) monitoring stoichiometry changes during ion track formation in GaN and b) hydrogen loss in amorphous Al_2O_3 thin films.

(1) C. Grygiel et al., Online in-situ X-ray diffraction setup for structural modification studies during swift heavy ion irradiation, Rev. Sci. Instr. 83 (2012) 013902

(2) C. Rotaru et al., Track formation in two amorphous insulators, vitreous silica and diamond like carbon: Experimental observations and description by the inelastic thermal spike model, Nucl. Instr. Meth. B 272 (2012) 9

10 - Others

Mo-PA61

Collisions of ions with charged nanodroplets in liquid metal source

HASANOV, Ilkham*; GURBANOV, Ilgar; AKBAROV, Elchin; NASIBOV, Ilgar

In a mode of charged nanodroplets generation in liquid metal source, fast ions (In, Sn, Au, Ge) are passing through droplets and losing a part of energy at collisions. Generation of nanodroplets is accompanied by excitation of capillary waves on a surface of the liquid emitter that results in high-frequency modulation of an ion current. In experiments droplets with the sizes of 2-20 nanometers and a characteristic specific charge of $5 \cdot 10(4)$ C/kg were registered. Energy spectra of ions were defined by means of the filter of speeds with cross-section static electromagnetic fields. Reduction of energy of ions In^+ in near axis areas of a beam makes 4 % in conditions of the executed measurements. Outside of this area losses of energy are not present, as nanodroplets extend along a beam axis. Penetration depth of the accelerated ions in liquid indium is estimated within the frames of the model of Linhard-Scharff-Schiott considering interaction of ions with nucleus of a target. Presumably, droplets with the sizes about 1 nanometer are intensively generated in an ion source, at collision with which loss of ion energy basically occurs. The part of ions is neutralized at collisions that lead to occurrence of a stream of fast atoms and reduction of a current density in the center of a beam. Similar interaction between components is necessary for considering in ion-beam systems with complex compose where there is a relative movement of the various charged particles.

References.

1. I.Gasanov and I.Gurbanov. Jap. Jour. App. Phys., 47, No 10, 8226 (2008).
2. I.Gasanov and I.Gurbanov. Rev. Sci. Inst., 83 02B906 (2012).

10 - Others

Mo-PA62

Projectile fragment emission in the fragmentation of silicon on carbon and polyethylene targets at 788 A MeV

ZHANG, Dong-Hai 1*; LI, Jun-Sheng 1; KODAIRA, Sadoshi 2; YASUDA, Nakahiro 3

1 Institute of Modern Physics, Shanxi Normal University, China; 2 Radiation Measurement Research Section, National Institute of Radiological Sciences, Japan; 3 The Research Institute of Nuclear Engineering, University of Fukui, Japan

The emission angle and the transverse momentum distributions of projectile fragments (PFs) produced in fragmentation of silicon on carbon and polyethylene targets at 788 A MeV are measured. It is found that the average emission angle and transverse momentum increase with the decrease of the charge of PFs for the same target, and no obvious dependence of angular and transverse distribution on the mass of target nucleus is found for the same PF. The cumulated squared transverse momentum distribution of PF can be well explained by a single Rayleigh distribution. The temperature parameter of PF emission source do not depend on the size of PF and mass of target for PF with charge $5 < Z < 14$.

11 - Simulations

Mo-PA63

Phase Field Modeling of Irradiation Damage

SCHLÜTER, Alexander 1*; KUHN, Charlotte 1; MÜLLER, Ralf 1; TOMUT, Marilena 2; TRAUTMANN, Christina 2

1 TU Kaiserslautern; 2 GSI, Darmstadt

Intense high-energy particle beams hitting a solid almost instantaneously deposit a large amount of energy in the irradiated material. This causes thermal expansion and consequently elastic waves spreading in the body, which may even cause disastrously macroscopic fracturing. The intention of the phase field model presented in this talk is to predict and analyze this type of structural failure. The development of reliable numerical models that can predict such failure mechanisms is of primary interest for high-power accelerator facilities.

The model regards the irradiated body as a linear elastic solid and neglects effects like phase transitions, i.e. melting, vaporization or ionization. The thermo-mechanical behavior is described by means of the displacement and temperature fields. An additional scalar phase field variable is introduced in order to represent cracks in a regularized way. The core of the model is an energy functional that includes elastic energy as well as fracture energy. The crack propagation law is then found by applying Hamilton's principle to the fracture problem,

which resembles Griffith's energy criterion of fracture mechanics. Eventually, this approach yields a set of coupled Euler-Lagrange equations that are solved with the finite element method.

The effect of the ion-beam interaction with graphite is modeled by prescribing the induced temperature field, i.e. the thermal strains. Alternatively, mechanical input is used whenever available from experiments or other simulations.

11 - Simulations

Mo-PA64

IMPROVEMENT OF ETACHA TOWARDS LOW VELOCITIES AND MANY ELECTRON IONS

LAMOUR, Emily 1; ROZET, Jean-Pierre 1*; PRIGENT, Christophe 1; TRASSINELLI, Martino 1; VERNHET, Dominique 1; FAINSTEIN, Pablo D. 2; GALASSI, Mariel E. 3; RAMIREZ, César A. 3; RIVAROLA, Roberto D. 3

1 Institut des NanoSciences de Paris - UPMC; 2 Centro Atomico Bariloche - CNEA; 3 Instituto de Fisica Rosario – UNR

Ab initio calculations of charge state distributions of fast ions at the exit of solid targets are useful in many circumstances, as in the context of energy loss in matter and for the design, or analysis, of atomic or nuclear physics experiments. The ETACHA code was initially developed to calculate charge state distributions of fast few-electrons ions with at most 28 electrons, and based on the calculation of cross sections for mono-electronic atomic collision processes in the independent electron approximation and at high velocities [1]. However, in the present days, many experiments take place in the intermediate velocity regime, where the stopping power is at maximum and where there is an active research prospective on exotic nuclei, atomic physics and plasma physics for instance. We feel especially concerned with future experiment at SPIRAL2 facility and warm dense matter studies with intense lasers or XFEL. In these cases, previously used Born1 type calculations break down, and more sophisticated theories are needed.

Moreover, more states have to be included. Several improvements have been made, and at present the model allows to deal with ions carrying up to 60 electrons ($n = 4$ shell), and more refined calculations are performed for ionization and excitation cross sections. Comparison with experiment for systems such as 30 MeV/u ^{56}Pb ions in carbon and silicon targets or 0.05 – 0.5 MeV/u C ions in aluminum, shows very good agreement with the new fully ab initio calculations of the ETACHA code. This new code will be available upon request at the time of the conference.

[1] J.P. Rozet, C. Stéphan and D. Vernhet, Nucl.Inst. and Meth. B 107, 67-70 (1996)

Hybrid model of sub-picosecond excitation of solids in nanometric tracks of swift heavy ions

VOLKOV, Alexander 1,2,3*; GORBUNOV, Sergei 3; MEDVEDEV, Nikita 4; RYMZHANOV, Ruslan 5; TEREKHIN, Pavel 1

1 NRC Kurchatov Institute, Kurchatov Sq. 1, 123182, Moscow, Russia; 2 FLNR, JINR, Joliot-Curie 6, 141980 Dubna, Russia; 3 LPI of the Russian Academy of Sciences, Leninskij prospekt, 53, 119991 Moscow, Russia 4 CFEL at DESY, Notkestr. 85, 22607 Hamburg, Germany; 5 FLNR, JINR, Joliot-Curie 6, 141980 Dubna, Russia

A hybrid microscopic model of material excitation (Al_2O_3 , SiO_2 , Si, C, Mg_2SiO_4 , LiF etc) in the nanometric vicinity of a trajectory of a swift heavy ion (SHI tracks, $E > 1$ MeV/amu) consists of three coupled modules. The original Monte Carlo (MC) code TREKIS is used to simulate the kinetics of excited electrons, valence and core holes (~ 10 fs after the ion impact). After finishing of ionization cascades, the data from the MC simulations are used as an input for an approach describing spatial spreading of thermalized electrons and holes (up to ~ 100 fs). A molecular dynamics model (MD) describes lattice excitation due to its interaction with the relaxing electronic ensemble in a track (> 100 fs).

Cross sections used in MC and MD models are based on the Dynamic Structure Factor - Complex Dielectric Function (DSF-CDF) formalism that enables taking into account collective responses of the electronic and atomic subsystems of a target to excitations. This model provides quantitative estimations of the key parameters governing the kinetics of track excitation: temporal evolutions of the radial distributions of generated fast electrons, valence and core holes when electron motion randomizes turning from ballistic to diffusive spreading within 10 to 100 fs, and the rate of energy exchange between the electronic and atomic subsystems for different modes of collective response of the lattice to excitations induced by electrons of different energies. Effects of the energy of valence holes on structure transformations in a SHI track are investigated because the excess energy accumulated in free electrons is not sufficient to initiate these transformations. The initial relaxation of the lattice in a track is also investigated demonstrating thermalization of lattice excitation and an excitation front moving from the ion trajectory. These results give abilities to form the basis of quantitative models of structure transformations in solids irradiated with swift heavy ions.

Elasticity model for the thermal response of ion tracks in quartz

NORDLUND, Kai 1*; AFRA, Boshra 2; KLUTH, Patrick 2

1 University of Helsinki; 2 ANU

We have studied the thermal response of amorphous SiO_2 ion tracks embedded in crystalline quartz (c-SiO_2) by means of small-angle x-ray scattering and a new analytical elasticity model [1]. During in situ annealing between room temperature and 620°C , we observe an irreversible expansion of the track cylinders followed by a reversible contraction. The reversible elastic response of the tracks is analyzed by developing an analytical model based on continuum elasticity theory of an infinitely long cylindrical elastic

inclusion in an infinite elastic medium. The model is implemented using the temperature-dependent elastic properties of bulk amorphous and crystalline SiO₂ for the inclusions and the matrix, respectively. Also the thermal expansion of the amorphous and crystalline material is implemented in the model. The results show excellent agreement between the experimental and calculated track radii, both for the first irreversible and following reversible annealing cycles. A high initial interface pressure between the tracks and the matrix is apparent from the calculations.

[1] B. Afra, K. Nordlund, M. D. Rodriguez, T. Bierschenk, C. Trautmann, S. Mudie and P. Kluth, Phys. Rev. B 90, 224108 (2014)

11 - Simulations

Mo-PA67

Effect of valence holes kinetics on material excitation in tracks of swift heavy ions

RYMZHANOV, Ruslan 1*; MEDVEDEV, Nikita 2; VOLKOV, Alexander 1,3,4

1 FLNR, JINR, Joliot-Curie 6, 141980 Dubna, Russia; 2 CFEL at DESY, Notkestr. 85, 22607 Hamburg, Germany; 3 NRC Kurchatov Institute, Kurchatov Sq. 1, 123182 Moscow, Russia; 4 LPI of the Russian Academy of Sciences, Leninskij prospekt, 53, 119991 Moscow, Russia

A swift heavy ion (SHI) penetrating through a solid target excites the electron subsystem of a material. A considerable part of the excess energy of the electron subsystem is accumulated in valence holes. Spatial redistribution of these valence holes can affect relaxation kinetics of the electron subsystem resulting in ionization of new electrons and energy transfer to the target lattice. A new version of our Monte-Carlo code (TREKIS) is applied to study the effect of holes propagation on the kinetics of the electron subsystem of Al₂O₃ and Si in an SHI track. The cross sections of interaction of charged particles (ion, electrons, holes) with a target are calculated via the complex dielectric function (CDF) formalism, which accounts for peculiarities of collective response of the electron subsystem in SHI tracks to excitation.

The inelastic and elastic mean free paths of holes and electrons in a solid target are calculated. These mean free paths determine the kinetics of holes in the vicinity of the ion trajectory. Heavy holes in Al₂O₃ (mass of 6.2 me) have shorter mean free paths than those of electrons, whereas light holes in Si (mass of 0.35 me) have longer mean free paths resulting in faster propagation of valence holes in silicon vs aluminum dioxide.

The study also demonstrates that the energy deposited by valence holes into the lattice is comparable to the energy transferred by excited electrons. We compare radial distributions of the densities and energies of excited electrons as well as of holes in the valence band at different times to those obtained under the assumption of immobile holes used in earlier works. The comparison demonstrates a significant difference within the track core where the majority of slow electrons and valence holes are located at femtosecond timescales after the ion impact. Far from the track core, where most of the fast electrons are cascading, difference is only minor.

THE ROLE OF THE EFFECTIVE SOLID ANGLE IN THE DETERMINATION OF THE ELECTRON YIELD OF METASTABLE PROJECTILE AUGER STATES

BENIS, Emmanouil 1*; ZOUROS, Theo 2*; DOUKAS, Spiros 1*; MADESIS, Ioannis 2; DIMITRIOU, Anastasios 3; LAOUTARIS, Aggelos 4; PARENTE, Fernando 5; MARTINS, Conceicao 5; MARQUES, Jose Pires 6; INDELICATO, Paul 7; SANTOS, Jose Paulo 5

1 University of Ioannina; 2 Dept. of Physics, Univ. of Crete, P.O Box 2208, GR 71003 Heraklion, Greece 3 Tandem Accelerator Laboratory, INPP, NCSR Demokritos, GR 15310 Ag Paraskevi, Greece; 4 Dept. of Applied Physics, National Technical University of Athens, GR 15780, Zographou, Greece; 5 LIBPhys, Dep. Física, FCT, Universidade NOVA de Lisboa, 2829-516 Caparica, Portugal; 6 BiolSI - Biosystems & Integrative Sciences Institute, Faculdade de Ciências da Universidade de Lisboa, Campo Grande, C8, 1749-016 Lisboa, Portugal; 7 Laboratoire Kastler Brossel, ENS, CNRS, UPMC, Case 74; 4, place Jussieu, 75005 Paris, France;

The $1s2s2p$ 4P metastable state life time formed by single electron capture (EC) in MeV/u He-like-ion - atom collisions is long (10-6-10-9s). In electron measurements, where the spectrometer lies in the direct path of the ion, electrons are measured at 0° to the beam and metastable projectile states Auger decay all along its path towards the spectrometer. Thus, the overall detection solid angle varies with the electron emission position and the determination of the Auger yields is not straightforward. Here, the SIMION electron optics software is used to treat the problem in an effective Monte Carlo simulation that includes τ obtained using the MCDF method. The experimental setup involving a hemispherical deflector analyzer with injection lens and PSD was accurately modeled. Random electron distributions in electron energy and emission angles were used to simulate the metastable Auger decay along the beam path, while the number of electrons was recorded. A systematic study based on the above procedure allowed for the accurate determination of the solid angle correction factor for the 4P decay in excellent agreement with measured electron line shapes of both metastable and prompt Auger projectile states formed by EC in collisions of 25 MeV $F7^+$ with H_2 [1] and 12 MeV $C4^+$ with Ne. These results are important in the accurate evaluation of the 4P/2P ratio of Auger yields [2], whose observed non-statistical production by electron capture into He-like ions awaits further resolution [3].

References

[1] M. Zamkov et al., Phys.Rev.A65, 062706 (2002)

[2] <http://apapes.physics.uoc.gr>

[3] T.J.M. Zouros et al., Phys. Rev. A77, 050701R (2008)

Co-financed by the European Union (European Social Fund—ESF) and Greek national funds through the Operational Program “Education and Lifelong Learning” of the National Strategic Reference Framework (NSRF)—Research Funding Program: THALES. Investing in knowledge society through the European Social Fund (Grant No. MIS 377289).

Extrapolation of the inelastic thermal spike model developed for swift heavy ions to describe surface modifications in CaF₂ induced by highly charged ions.

TOULEMONDE, Marcel 1; DUFOUR, Christian 1*; KHOMORENKOV, Vladimir 1; WANG, Yuyu 2; WANG, Zhiguang 2; AUMAYR, Fritz 3

1 CIMAP, Caen, France; 2 Institute of Modern Physics, Lanzhou, RP China; 3 Institute of Applied Physics, TU Wien, Austria

Potential energy carried by slow highly charged ions (HCI) [1], i.e., the sum of binding energies of all missing electrons, is used to induce surface modification at a nanometric scale. In the continuation of experiments regarding surface modifications on CaF₂ by El-Said et al. [2] using HCI and by Khalfaoui et al. [3] using swift heavy ions (SHI), Wang et al. [4] have shown that there is an experimental linear relationship between the electronic energy loss and the deposited potential energy, leading to an additive interaction of two mechanisms of energy deposition. This relation establishes a link between the fraction (F) of the deposited potential energy and its depth (d) of deposition near the sample surface, $d/F = 4.3$ nm. Such link suggests also that the hillocks induced by slow HCI may be described by models developed to predict material modifications induced by SHI, especially the inelastic thermal spike model [5], recently applied for CaF₂ [6]. Here it is proposed to apply this model to hillock formation by highly charged ion in a three dimensional geometry [6,7] for CaF₂ to quantify the potential energy threshold and the depth of material modifications.

[1] F. Aumayr et al. J. Phys. Cond. Matt. 23, 393001 (2011).

[2] A.S. El-Said, et al., Phys. Rev. Lett. 100, 237601 (2008).

[3] N. Khalfaoui et al. Nucl. Instr. Meth. Nucl. Instr. Meth. B 240, 819 (2005)

[4] Y. Y. Wang et al., in preparation.

[5] M. Toulemonde, et al. Nucl. Instr. Meth. B 277, 28 (2012).

[6] M. Toulemonde et al. Phys. Rev. B 85, 054112 (2012).

[7] Z.G. Wang et al. Nucl. Instr. Meth. B 209, 194 (2003)

[8] C. Dufour et al. J. Phys. :Appl. Phys. 45, 065302 (2012)

Measurement of local temperature around the impact points of fast ions

HAYASHI, Hiroaki 1*; KITAYAMA, Takumi 1; NAKAJIMA, Kaoru 1; NARUMI, Kazumasa 2;
SAITOH, Yuichi 2; MATSUDA, Makoto 3; SATAKA, Masao 3; TSUJIMOTO, Masahiko 4;
TOULEMONDE, Marcel 5; KIMURA, Kenji 1

1 Department of Micro Engineering, Kyoto University; 2 Takasaki Advanced Radiation Research Institute, JAEA; 3 Nuclear Science Research Institute, JAEA; 4 Institute for Integrated Cell-Material Sciences, Kyoto University; 5 Centre Interdisciplinaire de Recherches *Ions Laser (CIRIL)

When a swift heavy ion penetrates through a solid, a narrow trail of damage can be formed along the ion trajectory, which is called an ion track. There are several models proposed to explain the formation of the ion track. Among them, inelastic thermal spike (i-TS) model seems most reasonable because it quantitatively explains the track radius and the threshold stopping power for track formation. According to the i-TS model, ion tracks are formed if the lattice temperature of the thermal spike exceeds the melting point (T_m) of the target solid. Because the processes of track formation occur in a very short time period (T_m) and in a very localized area of nm size, it is difficult to measure the lattice temperature directly.

In this presentation, we present a method to estimate the temperature of thermal spike experimentally by observing the desorption of gold nanoparticles deposited on the target surface. Previous molecular dynamics simulations demonstrated that gold nanoparticles deposited on a target surface are desorbed when they are heated above the (T_m) of gold [1]. By utilizing such a desorption mechanism, the temperature around the impact points is measured. Gold nanoparticles deposited on amorphous silicon nitride and amorphous silicon dioxide films are irradiated with ~MeV C₆₀ and 420 MeV Au ions, and observed using transmission electron microscopy. The ion tracks are clearly seen as bright spots and the gold nanoparticles disappear from a surface area around each ion track. This indicates that the surface temperature of the area was raised above the (T_m) of gold (1338 K) by the irradiation. For comparison, the temperature evolution around the ion track is calculated using the i-TS model. The calculated area, where the temperature exceeds the (T_m) of gold, is roughly in agreement with the observed nanoparticle-cleared area.

[1] C. Anders et al., *Nucl. Instr. and Meth. in Phys. Res. B* 267 (2009) 2503.

POSTERS

Session B

Tuesday, 3:40 – 5:10 pm

* Primary author
Presenting author

Study of the water-to-air stopping power ratio for swift hadron impact

GALASSI, Mariel 1*; TESSARO, Veronica 2; QUIROGA, Flavia 2; MIRANDOLA, Alfredo 3; MAIRANI, Andrea 3; MOLINELLI, Silvia 3; VILCHES-FREIXAS, Gloria 3; CIOCCA, Mario

1 Institute of Physics, Rosario National University; 2 Cordoba National University; 3 National Center of Oncological Hadrontherapy of Italy (CNAO)

In particle therapy, the knowledge of the water-to-air stopping power ratio (STPR) is necessary for accurate ionization chamber dosimetry. According to the protocol provided by the International Atomic Energy Agency, Technical Report TRS-398, the STPR must be determined taking into account the entire particle-energy spectrum at the point of interest. For proton beams, it can be calculated using a semi-empirical law (obtained by fitting the results from a Monte Carlo code) as a particle range function. However, due to the complexity of the particle-energy spectrum for heavier ions, the protocol recommends to take a constant value of 1.13 with an estimated uncertainty of 2%.

In a recent work, a parametrization of the water-to-air stopping power ratio is proposed, but it depends strongly on the ionization potentials of water and air used [1]. Other authors propose an approach based on experimental measurements of water-equivalent thicknesses of air gaps [2].

In the present work, stopping power of antiprotons, protons and carbon ions in liquid water and air are calculated using a distorted-wave model to approximate the ionization cross sections required [4]. Taking into account only the primary particle spectrum (at the entrance channel), the water-to-air STPR can be approximated by the ratio of the stopping powers of water and air. The ratio of theoretical stopping powers as a function of the incident energy is compared with the obtained using the values recommended by ICRU Reports 49 (for protons) and 73 (for carbon ions). Bragg peaks for mono-energetic proton and carbon ion beams, measured at the National Center of Oncological Hadrontherapy of Italy (CNAO), were used to determine the practical range of these particles as a function of the incident energy. These values were employed to obtain the STPR from the semi-empirical laws proposed in the literature and compared with the theoretical results.

[1] A. Lühr et al, Phys. Med. Biol. 56, 2515-2533 (2011).

[2] D. Sánchez-Parcerisa et al, Phys. Med. Biol. 57, 3629-3641 (2012).

[3] M. E. Galassi et al, Phys. Rev. A 62,02270 (2000)

Electron emission in transfer ionization processes for Ne⁸⁺-He collisions

MA, Xinwen 1; ZHANG, Ruitian 1*; FENG, Wentian 1; ZHU, Xiaolong 1; GUO, Dalong 1; GAO, Yong 1;

1 Institute of Modern Physics, Chinese Academy of Sciences
x.ma@impcas.ac.cn

The momentum projecting techniques have been well applied so as to explore the mechanisms of electron emissions as well as the dynamical effects which influence the

momentum distribution of the electrons emitted in ion-atom collisions [1-3]. Usually, the emitted electrons were projected onto the scattering plane, which is defined as the plane containing the initial and the final momentum vectors of the projectile.

It is well known that the ejected electrons are influenced by a combined Coulomb potential from the recoil ions and the projectile ions. Qualitatively, this effect strongly depends on the velocity and the charge state of the projectile. In the present work, we investigate the electron emission in transfer ionization for 80 keV/u Ne^{3+} -He collisions. It is found that electrons are sharply localized around the projectile; this is caused by the projectile charge state effects. Additionally, there are two weak ridges circled around the projectile, which are from auto-ionized decay of doubly excited states of Ne^{6+} ($1s23l3l'$) and Ne^{6+} ($1s23l4l'$) formed via double electron capture processes. The corresponding energies are approximately 47 eV and 85 eV, these are consistent with the theoretical calculations [4].

This work was partially supported by the Major State Basic Research Development Program of China (973 Program, Grant No. 2010CB832902) and by the National Natural Science Foundation of China under Grants Nos. 10979007, 10974207 and 11274317.

References

- [1] R. Dörner, H. Khemliche, M. H. Prior et al., Phys. Rev. Lett. 77 4570 (1996).
- [2] M. A. Abdallah, C. L. Cocke, W. Wolff et al., Phys.Rev.Lett. 81 3627(1998).
- [3] X. Ma, R. T. Zhang, S. F. Zhang et al., Phys. Rev. A 83 052707(2011).
- [4] Z. Chen and C. D. Lin, Phys. Rev. A 48 1298(1993).

01 - Atomic physics + Electronic excitation

Tu-PB3

Forward Secondary Electron Emission from Carbon Foil induced by Swift di-atom cluster ions

KANEKO, Toshiaki 1*; OGAWA, Hidemi 2;

1 Okayama University of Science; 2 Nara Women's University;

Secondary electron (SE) emission from solid surfaces under irradiation of swift ions has been studied intensively as one of important elementary processes [1-3]. Regarding the MeV/atom carbon cluster ion impact, where the low energy electrons are dominantly emitted, the SE yield per atom was known to be suppressed in comparison with single ion incidence at equivalent speed [4-5]. Mechanism of this 'negative cluster effect' is not so clear at present. On the other hand, the energy spectra of SE's with higher energy (e.g. Binary electrons) was observed under MeV/u light ion incidence [6]. In this study, we calculate the energy spectra of the SE's from carbon emitted in the forward direction under swift carbon cluster-ion incidence. The electrons of a target are described in terms of Hartree-Fock wave functions. The calculated SE energy spectra represent the alignment effect, or the orientation dependence of an incident cluster, which is different from those obtained by single ion incidence. This means that investigation of the energy spectra in the forward will show the cluster effect. We also present the energy spectra of randomly-oriented cluster incidence.

References:

- [1] M. Roesler, et al., 'Particle Induced Electron Emission : I', Springer-Verlag (1991).

- [2] D. Hasselkamp, et al., 'Particle induced Electron Emission: II', Springer-Verlag (1991).
- [3] H. Ogawa et al., Nucl.Instr.Meth. B269 (2011) 968
- [4] H. Kudo et al., Vacuum 84, 1014 (2010).
- [5] T. Kaneko et al., J. Phys. Soc. Jpn. 75, 034717 (2006).
- [6] H. Ogawa et al, Nucl. Instr. Meth. B315 (2013) 291.

01 - Atomic physics + Electronic excitation

Tu-PB4

X-ray emission during charging and de-charging of insulators irradiated by swift ions

ROTHARD, Hermann 1*; HAGMANN, Siegbert 2; DE FILIPPO, Enrico 3; VOLANT, Claude 4; LANZANO, Gaetano 3

1 CIMAP-Ganil CNRS; 2 Goethe-Universität Frankfurt (UFfm-IKP)/ GSI-Darmstadt; 3 INFN, Sezione di Catania; 4 DAPNIA/SPhN CEA/Saclay

During irradiation of polymers (Mylar, polypropylene) with swift ion beams, due to secondary electron ejection, the thin insulating foils start charging up until eventually, a sudden de-charging occurs. This phenomenon was studied via the measurement of the slowing down of fast electrons by the time-of-flight (TOF) method at LNS/Catania and at GANIL/Caen [1-3] with several projectiles (C, O, Kr, Ag, Xe; 20-64 MeV/u).

The charge build-up, deduced from convoy- [1,3] and binary encounter [2,3] electron peak shifts, leads to target material dependent potentials (6.0 kV for Mylar, 2.8 kV for polypropylene). The number of projectiles needed for charging up, deduced from the charging-up time constant, is inversely proportional to the electronic energy loss [2,3]. For low beam currents, charging-up time, energy shift corresponding to maximum charge build-up, and time of de-charging are regular. When the beam current is increased, the time intervals become irregular.

Here, we focus on another puzzling finding: The intensity of emitted x-rays during beam-foil interaction is correlated with the charging-up and the sudden de-charging. The X-rays probably stem from the de-excitation of the beam-foil excited projectiles.

References:

- [1] G. Lanzanò, E. De Filippo, S. Hagmann, H. Rothard, C. Volant, Rad. Eff. and Defects in Solids 162 (2007) 303.
- [2] E. De Filippo, G. Lanzano, F. Amorini, G. Cardella, E. Geraci, L. Grassi, E. La Guidara, I. Lombardo, G. Politi, F. Rizzo, P. Russotto, C. Volant, S. Hagmann, H. Rothard, Phys. Rev. A82 (2010) 062901.
- [3] E. De Filippo, G. Lanzano, F. Amorini, E. Geraci, L. Grassi, E. La Guidara, I. Lombardo, G. Politi, F. Rizzo, P. Russotto, C. Volant, S. Hagmann, H. Rothard, Phys. Rev. A83 (2011) 064901

Sputtering analysis of silicates by XY-TOF-SIMS: astrophysical applications

MARTINEZ, Rafael 1*; LANGLINAY, Thomas 2; DOMARACKA, Alicja 2; ROPARS, Frédéric 2; ROTHARD, Hermann 2; PONCIANO, Cassia 3; DA SILVEIRA, Enio 3; PALUMBO, Maria Elisabetta 4; STRAZZULLA, Giovanni 4; BRUCATO, John 5; HIJAZI, Hussein 6; BODUCH, Philippe 2; CASSIMI, Amine 2;

1 UNIFAP, Brazil; 2 CIMAP-Ganil; 3 PUC-Rio; 4 Osservatorio Astrofisico di Catania; 5 Osservatorio Astrofisico di Arcetri, Firenze; 6 Physics Division, Oak Ridge National Laboratory;

Silicates are the dominant material of many objects in the Solar System, e.g. asteroids, the Moon, the planet Mercury and meteorites. Ion bombardment by cosmic rays and solar wind may alter the reflectance spectra of irradiated silicates by inducing physico-chemical changes known as "space weathering". Furthermore, sputtered particles contribute to the composition of the exosphere of planets or moons. Mercury's complex particle environment surrounding the planet is composed by thermal and directional neutral atoms (exosphere) originating via surface release and charge-exchange processes, and by ionized particles originated through photo-ionization and again by surface release processes such as ion induced sputtering. As a laboratory approach to understand the evolution of the silicate surfaces and the Na vapor (as well as, in lower concentration, K and Ca) discovered on the solar facing side of Mercury, we measured sputtering yields, velocity spectra and angular distributions of secondary ions from terrestrial silicate analogs. Experiments were performed using highly charged MeV/u and keV/u ions at GANIL in a new UHV set-up (under well controlled surface conditions) [1]. Other experiments were conducted at the Pontifical Catholic University of Rio de Janeiro (PUC-Rio) by using Cf fission fragments (~ 1 MeV/u). Nepheline, an aluminosilicate containing Na and K, evaporated on Si substrates (wafers) was used as model for silicates present in Solar System objects. Production yields, measured as a function of the projectile fluence, allow to study the possible surface stoichiometry changes during irradiation. In addition, from the energy distributions $N(E)$ of sputtered particles it is possible to estimate the fraction of particles that can escape from the gravitational field of Mercury, and those that fall back to the surface and contribute to populate the atmosphere (exosphere) of the planet.

The CAPES-COFECUB French-Brazilian exchange program, a CNPq postdoctoral grant, and the EU Cost Action "The Chemical Cosmos" supported this work.

References:

[1] H.Hijazi, H. Rothard, et al. Nucl. Instrum. Meth. B269 (2011) 1003-1006

Thickness dependent sputtering and surface enhanced Raman scattering activity of gold thinfilms by 120 MeV Au ion irradiation

MISHRA, Naresh 1*; DASH, Priyadarshini 2; SAHOO, Pratap 3; SOLANKI, Vanaraj 4; SINGH, Uday 5; AVASTHI, Devesh 5;

1 Utkal University, Bhubaneswar, India; 2 U.N. (Auto.) College of Sc. and Tech., Adaspur, Cuttack, India; 3 National Institute of Science Education and Research, Bhubaneswar, India; 4 Institutes of Physics, Bhubaneswar, India; 5 Inter-University Accelerator Centre, New Delhi, India;

Gold thin films of varying thickness (10-100 nm) grown on silica substrates by e-beam evaporation method were irradiated by 120 MeV Au ions at fluences of 3×10^{12} and 1×10^{13} ions cm^{-2} . Irradiation induced modifications of these films were probed by glancing angle X-ray diffraction (GAXRD), atomic force microscopy (AFM), Rutherford Backscattering Spectrometry (RBS) and surface enhanced Raman scattering (SERS). Irradiation didn't affect the structure, the lattice parameter or the crystallite size, but changed the texturing of grains from [111] to [220]. RBS indicated thickness dependent sputtering on irradiation. The sputtering yield was found to linearly decrease with increasing thickness. AFM indicated linear increase of roughness with increasing irradiation fluence for films of all thickness. Power spectral density analysis of AFM images indicated progressive dominance of volume diffusion controlled mass transport over surface diffusion with increasing ion fluence. In agreement with the AFM observation, the gold nanostructures on the surface of 20 nm thick film were found to increase the SERS signal of acridine orange dye attached to these structures. The SERS peaks were amplified by many folds with increasing ion fluence. The effect of 120 MeV Au ion irradiation on the grain texture, surface morphology and SERS activity in addition to the thickness dependent sputtering in gold thin films are explained by the thermal spike model of ion-matter interaction.

Carbon monoxide ice irradiated by swift heavy ions: radiolysis and sputtering

MEJÍA, Christian 1,2*; BODUCH, Philippe 2; LV, Xue Yang 2; DOMARACKA, Alicja 2; ROTHARD, Hermann 2; FROTA DA SILVEIRA, Enio 1;

1 PUC-Rio; 2 CIMAP-CNRS

Pure carbon monoxide ices, deposited from gas phase CO at 15 K on IR transparent CsI windows were bombarded by energetic heavy ions (O, Ne, Ni, Fe, Zn, and Kr) with energies between 0.3 and 15 MeV/nucleon. These projectiles are used to simulate the energy deposited in interstellar CO ices by cosmic rays and the corresponding chemical and physical changes after cosmic radiation–solid–collision. The experiments were performed at the SME and IRRSUD beam lines of the heavy ion accelerator facility GANIL in Caen/France as described in [1].

The column densities of CO molecules and of the synthesized species CnOm were monitored by mid-infrared spectroscopy (FTIR). The CO destruction (σ_d) and CO² formation (σ_f) cross sections were determined and compared with previous experiments.

They show a linear dependence with the quantity of energy deposited by inelastic collision with target electrons, the electronic energy loss (S_e). Additionally, it is confirmed that the sputtering yield (Y_0) exhibits a quadratic dependence on S_e , ($Y_0 \propto S_e^2$) [1,2].

References:

- [1] Seperuelo Duarte, E., Domaracka, A., Boduch, P., Rothard, H., Dartois, E., & Da Silveira, E. F. 2010. Laboratory simulation of heavy-ion cosmic-ray interaction with condensed CO. *Astronomy and Astrophysics*, 512, 71.
 [2] Brown, W., Augustyniak, W., Brody, E., Cooper, B., Lanzerotti, L., Ramirez, A., Evatt, R., & Johnson, R. 1980. Erosion and molecule formation in condensed gas films by electronic energy loss of fast ions. *Nuclear Instruments and Methods*, 170, 321.

02 - Sputtering + Desorption

Tu-PB8

Radiolysis and sputtering of carbon dioxide ice induced by swift Ti, Ni, and Xe ions

MEJÍA, Christian 1, 3*; BENDER, Markus 2; TRAUTMANN, Christina 2; SEVERIN, Daniel 2; BODUCH, Philippe 3; DOMARACKA, Alicja 3; LV, Xue Yang 3; MARTINEZ, Rafael 3; ROTHARD, Hermann 3; BORDALO, Vinicius 4

1 PUC-Rio; 2 GSI, Darmstadt; 3 CIMAP; 4 UNIFAP, Brazil 5 Observatorio Nacional, Rio de Janeiro, Brazil;

Solid carbon dioxide (CO_2) is found in several bodies of the Solar System, the interstellar medium (ISM) and young stellar objects, where it is exposed to cosmic and solar wind radiation [1]. In this work, the chemical and physical changes induced by heavy irradiation of pure solid CO_2 at low temperature ($T=15\text{-}25\text{ K}$) are analyzed. The experiments were performed with Ti (570 MeV) and Xe (630 MeV) ions at the M-branch of GSI/Darmstadt and with Ni ions (46 and 52 MeV) at IRRSUD GANIL/Caen. The evolution of the thin CO_2 ice films (deposited on a CsI window) was monitored by mid-infrared absorption spectroscopy (FTIR) [1]. The dissociation rate of CO_2 , determined from the fluence dependence of the IR absorption peak intensity, is found to be proportional to the electronic stopping power S_e . We also confirm that the yield shows a quadratic increase with electronic stopping power [1,2]. Furthermore, the production rates of daughter molecules such as CO, CO_3 , C_3 and O_3 were analyzed and found to be linear in S_e .

References

- [1] E. Seperuelo Duarte, P. Boduch, H. Rothard, T. Been, E. Dartois, L.S. Farenzena, E.F. da Silveira, *Astronomy & Astrophysics* 502(2009) 599.
 [2] W.L. Brown, W.M. Augustyniak, K.J. Marcantonio, E.H. Simmons, J.W. Boring, R.E. Johnson, C.T. Reimann, *Nucl. Instr. Meth.* B1(1984) 307

Nanoporous Graphene/PET Composites

SCHLEBERGER, Marika 1; OCHEDOWSKI, Oliver 1*; MEYER, Jens 1; HIERZENBERGER, Anke 1; TOIMIL-MOLARES, Maria Eugenia 2; ULBRICHT, Mathias 1;

1 Universität Duisburg-Essen; 2 GSI, Darmstadt, Germany

As the most prominent member of the material class of two dimensional crystals, graphene is envisaged to have a place in a lot of future applications like sensors, ultrathin membranes or transparent electrodes. To be used in filtration applications or as a nanoresonator, graphene has to be partially suspended on a supporting substrate. In this contribution we present a facile way to create suspended graphene sheets on top of a thin porous polyethylene terephthalate (PET) film. Graphene/PET composites are prepared by transferring graphene grown by chemical vapour deposition from the copper foil to the PET film. This composite is irradiated at GSI with swift heavy ions (2.25 GeV Au²⁶⁺, 1 ion/μm²). The ions create nanoscale defects directly in graphene and a latent track in the polymer [1,2,3]. By etching the irradiated composite in NaOH, suspended graphene is fabricated. The graphene sheet is supported on top of a nanopore in the supporting polymer film with a defect in the graphene sheet at the center. The size of the defect in graphene can be modified by the irradiation parameters eg. ion energy or angle of incidence. We will present experimental data from atomic force and scanning electron microscopy techniques as well as membrane performance characterization such as gas flow/pore dewetting permporometry and water permeability measurements.

References

- [1] Fleischer et al., Nuclear tracks in solids. Berkeley: University of California (1975)
- [2] Akcöltekin et al., Appl. Phys. Lett. 98, 103103 (2011)
- [3] Ochedowski et al., Appl. Phys. Lett. 102, 153103 (2013)

A structural recovery study in high temperature swift heavy ion irradiated graphite

PELLEMOINE, Frederique 1*; AVILOV, Mikhail 1; TRAUTMANN, Christina 2; BENDER, Markus 2; EWING, Rodney C. 3; FERNANDES, Sandrina 1; LANG, Maik 4; MITTIG, Wolfgang 5; SCHEIN, Mike 1; SEVERIN, Daniel 2; TOMUT, Marilena 2;

1 Michigan State University - Facility for Rare Isotope Beams; 2 GSI, Darmstadt; 3 Stanford University; 4 University of Tennessee; 5 Michigan State University -NSCL;

To study the feasibility of using graphite as a high-power target material for secondary nuclear beam production for the Facility for Rare Isotope Beams FRIB (USA) and the Facility for Antiproton and Ion Research FAIR (Germany), polycrystalline thin graphite foils were irradiated at GSI with a 8.6 MeV/u ¹⁹⁷Au beam with additional Ohmic heating of the foil up to 1600 °C [1]. The radiation damage accumulation and recovery was monitored by in-situ electrical resistance measurements during and after stopping of irradiation and heating, until stabilization at room temperature occurred. The dependence of electrical resistance on ion fluence and on irradiation temperature shows that the saturation value is reached faster at

low irradiation temperatures due to a less efficient recombination of the irradiation produced defects. Visual inspection of the irradiated graphite foils showed that the observed swelling and dimensional changes in the irradiated region are diminished with increasing irradiation temperature. At irradiation temperatures higher than 1200°C no visible foil deformation was observed after irradiation up to a fluence of 10^{15} ions/cm². Work reported here extends the investigation of the structural changes in GeV heavy ion irradiated isotropic graphite with increasing irradiation temperature, using synchrotron X-ray diffraction. A nearly complete recovery of the interplanar spacing along the c-axis at high irradiation temperatures was found.

This material is based upon work supported by the U.S. Department of Energy Office of Science under Cooperative Agreement DE-SC0000661, the State of Michigan and Michigan State University.

References:

[1] S. Fernandes et al., Nucl. Instrum. Methods Phys. Res. B 314 (20013) 125-129.

Swift heavy ion induced effects in novel copper-diamond and molybdenum-carbide graphite composite materials

TOMUT, Marilena 1*; XU, Yuan 2; ROSSI, Adriana 3; KITZMANTEL, Michael 4;
NEUBAUER, Eric 4; BIZZARO, Stefano 5; TRAUTMANN, Christina 1; BOLZ, Philip 2;
FERHATI, Redi 6; BOLSE, Wolfgang 7; CARRA, Federico 3; QUARANTA, Elena 3;
HERMES, Pascal 3; BERTARELLI, Alessandro 3; REDAELLI, Stefano 3;

1 GSI, Darmstadt; 2 Technische Universität Darmstadt, Germany; 3 CERN, Geneva, Switzerland; 4 RHP-Technology GmbH, Seibersdorf, Austria; 5 Brevetti Bizz, Verona, Italy; 6 University of Stuttgart, Germany; 7 Institute for Semiconductor Optics and Functional Interfaces, Stuttgart University

Innovative carbon-based composites such as copper-diamond (Cu-CD), originally developed for thermal management applications and molybdenum-carbide graphite (Mo-Gr), purposely developed for high energy physics applications, are showing a very promising combination of thermal, electrical, and mechanical properties for application in beam protection elements for high-power accelerators. Nevertheless, nothing was known about their structural and dimensional stability and about degradation of functional properties under irradiation. Within the EU, FP7, EuCARD-2 project [1], an intense campaign for testing radiation hardness using different particle beams and energies is taking place at GSI Helmholtzzentrum für Schwerionenforschung in Germany, at Brookhaven National Laboratory in US and at Kurchatov Institute in Russia. First radiation hardness tests with GeV heavy ions (U238, Bi209 and Au197) were performed at the UNILAC accelerator at GSI. Cu-CD composites are produced by Rapid Hot Pressing (RHP) of metallic Cu, with addition of small quantities of boron powder, mixed with small synthetic diamonds. Mo-Gr composites are processed by Liquid Phase Sintering of molybdenum powder, graphite flakes and pitch-based carbon fibers at temperatures higher than 2000 °C. Ion irradiation-induced structural modification of the composites is investigated by means of Raman Spectroscopy, X-ray diffraction and in situ and off-line scanning electron microscopy. Online infrared thermography during irradiation and off-line laser flash analysis were used to monitor ion-induced deformation and thermal diffusivity degradation, respectively. Hardening and Young modulus changes were

characterized by nanoindentation. The outcome of these investigations allowed us to perform several optimization steps for internal stresses release in the Mo-Gr composite processing, resulting in improved stability under irradiation.

References:

[1] <http://eucard2.web.cern.ch>

03 - Metals + Carbon-based materials

Tu-PB12

Mechanism of the Defect Formation in Supported Graphene by Energetic Heavy Ion Irradiation: the Substrate Effect

WEISEN, Li 1*; JIANMING, Xue 1*;

1 Peking University;

The irradiation effects in SiO₂ supported graphene has been investigated by both experiment and molecular dynamics (MD) simulation. Defect production probability measured with Raman spectra clearly indicates that it is the nuclear collision process between target atom and the incident ions which dominates the defect production, and MD simulations agree quantitatively with experimental data while neglecting the electronic energy loss (Se) process. However, when Se is high enough and exceeds a threshold value of 2.3 keV/nm, the electronic sputtering from substrates would greatly increase the final defect number. Further analysis of the MD simulation shows surprisingly that, both the defect production probability and forms are determined by the indirect damage originating from SiO₂ substrate, while the direct interaction between the graphene and the incident ions is less important. Our results quantify the defects produced in these two processes, revealing a substrate controlled defect production mechanism in ion irradiation effects of supported graphene.

03 - Metals + Carbon-based materials

Tu-PB13

Hardness change in various compositional ZrCuAl bulk metallic glasses by swift heavy ion irradiation

KOBAYASHI, Kazuki 1*; HORI, Fuminobu 1*; ISHII, Koji 1; IWASE, Akihiro 1; YOKOYAMA, Yoshihiko 2; ISHIKAWA, Norito 3;

1 Department of Materials Science, Osaka Prefecture University; 2 Institute of Metals Research, Tohoku University; 3 Japan Atomic Energy Agency, Takasaki Advanced Radiation Research Institute;

This study involves the investigation of defect induced local structure and hardness change in various compositional ZrCuAl ternary bulk size amorphous alloys with swift heavy ion irradiation. So far, we have reported the hardness can be changed for eutectic Zr₅₀Cu₄₀Al₁₀ bulk glassy alloy by electron and ion irradiations. Additionally, different atomic relaxation process and mechanical features depending on chemical composition for Zr-based bulk amorphous alloys have been reported. In order to estimate radiation effects for various compositional bulk amorphous alloys, positron annihilation lifetime, Doppler broadening and

micro Vickers hardness measurements have been performed for bulk size (more than 100 mm length with 6mm diameter rod shape) of $\text{Zr}_{50}\text{Cu}_{40}\text{Al}_{10}$, $\text{Zr}_{55}\text{Cu}_{35}\text{Al}_{10}$, $\text{Zr}_{60}\text{Cu}_{30}\text{Al}_{10}$ and $\text{Zr}_{65}\text{Cu}_{25}\text{Al}_{10}$ amorphous alloys before and after 200 MeV Xe and 2.3 GeV Au ion irradiation with a fluence of $2 \times 10^{12} \sim 5 \times 10^{13}$ ions/cm². Radiation induced softening was observed in all composition alloys. Change in micro Vickers hardness ΔH_v decreases with increasing of Zr concentration in any composition alloys and irradiation fluences. That is, the irradiation softening is suppressed in higher Zr concentration alloys. Also, we observed that the changing trend of ΔH_v by heavy ion irradiation is consistent with that of positron lifetime, suggesting that softening caused by open volume, which size corresponds to a single or small vacancy cluster in crystal, shrinking locally during irradiation. However, the positron lifetime does not change in case $\text{Zr}_{60}\text{Cu}_{30}\text{Al}_{10}$ and $\text{Zr}_{65}\text{Cu}_{25}\text{Al}_{10}$ alloys even though the hardness decreases in all alloys. This result shows that not only open volume but also another domain or something may affect the hardness change by heavy ion irradiation.

Swift heavy ion-induced radiation damage in isotropic graphite studied by micro-indentation and in situ electrical resistivity

HUBERT, Christian 1*; SEVERIN, Daniel 1; TRAUTMANN, Christina 1; KUPKA, Katharina 1; BENDER, Markus 1; VOSS, Kay-Obbe 1; ROMANENKO, Anton 1; TOMUT, Marilena 1

1 GSI, Darmstadt

New high-power ion accelerators such as FAIR (Facility for Antiproton and Ion Research) will provide unprecedented beam energies and highest intensities. Under these extreme conditions, specific accelerator components including production targets and beam protection modules are facing the risk of degradation due to radiation damage. To ensure safe operation and less frequent maintenance shut-downs, optimized material solutions are needed. Due to its low atomic number combined with excellent thermo-physical properties and radiation hardness, high-density isotropic graphite is presently the most promising material candidate. A series of graphite samples were irradiated at the UNILAC (GSI, Darmstadt) with 4.8 MeV/u ^{132}Xe , ^{152}Sm , ^{197}Au , and ^{238}U ions applying fluences between 1×10^{11} ions/cm² and 1×10^{14} ions/cm². This specific energy was selected to be close to the Bragg-peak maximum and to avoid too intense radioactivation of the samples. The overall damage accumulation and its dependence on energy loss of the ions were studied by in situ 4-point resistivity measurements. With increasing fluence, the electric resistivity increases due to disordering of the graphitic structure. Vacancy clusters, dislocation loops, and the formation of new grain boundaries reduce the free mean path of the electrons, thus decreasing the conductivity of the material. Irradiated samples were also analyzed offline by means of micro-indentation in order to characterize mesoscale effects such as beam-induced hardening and stress fields within the specimen. With increasing fluence and energy loss, hardening becomes more pronounced.

Activation of accelerator construction materials by heavy ions

KATRIK, Peter 1*; HOFFMANN, Dieter H.H. 1; MUSTAFIN, Edil 2; PAVLOVIČ, Márius 3; STRASIK, Ivan2

1 Technische Universität Darmstadt; 2 GSI Helmholtzzentrum für Schwerionenforschung GmbH; 3 Slovak University of Technology in Bratislava

The activation data of aluminium target irradiated by 200 MeV/u ^{238}U ion beam are presented in the paper. The target was irradiated in the stacked-foil geometry and analysed using gamma-ray spectroscopy. The purpose of the experiment was to study the role of primary particles, projectile fragments, and target fragments in the activation process using the depth profiling of residual activity. The study brought information on which particles contribute dominantly to the target activation. The experimental data were compared with the Monte Carlo simulations by FLUKA2011.2c.0 code. This study is a part of a broader research program devoted to material activation by heavy ions performed with higher beam energies (≥ 500 MeV/u) at GSI Darmstadt. The whole set of activation data is important for evaluating of simulation codes and data libraries.

Swift heavy ion beam induced effects in carbon-based stripper foils

KUPKA, Katharina 1*; TOMUT, Marilena 1; HUBERT, Christian 2; DUNLAP, Anthony 2; ROMANENKO, Anton 1; TRAUTMANN, Christina 1

1 GSI, Darmstadt; 2 Technische Universität Darmstadt

Amorphous (aC) and diamond-like carbon (DLC) foils are commonly applied in accelerator technology for electron stripping of ion beams. At the planned antiproton and ion facility FAIR at GSI, Darmstadt, thin solid stripper foils could provide an option for directly delivering an intermediate charge state to the heavy ion synchrotron, SIS 18, in order to mitigate space charge limitations during high-intensity operation.

High beam intensities and a pulsed beam structure as foreseen at FAIR pose new challenges to the stripper foils which experience enhanced degradation by radiation damage, thermal effects, and stress waves. In order to ensure a reliable working carbon stripper foil, the prediction and increase of its lifetime is therefore of great interest.

This work presents an experimental contribution to understanding response and failure mechanisms of different carbon-based foils to swift-heavy ion beams of different beam structures: Amorphous carbon, DLC, and carbon nanotube-based (CNT) foils were irradiated with 4.8 MeV/u ions of different duty cycles such as ^{197}Au (5 Hz, 0.5 ms and 50 Hz, 4ms), ^{209}Bi beam (3.4 Hz, 0.5 ms), and ^{238}U (1Hz, 0.1 ms) applying fluences up to 5×10^{14} ions/cm². Beam-induced structural changes of the carbon-based materials were investigated by Scanning Electron Microscopy and by Raman and infrared Spectroscopy.

Properties' modifications of giant magnetocaloric thin films with highly charged ions

TRASSINELLI, Martino 1*; MARANGOLO, Massimiliano 1; PRIGENT, Christophe 1; ROZET, Jean-Pierre 2; STEYDLI, Sébastien 1; ZHENG, Yunlin 1; VERNHET, Dominique 1; BERNARD-CARLSSON, Louis 1; CERVERA, Sophie 1; EDDRIEF, Mahmoud 1; ETGENS, Victor H. 1; GAFTON, Vasilica 1; HIDKI, Sarah 1; LACAZE, Emmanuelle 1; LAMOUR, Emily

2

1 Insitut des NanoSciences de Paris; 2 Institut des NanoSciences de Paris - UPMC

Modifications of material properties by ion impact, and in particular changes in magnetic features, have been extensively studied in the last decades. Nevertheless, previous studies were focused mostly on materials exhibiting a second-order magnetic transition under impact of singly charged ions whilst, here, we investigate thin film presenting a first-order magneto-structural transition, namely MnAs, irradiated with slow highly charged ions, i.e. Ne^{9+} of 90 keV ($v=0.4$ a.u.). Indeed MnAs is one of the more promising candidates for developing magnetic refrigeration since it exhibits giant magnetocaloric effect (GMCE) associated to its phase transition close to room temperature (at $T_c=40^\circ$). Up to now, the practical use of GMCE materials for real refrigerator systems is blocked by the presence of a large thermal hysteresis in the magnetization cycle, which is typical of first-order transition materials. Differently from other means applied previously to reduce the thermal hysteresis (like doping, external strains, ...), ion collisions induce new defects that act as seeds for the nucleation of one phase with the other during the transition. Consequently, the thermal hysteresis is entirely suppressed whereas other structural and magnetic properties are only slightly affected. In particular, the large refrigeration power of MnAs thin film related to GMCE is preserved which opens new routes for magnetic refrigeration.

Characterization of defects and influence of the composition in $\text{Al}_x\text{Ga}_{1-x}\text{N}$ nitrides under SHI Irradiation

MOISY, Florent 1*; SALL, Mamour 2; GRYGIEL, CLARA 2; BALANZAT, Emmanuel 2; MONNET, Isabelle 1

1 CIMAP; 2 CIMAP-GANIL

In the III-V Nitride semiconductor family, $(\text{Al,Ga})\text{N}$ ternary alloys can cover different gap values from 3.4 eV (GaN) to 6.2 eV (AlN). In order to integrate these materials in devices working in harsh environment (outer space or nuclear plants), their behavior under irradiation needs to be known. In this presentation, results obtained on $\text{Al}_x\text{Ga}_{1-x}\text{N}$ ($x=0$; 0.1; 0.3; 0.5; 0.7; 0.85 and 1) wurtzite epilayers, grown on c-plane sapphire substrates, irradiated with Swift Heavy Ions (SHI) at GANIL facility, are presented. Using different ions at different energies and fluences, a large variation of ENSP (Electronic to Nuclear Stopping Power) ratio can be obtained. Thus, the contribution of electronic excitations and ballistic collisions

on the damage created by irradiation can be discussed. Optical absorption spectra exhibit absorption bands in the gap of the nitride layers (at 3.4 and 4.7 eV in AlN and 2.8 eV in GaN) resulting from the creation of new energy levels related to the creation of point defects. The position of these absorption bands varies as a function of the composition. It was previously shown that colored center creation observable at 4.7 eV in AlN after irradiation could come from N-vacancies related defects and that a synergy between electronic excitations and ballistic collisions can explain their formation [1]. In GaN, the absorption band at 2.8 eV could be linked to Ga-sublattice related defects, however, mechanisms of creation of these defects in GaN is not totally elucidated. The influence of the composition on the absorption bands and on the synergy is discussed here by varying the Ga ratio introduced in the $\text{Al}_x\text{Ga}_{1-x}\text{N}$ alloys. Transmission Electron Microscopy characterizations were also done to follow the structural modifications induced (for example to see ion track formation).

Reference

[1] M.Sall, I.Monnet, C.Grygiel, B.Ban d'Etat, H.Lebius, S.Leclerc and E.Balanzat, Europhys. Lett. 102 2600

Temperature dependence of growth and shape evolution of nanoscale voids in amorphous Ge on SHI irradiation

HOODA, Sonu 1*; KHAN, Saif Ahmad 1; KABIRAJ, Debdulal 1; UEDONO, Akira 2; SELLAIAN, Selvakumar 2; ASHOKAN, K 1; KANJILAL, Dinakar 1

1 Inter University Accelerator Centre, New Delhi; 2 Division of Applied Physics, Faculty of pure and applied physics, University of Tsukuba, Japan

Void formation on swift heavy ion (SHI) irradiation of amorphous germanium (a-Ge) layers due to local melting and re-solidification during high electronic energy deposition results in volume expansion of amorphous layer. The present study focuses on the temperature dependent growth dynamics and shape evolution of porous structures in a-Ge due to SHI irradiation. The a-Ge layers were prepared by multiple low energy Ar ion implantations in single crystalline Ge with damage formation of ~ 7 DPA. Further, these a-Ge layers were irradiated using 100 MeV Ag ions at two different temperatures (77 K and 300 K). A mono-energetic positron beam was used in Doppler broadening spectroscopy to probe the open volume in Ge samples. The spectra indicate presence of open volume of the defects in the prepared a-Ge layer as compared to c-Ge and this open volume started to increase on SHI irradiation above the ion fluence of $5 \times 10^{11} \text{ Ag cm}^{-2}$. After SHI irradiation substantial volume expansion of a-Ge layer was detected with the help of a stylus profiler. Cross-section Scanning Electron Microscopy (XSEM) studies show that the expanded a-Ge layer consists of nanoscale voids. It is observed that the voids are of spherical shape at low ion irradiation fluence. The voids grow in size and change to prolate spheroid shape with increasing ion fluence. The major axis of prolate spheroid is observed to be aligned approximately along the ion beam direction which has been confirmed by irradiation at two different angles. Relative swelling increases with increasing irradiation fluence and tend to saturate at higher fluences. Irradiation at low temperature exhibits enhanced relative swelling of amorphous

layer and growth rate of voids. Aspect ratio of voids also follows the similar fluence dependence behavior. The change in shape is a consequence of combination of compressive strain and plastic flow developed due to thermal spike generated by an incident SHI.

Raman study of gallium nitride under swift heavy ions

MOISY, Florent 1*; SALL, Mamour 2; GRYGIEL, CLARA 2; BALANZAT, Emmanuel 2;
SIMON, Patrick 3; MONNET, Isabelle 1

1 CIMAP; 2 CIMAP-GANIL; 3 CEMHTI

Nitride semiconductors are interesting materials because of their properties suitable for high power and high frequency optoelectronic devices. In order to use these materials, for example in the outer space, it is important to study their behavior under Swift Heavy Ions (SHI) irradiation. In this work, wurtzite GaN epilayers, grown on c-plane sapphire substrates, have been irradiated with SHI (Xe, Ar, U,...) at different energies and fluences at GANIL facility. Thus, different ENSP (Electronic to Nuclear Stopping Power) ratios are explored in order to investigate the contribution of electronic excitations and ballistic collisions on the damages created by irradiation. Here, Raman scattering spectroscopy has been used to study structural modifications induced in the GaN layers. Indeed, a continuum and three new modes appear after irradiation at approximately: 200 cm^{-1} , 300 cm^{-1} and 670 cm^{-1} . This phenomenon is attributed to Disorder Activate Raman Scattering (DARS), where spectra are driven by the Phonon Density of States (DOS), resulting from a loss of translation symmetry of the lattice. Moreover, it appears that the new modes at 200 cm^{-1} and 300 cm^{-1} come from Ga-sublattice related defects whereas the one at 670 cm^{-1} comes from N-sublattice related defects. UV-visible absorption spectra exhibit an absorption band at 2.8 eV which is linked to the new Raman mode at 300 cm^{-1} . Annealing analysis of both the absorption band and the Raman mode indicates that the corresponding defect could be a Ga-vacancy likely linked to another element. Raman spectra also exhibit a high-frequency shift of the strong E2 mode as a function of the fluence, which indicates that biaxial stresses are induced in the c-plane. Mechanisms responsible of this stress are discussed: an effect of the Se is clearly shown but a complementary effect of atomic displacements cannot be excluded.

Swift heavy ion damage in $\text{Mg}_x\text{Ni}_{1-x}\text{Al}_2\text{O}_4$ spinel

PERLOV, Brandon 1*; SHAMBLIN, Jacob 1; SCHAURIES, Daniel 2; TRAUTMANN, Christina 3; KLUTH, Patrick 2; EWING, Rod 4; LANG, Maik 1

1 University of Tennessee; 2 Australian National University; 3 GSI Helmholtzzentrum für Schwerionenforschung; 4 Stanford University

The radiation response of cubic MgAl_2O_4 spinel is studied extensively due to its potential applications throughout the nuclear fuel cycle, such as nuclear waste-forms and inert matrices for minor actinide transmutation. Magnesium aluminate spinel is highly resistant to damage from neutron and swift heavy ion irradiation [1,2]. Within a single ion track, the transformation to the rock-salt structure was observed [2]. The present study investigates swift heavy ion effects on the spinel structure AB_2O_4 ($\text{B}=\text{Al}$) with varying A-site cation occupation. Polycrystalline samples of magnesium nickel aluminate spinel ($\text{Mg}_{1-x}\text{Ni}_x\text{Al}_2\text{O}_4$ with $x = 0, 0.4, 0.6, 1$) were irradiated at room temperature with 2.2 GeV Au ions to a fluence of $6 \times 10^{12} \text{ cm}^{-2}$ and characterized using total neutron scattering experiments at the NOMAD (Nanoscale-Ordered Materials Diffractometer) beamline of the Spallation Neutron Source of Oak Ridge National Laboratory. Pair distribution function (PDF) analysis was used to characterize the local structure of the different spinel compositions before and after irradiation. The results were compared to ion track radii data obtained by small angle x-ray scattering (SAXS) experiments at the Australian Synchrotron. This radiation behavior can be explained in terms of the modifications to the spinel structure by cation substitution. Increasing the nickel concentration results in relatively large changes in the $\langle\text{A-O}\rangle$ and $\langle\text{B-O}\rangle$ bond distances and coordination compared with MgAl_2O_4 . These structural changes lead to a higher susceptibility to radiation damage for increasing Ni-content in agreement with the SAXS measurements. Interestingly, swift heavy ion irradiation of Mg-rich compositions has a similar disordering effect as substituting Mg with Ni at the A-site.

References

- [1] C. Kinoshita, K. Fukumoto, K. Fukuda, F.A. Garner, G.W. Hollenberg, J. Nucl. Mat. 219 (1995) 143.
- [2] T. Yamamoto, M. Shimada, K. Yasuda, S. Matsumura, Y. Chimi, N. Ishikawa Nuc. Instr. Meth. B 245 (2006) 235.

Surface track formation in SrTiO₃

MEINERZHAGEN, Florian 1*; BUKOWSKA, Hanna 1; BREUER, Lars 1; BENDER, Markus 2; SEVERIN, Daniel 2; SCHLEBERGER, Marika 1

1 Universität Duisburg-Essen; 2 GSI, Darmstadt

Irradiation by swift heavy ions with kinetic energies of several tens of MeV under glancing angles of incidence leads to characteristic permanent modifications in insulating materials [1,2]. The size and length of these modifications can be varied by the energy of the projectile and the angle of incidence. To analyze these modifications in detail and without surface contaminations from ambient conditions, we have built a new set-up at the M branch of the UNILAC at the GSI for in-situ investigations under ultra high vacuum conditions by scanning probe microscopy. One of the materials investigated with this new set-up is SrTiO₃ for which it has been shown that chains of hillocks occur after irradiation under glancing angles of incidence [1]. Our high-resolution non-contact frequency modulated atomic force microscopy measurements after irradiation with ²³⁸U with a kinetic energy of 3.6 MeV/amu and an angle of incidence of 4 degree revealed a hitherto undisclosed feature. In the very beginning of the typical chains of hillocks, we observe a narrow (~ 22 nm) and shallow (~ 0.8 nm) rift, very similar to the feature observed in SiC [2]. In terms of physical mechanisms this obvious loss of material could be explained either within the thermal spike model [3] or by a Coulomb explosion [4]. In our presentation we will discuss how an in-situ analysis of the emitted particles by a time-of-flight-mass-spectrometer in combination with a pulsed VUV laser for post-ionization might enable us to unravel the physical mechanisms behind this phenomenon.

References

- [1] Akcöltekin, Peters et al. Nature Nanotechnology 2, 290 - 294 (2007)
- [2] Ochedowski, Osmani et al. Nature Communications 5, 3913
- [3] Toulemonde, Dufour, Paumier. Phys. Rev. B 46 (1992) 014362
- [4] Fleischer et al. J. Appl. Phys. 36, 3645 (1965)

Modifications of the microstructure and electronic properties of rutile TiO₂ thin films with 79 MeV Br ion irradiation

MISHRA, Naresh 1*; RATH, Haripriya 2; DASH, Priyadarshini 2; SINGH, Udai 3; KANJILAL, Dinakar 4; AVASTHI, Devesh 4

1 Utkal University, Bhubaneswar, India; 2 U.N. (Auto.) College of Sc. and Tech., Adaspur, Cuttack, India; 3 KIIT University, Bhubaneswar, India; 4 Inter-University Accelerator Center, New Delhi, India

The rutile phase of TiO₂ is the most promising alternative gate insulator due to its good thermal and chemical stability on silicon, higher dielectric constant than SiO₂, large band gap and high transmittance in the visible spectral range. Microstructure and electronic properties of rutile thin films play a crucial role in this application. The present study probes into the modification of these properties in rutile TiO₂ thin films, induced by 79 MeV Br ion irradiation. The films were deposited on Si (100) substrates by dc magnetron sputtering. Post deposition thermal annealing at different temperatures up to 1000 °C indicated the occurrence of phase transformation directly from amorphous to rutile structure without the conventionally observed intermediate anatase phase of TiO₂. The films annealed at 1000 °C were preferentially oriented along [101]. Irradiations did not induce new XRD peaks corresponding to any other phases of TiO₂. The alignment of the grains in the film however changed due to irradiation. In addition, the total area under all the XRD peaks decreased with increasing ion fluence. Fitting of the fluence dependence of the XRD peak area to the Poisson equation yielded the radius of ion tracks as 2.4 nm. We extracted the track radius by both the analytical and inelastic thermal spike models and found that the latter yield a value of the track radius, which closely matches with our experimentally observed value. Irradiation also caused a decrease in the band gap of the films in the low fluence regime. Beyond a fluence of 1×10^{12} ion cm⁻², the band gap increased. The decrease of the band gap in the low fluence regime can be understood based on the formation of irradiation induced localized states. The increase of the band gap in the high fluence regime is a characteristic of the amorphous TiO₂ as indicated from the XRD study. Surface of the films was found to smoothen under Br ion irradiation due to dense electronic excitation. A detailed power spectral density analysis of the surface topography indicated surface diffusion is the dominant mechanism of the smoothening process under 79 MeV Br ion irradiation.

Defect-enhanced amorphous track formation in complex oxides

ZHANG, Yanwen 1*; ZARKADOULA, Eva 1; SACHAN, Ritesh 1; XUE, Haizhou 2; JIN, Ke 2;
WEBER, William 2

1 Oak Ridge National Laboratory; 2 The University of Tennessee

The interaction of ions with solids results in energy loss to both atomic and electronic systems. The material response to such energy deposition are complex and not well understood due to dependencies on electron-electron scattering processes, electron-phonon coupling, localized electronic excitations, diffusivity of charged defects, and solid-state radiolysis. Compared to defect-free crystal, thermal conductivities of the electronic and the atomic systems can be significantly reduced due to preexisting defects, and the electron-phonon coupling becomes stronger. Utilizing an integrated computational and experimental approach, we investigate the separate and combined effects of nuclear and electronic energy loss on the response of ceramics to ion irradiation. A colossal synergy, orders of magnitude larger than anything previously reported, has been discovered to occur between electronic energy loss by ions and pre-existing atomic defects created by elastic energy loss in single-crystal strontium titanate (SrTiO_3). This synergy results in the formation of nanometer-sized amorphous tracks, but only in the region with pre-existing defects. These defects decrease the electronic and atomic thermal conductivities and increase the electron-lattice coupling, which highly localizes the thermal spike for each ion, resulting in the formation of an amorphous track. This work identifies a major gap in fundamental understanding on the role of defects in electronic energy dissipation and electron-lattice coupling. As SrTiO_3 is a foundational material in functional microelectronics, the work also provides new insights for creating novel interfaces and nanostructures to functionalize thin-film structures, including tunable electronic, magnetic and optical properties. This work was support by U.S. DOE, BES, MS&ED.

Degradation of ionic crystals during irradiation with relativistic heavy-ions: An in-situ Resonant Ultrasound Spectroscopy study

ALENCAR, Igor 1*; HAUSSÜHL, Eiken 1; WINKLER, Björn 1; TRAUTMANN, Christina 2;
VOSS, Kay-Obbe 2; SEVERIN, Daniel 2

1 Goethe-Universität, Frankfurt am Main; 2 GSI, Darmstadt

Ion irradiation is a powerful technique to tailor and probe the properties of solids. In order to understand the response of matter at extreme conditions caused by the irradiation with swift heavy ions, in-situ (on line) measurements are highly desirable. In this context, we have

recently shown the capability of Resonant Ultrasound Spectroscopy (RUS) to monitor the sample temperature and its integrity during irradiation with relativistic heavy-ions [1]. In this work, we present new RUS measurements recorded during the irradiation of NaCl and KCl with 350 MeV/u Bi ions available at the GSI synchrotron SIS, complementing the previous investigation of NaCl and CaF₂ with 250 MeV/u U ions [1]. The ion energies were sufficiently high to penetrate macroscopic samples of several mm in dimension. Applied ion fluences were 3×10^{11} and 6×10^{11} cm⁻² using a flux of 2×10^7 and 8×10^7 cm⁻² s⁻¹ for Bi and U ions, respectively. As expected, coloration of the ionic crystals [2] was observed after irradiation. Sample degradation can be inferred from changes in the resonance frequencies uncorrelated with the ion flux. Moreover, all spectra recorded after irradiation of the samples show differences when compared to those recorded before irradiation. Additional Raman spectroscopic data showed the whole one-phonon density of states. This is a consequence of the local loss of translational symmetry due to the presence of point defects and their agglomerates. An independent ion irradiation experiment with CaF₂ showed that the observation of these phonons starts at ion fluences of 1×10^{11} cm⁻² [3]. Hence, we will discuss the conditions and possible causes for degradation in these macroscopic samples.

Financial support from German Federal Ministry of Education and Research (BMBF, projects 02NUK019E and 02NUK021F) is gratefully acknowledged.

References

- [1] Alencar et al., Acta Mater., accepted.
- [2] Schwartz et al., Nucl. Instr. Meth. B209 (2003) 73.
- [3] Alencar et al., Appl. Phys. Lett., to be submitted.

05 - Insulators

Tu-PB26

Is the shape elongation mechanism of embedded nanoparticles via underdense track cores acceptable?

AMEKURA, Hiroshi 1*; MOTA SANTIAGO, Pablo 2; KLUTH, Patrick 2; CHETTAH, Abdelhak 3; AVASTHI, Devesh 4; OKUBO, Nariaki 5; ISHIKAWA, Norito 6

1 National Institute for Materials Science; 2 The Australian National University; 3 Université 20 Août 1955, Skikda; 4 IUAC; 5 JAEA; 6 Japan Atomic Energy Agency

The elongation of metal nanoparticles (NPs) in silica induced by swift heavy ion (SHI) irradiation has been receiving much attention. Recently, Leino et al. [1] have succeeded in the reproduction of the shape elongation of NPs by classical molecular dynamics (MD) simulations which adapted to transient temperature profiles calculated by the inelastic thermal spike (i-TS) model. They interpreted that the shape elongation was induced as consecutive dynamic crystal-liquid-crystal phase transitions of a NP with the flow of liquid phase into an underdense track core in silica. It was reported that the underdense track cores are formed in silica with overdense shells [2]. The cores and shells were ascribed to

vaporized and molten regions of silica by the i-TS effect, respectively [2]. Since the vaporization in silica tracks requires relatively high energy stopping Se, the NP elongation was expected only under high-Se irradiation. However, we evaluated the Se dependence on the elongation efficiency of NPs [3] and found that the elongation was induced with even low Se of 3 keV/nm, while the vaporization of tracks required Se much higher than 6 keV/nm. Consequently, our experimental observation is inconsistent with either of the previous interpretations of the MD results, i.e., “the elongation via underdense tracks” or “the underdense cores made by vaporization”. In the present work, the irradiation experiments with low Se where the vaporization silica is not expected, are performed to test the two interpretations.

References

- [1] A.A. Leino, et al., Mat.Res. Lett. 2, 37 (2013).
- [2] P. Kluth, et al., Phys. Rev. Lett. 101, 175503 (2008).
- [3] H. Amekura, et al. Nanotechnology 25, 435301 (2014).

05 - Insulators

Tu-PB27

Raman spectra of malachites ($\text{Cu}_2[(\text{OH})_2/\text{CO}_3]$) after ion irradiation

SCHÖPPNER, Nicole 1*, GLASMACHER, Ulrich A. 1; BURCHARD, Michael 1;
TRAUTMANN, Christina 2

1 Institut für Geowissenschaften, Universität Heidelberg; 2 GSI, Darmstadt

Within geosciences, the use of fission tracks in various minerals as a thermochronological analytical technique is of major importance. For track dating, natural samples are typically etched, converting the nanoscopic tracks into open channels which can be visualized and counted under an optical microscope. Due to channel overlapping, large track densities cannot be analyzed. For future quantification of fission tracks we investigate alternative methods such as Raman spectroscopy. For large track densities, the amplitude, wavenumber position, and full width of half maximum of specific Raman bands change. Malachite ($\text{Cu}_2[(\text{OH})_2/\text{CO}_3]$) occurs in nature within copper deposits and can have 10 ppm uranium. Thus if the fission-track dating system could be applied to malachite, it would be possible to access large track densities and date the formation or temperature history of geological samples bearing malachite (e.g. copper deposits). In nature, malachite occurs as nano- to micro-sized crystalline mass with banded zonation's or as micro- to macro sized crystals. As the U-content varies in natural malachite, we used swift heavy ions to create well-defined track densities. Malachite crystals of different shape and size were irradiated at the UNILAC (GSI, Darmstadt) with ^{209}Bi ions (11.1 MeV/u) of fluences between $1 \cdot 10^6$ and $2 \cdot 10^{12}$ -ions/cm². The samples were investigated by Raman spectroscopy before and after irradiation. The crystal orientation has a direct influence on the amplitude of specific Raman bands (e.g. the doubly degenerated ν_3 (CO_3)₂- antisymmetric stretching mode at $\sim 1491 \text{ cm}^{-1}$). With increasing fluences the amplitudes of all Raman bands decrease. At the fluence of

1×10^{10} ions/cm² the surface of the malachite changes its color from green into black with Raman bands indicating graphite. The presentation will provide data on the differences of ion irradiated microcrystalline or nanocrystalline samples as well as brighter and darker parts of the zoned malachite samples.

Heat capacity and electron paramagnetic resonance measurements of ionic crystals irradiated with swift heavy ions

ALENCAR, Igor 1*; WINKLER, Björn 1; BAYARJARGAL, Lkhamsuren 1; BAUER, Johannes D. 1; HAUSSÜHL, Eiken 1; ENDEWARD, Burkhard 1; PRISNER, Thomas 1; TRAUTMANN, Christina 2

1 Goethe-Universität Frankfurt am Main; 2 GSI, Darmstadt

Point defects in ionic crystals are known to be trapping sites for electrons and holes. Irradiation of ionic crystals with heavy ions induces color centers by the non-radiative exciton decay mechanism [1] with a typical optical absorption in the spectral range of the band gap (~ 10 eV). While extensive Electron Paramagnetic Resonance (EPR) studies in alkali halides [2] and alkaline earth halides [3] were performed for samples irradiated with electrons, data for swift heavy ion irradiations are rather scarce. Furthermore, heat capacity measurements require mm-sized bulk crystals. Such samples can be exposed to ions of sufficiently large penetration at the heavy ion synchrotron SIS at GSI. We present heat capacity measurements at constant pressure (PPMS Quantum Design) and EPR (ESP300 X-band Bruker) measurements of NaCl, KCl, LiF and CaF₂ crystals irradiated with either 350 MeV/u Bi or 209 and 250 MeV/u U ions. The total ion fluences varied from 5×10 to 6×10^{11} cm⁻². Heat capacity differences between pristine and irradiated samples appear for temperatures below 100 K. At these temperatures, also the EPR signal displays additional features.

Financial support from German Federal Ministry of Education and Research (BMBF, projects 02NUK019E and 02NUK021F) is gratefully acknowledged.

References

- [1] Itoh, Adv. Phys. 31 (1982) 491.
- [2] Fryburg & Lad, Surf. Sci. 48 (1975) 353.
- [3] Beuneu et al., Radiat. Eff. Defects Solids 136 (1995) 175.

Swift heavy ion tracks in amorphous thin films and multilayers

KARLUSIĆ, Marko 1*; LEBIUS, Henning 2; BAN D'ETAT, Brigitte 2; BOGDANOVIĆ RADOVIĆ, Iva 1; JAKŠIĆ, Milko 1; ŠANTIĆ, Branko 1; RADIĆ, Nikola 1; SCHLEBERGER, Marika 3; BERNSTORFF, Sigrid 4; BULJAN, Maja 1;

1 Ruđer Bošković Institute, Zagreb, Croatia; 2 CIMAP, CEA-CNRS-ENSICAEN-UCBN, Caen, France; 3 Universität Duisburg-Essen, Duisburg, Germany; 4 ELETTRA Sincrotrone Trieste, Italy;

Recently we have demonstrated a new approach for the investigation of ion tracks in amorphous materials. Specially designed amorphous materials optimized for GISAXS measurements were shown to be suitable for ion track production and measurement [1]. Furthermore, ion tracks in those materials exhibit typical ion track specifics like the velocity effect [2]. In the present contribution two new developments are presented. Irradiation of flat solid surfaces by swift heavy ions under grazing incidence can result in the formation of surface ion tracks that are usually observed directly using an atomic force microscopy (AFM) [3]. However, to extract the statistical information (average ion track length, separation, size, internal structure and their statistical distributions), structural investigations with AFM are very time consuming. Here we introduce a new approach based on the grazing incidence small angle X-ray scattering (GISAXS) technique. GISAXS is used for the structural analysis of surface swift heavy ion tracks, enabling determination of the above-mentioned properties. Compared to AFM, GISAXS allows shorter measuring times with excellent statistics. Compared to our previous work where 15 MeV Si was the most energetic ion beam used [2], in the present work our research was extended to higher values of electronic energy loss by using 23 MeV I and 92 MeV Xe ion beams. New ion track phenomena were observed: after the grazing incidence irradiation, rift-like structures were observed on the surface, while after irradiation under large angles evidence for nucleation of nanoparticles by single ions was found.

References

- [1] M. Buljan et al., Determination of ion track radii in amorphous matrices via formation of nano-clusters by ion-beam irradiation, *Appl. Phys. Lett.* 101 (2012) 103112
- [2] I. Bogdanović-Radović et al., Conditions for formation of germanium quantum dots in amorphous matrices by MeV ions: Comparison with standard thermal annealing, *Phys. Rev. B* 86 (2012) 165316
- [3] M. Karlušić et al., Energy threshold for the creation of nanodots on SrTiO₃ by swift heavy ions, *New J. Phys.* 12 (2010) 043009

Raman spectra of gypsum after ion irradiation

SCHÖPPNER, Nicole 1*; GLASMACHER, Ulrich A. 2; BURCHARD, Michael 2;
TRAUTMANN, Christina 3

1 University of Heidelberg; 2 Institut für Geowissenschaften, Universität Heidelberg; 3 GSI, Darmstadt

Within geosciences, the effect of ion irradiation in various minerals of high importance for a better understanding of geological aspects. Our research was triggered by the question if crystal water of natural minerals is released due to radiation effects. To test the behavior of the water within the crystal lattice under irradiation, gypsum samples were exposed to swift heavy ions und subsequently analyzed by Raman spectroscopy. Natural gypsum single crystals ($\text{CaSO}_4 \cdot 2\text{H}_2\text{O}$) were irradiated at the UNILAC (GSI, Darmstadt) with 11,1 MeV/u 209Bi ions of fluences between $1 \cdot 10^6$ and $2 \cdot 10^{12}$ -ions/cm². The samples were analyzed by Raman spectroscopy. Details of the spectra depend on the crystal orientation. Significant changes in the Raman spectra of gypsum appear above fluences of $1 \cdot 10^{10}$ 209Bi-ions/cm². With increasing fluences the band intensities decrease. This applies especially to the ν_1 stretching mode at 3404 cm⁻¹ and the ν_3 stretching mode at 3492 cm⁻¹, which characterizes the Raman bands of H₂O. The amplitudes decrease is an indication of irradiation-induced release of water. Although the lattice water is set free, the mineral is not transformed to anhydrite (CaSO_4) which is the waterless sulfate. The bands remain at their characteristic gypsum position and do not shift to the anhydrite position. In addition it could be observed that the colorless and transparent sample turn into a hazy white color at a fluence of $3 \cdot 10^{11}$ 209Bi-ions/cm² and above.

Radiation-enhanced diffusion in Mg₂SiO₄ olivine bi-crystals

GARDES, Emmanuel 1*; BALANZAT, Emmanuel 1; GRYGIEL, Clara 2; LEBIUS, Henning 1;
MARQUARDT, Katharina 3; MONNET, Isabelle 1

1 CIMAP; 2 CIMAP-GANIL; 3 BGI-Bayreuth

Atomic diffusion plays a primary role in numerous phenomena that greatly modify the properties and enhance the aging of materials, especially under irradiation. For instance, these are (1) corrosion and oxidation, (2) phase transitions, (3) creep, (4) agglomeration of point defects provoking the formation of dislocation loops or cavities and concomitant swelling, (5) redistribution of chemical species leading to precipitation or dissolution of precipitates or to grain boundary segregation.

Irradiation introduces an excess of point defects that provokes a dramatic enhancement of atomic diffusion in materials. Radiation-enhanced diffusion can be several orders of magnitude faster than thermal diffusion and allows the transport of atomic species at

temperatures where they are usually virtually immobile. However, while radiation-enhanced diffusion is well documented and understood in metals, it is almost unexplored in ionic-covalent solids and the interest in these latter materials is continuously increasing.

Grain boundary diffusion is usually several orders of magnitude faster than volume diffusion and its potential additional enhancement under irradiation is of crucial importance since most of materials are and will be polycrystalline or composite.

We investigate here not only the influence of ion irradiation on volume (lattice) diffusion but also on grain boundary diffusion. We report preliminary results on model experiments performed on Mg_2SiO_4 olivine bi-crystals coated with Ni_2SiO_4 films so that Ni acts as diffusion tracer. The geometry of the samples allows for convenient and concomitant analysis of volume and grain boundary diffusion within the same sample using focused-ion-beam-assisted electron microscopy. Volume and grain boundary radiation-enhanced diffusion under 1 MeV/a-40Ar flux and at 500°C is compared to thermal diffusion.

06 - Optical properties of insulators

Tu-PB32

Accumulation of aggregate centers in LiF under swift heavy ion irradiation: the correction using depth-resolved photoluminescence data

DAULETBEKOVA, Alma 1; KIRILKIN, Nikita 2*; KOVALEV, Yuri 2; SKURATOV, Vladimir 2; VOLKOV, Alexei 3; AKILBEKOV, Abdirash 1;

1 L.N. Gumilyov Eurasian National University, Astana, Kazakhstan; 2 FLNR JINR, Dubna, Russia; 3 Nazarbayev University, Astana, Kazakhstan;

Optical absorption spectroscopy has been successfully used for quantitative analyses of single and complex electron centers in lithium fluoride irradiated with high energy heavy ions. In particular, track radii for different ion species and energies were deduced from optical absorption data as a function of ion fluence. Usually the average volume color center concentration is calculated by using the Smakula-Dexter formula and then divided by the projected ion range, R_p . Such an averaging may be a source of large inaccuracy if corresponding centers in a number detectable by optical absorption technique are created in the range less than R_p . Using laser confocal scanning microscopy we have measured the luminescence intensity of F2 and F3+ centers across depth of 1 MeV/amu Ar, Kr, Xe and 0.5-3 MeV/amu Bi ion irradiated LiF specimens. It was found that the luminescence signal ascribed to above centers in a broad range of ion fluences is proportional to the total absorbed dose and registered in layers with a thickness R_{eff} , much less than projected ion range. Application of realistic R_{eff} value instead of R_p may result in significant increase, up to 2 times, of the average volume color center concentration.

The study of optical property of sapphire irradiated with 73 MeV Ca ions

GOU, Jie 1*; ZHANG, Chonghong 1*; SONG, Yin 1;

1 Institute of Modern Physics, Chinese Academy of Sciences;

Single crystals of sapphire were irradiated with 73 MeV Ca ions at room temperature to fluences of 1.0×10^{13} , 5.0×10^{13} and 1.0×10^{14} ions/cm². Optical properties of these samples were characterized by ultraviolet-visible spectrometry (UV-VIS) and fluorescence spectrometer (PL). In UV-VIS spectra, it is observed the absorbance bands from oxygen single vacancy (F and F⁺ color centers) and vacancy pair (F₂⁺ and F₂⁽²⁺⁾ color centers). From the evolution of the absorbance intensity of these bands, it is seen that oxygen single vacancy initially increases rapidly and then becomes saturated in the fluence range from 1.0 to 5.0×10^{13} ions/cm². When the fluence is higher than 5.0×10^{13} ions/cm², oxygen single vacancy starts to increase again. Oxygen vacancy pair monotonically increases with fluence for all irradiated samples. The variation of oxygen single vacancy with fluence is probably associated with defect recovery and complex defect formation. From PL spectra, two emission bands around 3.1 and 2.34 eV are observed. The PL intensity of the emission band around 3.1 eV decreases for all irradiated samples. For the emission band around 2.34 eV, the PL intensity initially decreases, and then increases with fluence. Meanwhile, the peak position of the emission band around 2.34 eV gradually shifts to high energy direction with increase of fluence. The decrease of the intensity of emission bands around 3.1 and 2.34 eV could be induced by stress from the damage layer in the irradiated samples. The shift of peak position for the emission band around 2.34 eV is induced by the appearance of emission band from Al interstitials.

Photoluminescence in SiO₂/Si structures irradiated with 133-MeV Xe ions

KOMAROV, Fadei 1*; VLASUKOVA, Ludmila 1; YUVCHENKO, Vera 1; PARKHOMENKO, Irina 1; DAULETBEKOVA, Alma 2; ALZANOVA, Aliya 2;

1 Institute of Applied Physics Problems; 2 L.N. Gumilyov Eurasian National University;

Amorphous silicon dioxide (silica) is widely used in microelectronics and telecommunications owing to its large band gap and very low conductivity as well as to the perfect Si-SiO₂ interface. The interest in studying the interaction of swift heavy ions (SHI) with SiO₂ is due to a possible use of SHI for creation of Si-based light-emitting nanostructures by disproportionation of SiO₂ in the ion tracks [1]. Moreover, when the solar cells and MOS structures with insulating silica layers are in outer space equipment, they change their properties due to generation of defects. Thus, radiation induced defects in silica deserve special attention in modern electronic technology, too.

One micrometer-thick silicon dioxide layers were grown by PECVD on Si substrates at 300 °C and afterwards irradiated with 133-MeV Xe ions at the cyclotron DC60 (Astana, Kazakhstan) in the fluence range of 10^{10} - $5 \cdot 10^{14}$ cm⁻². According to SRIM 2010 the electronic stopping power for Xe ions in SiO₂ was 13.5 keV/nm. We have calculated track formation parameters in the frames of thermal spike model, too. The molten region radius

and lifetime for Xe ions in the SiO₂ were 5.9 nm and 20.5 ps accordingly. The triple band in visual range with maxima at 470, 550 and 660 nm was observed in PL spectrum of SiO₂ after the irradiation at fluence of 1010 cm⁻² and grew substantially with the ion fluence. The formation of Si-enriched nanostructures inside the tracks of swift ions as well as the formation of defect aggregates in tracks [2] is discussed as the possible sources of the observed photoluminescence.

[1] G. A. Kachurin, S. G. Cherkova, D. A. Marin, V. G. Kesler, V. A. Volodin, V. A. Skuratov, Nucl Instrum. Meth. B (2011) doi:10.1016/j.nimb.2011.08.053.

[2] K. Schwartz, C. Trautmann, A. S. El-Said, R. Newmann, M. Toulemonde, W. Knolle, Phys. Rev. B70 (2004) 184104.

06 - Optical properties of insulators

Tu-PB35

Response from Inorganic Scintillating Screens induced by high energetic Ions

LIEBERWIRTH, Alice 1*; FORCK, Peter 2; LEDERER, Stephan 1; ENSINGER, Wolfgang 1;

1 TU Darmstadt; 2 GSI

Scintillating Screens are a commonly used device for beam profile monitoring at accelerator facilities. For high energetic ion beams the characteristics and the reproducibility of the light emission for different materials is quite unknown, therefore possible differences in light yield and beam profile imaging have to be investigated. Investigations with seven inorganic scintillators (P43, P46, YAG:Ce, Aluminium oxide and Al₂O₃:Cr) were performed with high energy ion beams at GSI as research for the FAIR project. Beams of various ion species from Hydrogen to Uranium were extracted from SIS18 with 300 MeV/u and beam intensities between 10⁶ to 10¹⁰ particles per pulse. To study possible modifications or saturation effects of the scintillation yield, the pulse length of the ion beam was varied for slow extraction (300 ms-10 s) while fast extracted beams were fixed at 1 µs.

The beam response on the scintillation screens was recorded and analyzed with respect to light yield, statistical moments and emission spectra.

It can be shown that the light output for all targets is a linear function of the extracted beam intensity, independent of the chosen projectile. The light yield as function of beam current shows a nearly constant behavior for all targets and ions. This is also approved by unchanged luminescence spectra for each target during all measurements. Changes in calculated profile sizes can be explained by expected broadening of beam with increasing intensity.

Additional radiation hardness tests showed stability of the scintillator characteristics. All these results make each target to reliable devices for high energy beam alignment even under high intensities.

SPORT: A time-resolved setup for the study of swift heavy ion beam-induced luminescence

GARDES, Emmanuel 1; GRYGIEL, Clara 2; DURANTEL, FLORENT 3*; MONNET, Isabelle 1; SCHLEBERGER, Marika 4; BALANZAT, Emmanuel 1; BAN D'ETAT, Brigitte 1; CASSIMI, Amine 1; LEBIUS, Henning 1; ROPARS, Frédéric 1;

1 CIMAP; 2 CIMAP-GANIL; 3 lab. CIMAP-GANIL CNRS; 4 Universität Duisburg-Essen;

Swift heavy ions trigger a strong electronic excitation along their trajectory. This includes the creation of a significant amount of electron-hole pairs. Details about the type of excitation as well as the processes in the subsequent redistribution and relaxation of energy can be accessed by measuring the transient emission due to radiative recombination i.e., the luminescence. The dynamics is typically dependent on the sample temperature because quasi-particles can only form if their binding energy is higher than kT . Thus, this approach can be used to unravel different recombination mechanisms and their interplay.

The SPORT set-up (time-resolved optical spectrometer, SPectroscopie Optique Résolue en Temps), recently developed in CIMAP, is a new sub-nanosecond time-resolved instrument dedicated to studying the dynamics of UV-visible luminescence, at variable temperature, under high stopping power heavy ion irradiation [1].

We present our instrument and first results on materials irradiated with SHI beams. Especially, We measured the iono-luminescence of SrTiO_3 irradiated with 40 MeV Ar beams. This material has decay times adapted to SPORT, where different photo-excited carrier recombination mechanisms have been identified by time resolved photo luminescence and where ion-induced excitonic states have been postulated to play an important role [2].

[1] E. Gardes et al., Nucl. Instrum. Methods B 297 (2013) 39

[2] Y. Yamada et al, Phys. Rev. Lett. 102 (2009) 247401

Color center formation in alumina induced by heavy ions at high fluences

LEDERER, Stephan 1*; GÜTLICH, Eiko 2; LIEBERWIRTH, Alice 1; ZIMMERMANN, Jörg 3; ENSINGER, Wolfgang 1;

1 Technische Universität Darmstadt; 2 GSI Helmholtzzentrum für Schwerionenforschung; 3 Fraunhofer IWKS;

Scintillating screens are used at accelerator facilities for ion beam diagnostics with very high ion fluxes. However, during irradiation of the material, formation of color centers occurs. The increasing radiation damage leads to massive degradation of light yield, which is one of the main problems using the screens as an appropriate tool for beam imaging. Due to its radiation hardness, alumina is an interesting material for scintillation applications. Another advantage of using Al_2O_3 is that the understanding of its luminescence behavior is at an advanced stage.

Polycrystalline alumina samples (α -Al₂O₃, purity: 99.8 %) were irradiated with different ion species and different fluences at various energies at UNILAC within GSI (Darmstadt, Germany). Ion beam induced luminescence and emission spectra were monitored at wavelengths from 320 to 800 nm.

Results were evaluated according to Birks theory, to determine the critical half-life fluence and the material's radiation hardness. It could be shown that thermal annealing during irradiation leads to an extended life time of the scintillation screens. This condition is supported also by analysis of emission spectra and the observation of complex color center formation processes with increasing irradiation and temperature.

After irradiation, absorption measurements were performed to calculate the color center concentration using the Smakula-Dexter formula. For low doses, color center formation complies with exponential growth. For high doses, saturation in the concentration of color centers can be determined.

06 - Optical properties of insulators

Tu-PB38

Linear energy transfer effects on the time profiles of scintillation in Ce-doped LiCaAlF₆ Crystals

YANAGIDA, Takayuki 1*; KURASHIMA, Satoshi 2; IWAMATSU, Kazuhiro 3; KIMURA, Atsushi 2; TAGUCHI, Mitsumasa 2; FUJIMOTO, Yutaka 4; ASAI, Keisuke 4; KOSHIMIZU, Masanori 4;

1 Nara Institute of Technology; 2 JAEA; 3 University of Tokyo; 4 Tohoku University;

Rare-earth-doped LiCaAlF₆ is a promising scintillation material for thermal neutron detection. In particular, Ce-doped LiCaAlF₆ has attracted attention for its potential use in discrimination of neutron and gamma-ray detection events based on the behavior of the scintillation time profile: a fast scintillation component appeared during gamma-ray irradiation, whereas no such component was observed during thermal neutron irradiation. Because scintillation under neutron irradiation is generated via electronic excitation by energetic 3H and alpha rays produced by the nuclear reaction $6\text{Li}(n,\alpha)3\text{H}$, and because the linear energy transfer (LET) of the energetic particles is significantly higher than that of gamma rays, the difference in the temporal profiles may originate from LET effects. In this study, we analyzed the LET dependence of the temporal profiles of scintillation in Ce-doped LiCaAlF₆.

Temporal profiles of scintillation at different LETs were obtained using pulsed ion beams of 20 MeV H⁺, 50 MeV He²⁺, and 220 MeV C⁵⁺. A scintillation time profile at low LET was also obtained using a pulsed X-ray beam. A fast scintillation component was observed during X-ray irradiation. Because the X-ray energy was less than 30 keV, the observed fast component cannot be ascribed to Cherenkov radiation. On the basis of discussion in previous studies, this component is ascribed to lattice defects. The fast component was not observed during ion irradiation. This result indicates that the fast component is quenched at high LET, and the discrimination of thermal neutron and gamma-ray detection events based on this quenching is feasible. In addition, the rise behavior of the slow component, which is ascribed to emission from Ce³⁺ luminescence centers, was different at different LETs. This difference can be explained by interaction between excited states during energy transfer to the luminescence centers.

Oxygen loss induced by swift heavy ions of low and high dE/dx in PMMA thin films

THOMAZ, Raquel 1*; GUTIERRES, Leandro 2; JONDER, Morais 3; LOUETTE, Pierre 4; PIREAUX, Jean-Jacques 4; SEVERIN, Daniel 5; TRAUTMANN, Christina 5; PAPALÉO, Ricardo 2;

1 Pontifical Catholic University of Rio Grande do Sul (PUCRS); 2 Pontifical Catholic University of Rio Grande do Sul; 3 Federal University of Rio Grande do Sul; 4 Université de Namur; 5 GSI, Darmstadt;

*primary author

Investigations on the chemical modifications induced by swift heavy ions in PMMA thin films were carried out using beams of high dE/dx (2.2 GeV Bi, 1400 eV/Å) and low dE/dx (2 MeV H, 1.9 eV/Å). The induced chemical modifications were monitored by XPS for films with initial thickness of 5, 50 and 120 nm. For both beams, the irradiation decreased the amount of carbon atoms bound to oxygen (C=O and O-C-O), with a larger decrease of the carboxyl moiety, as expected. However, the chemical changes induced by light and heavy ions were qualitatively different. Surprisingly, for the same mean deposited energy density (the product of stopping power and fluence), proton irradiation induced a decrease of the C-O bonds up to ~20% larger than the irradiation with Bi ions. This suggests a greater importance of particle ejection by unzipping of PMMA chains at high dE/dx, which tends to keep the O/C ratio closer to the pristine value. The strong difference in electronic sputtering yields for H and Bi beams also resulted in distinct surface morphologies of the irradiated films.

Dose effect on H₂ emission and O₂ consumption in polyethylene radio-oxidized at various LET

FERRY, Muriel 1*; FROMENTIN, Elodie 2; NGONO-RAVACHE, Yvette 3; BALANZAT, Emmanuel 4; ESNOUF, Stephane 2; PELLIZZI, Eleonora 2; BOUGHATTAS, Imène 5; DURAND, Delphine 2; LEGAND, Solene 2; DAUVOIS, Vincent 2; DE COMBARIEU, Guillaume 6; COIGNET, Pascale 6; COCHIN, Florence 6;

1 CEA Saclay; 2 CEA; 3 CIMAP/CEA; 4 CNRS; 5 Commissariat à l'Energie Atomique; 6 AREVA;

To our knowledge, only a few studies have focused on the dose effect on hydrogen emission and oxygen consumption rates in polymers submitted to ionizing radiations. According to Chapiro [1], hydrogen radiation chemical yield is constant, until 2 MGy, in polyethylene submitted to gamma-rays under inert atmosphere. On the contrary, Mitsui [2] and Seguchi [3] indicate a decrease in hydrogen emission yield at doses above 1 MGy. This decrease was assigned either to hydrogen molecule readdition on double bonds formed during radiolysis [2] or to the protection of the polymer by radiation-induced trans-vinylenes formed

at lower doses [3]. More recently, the protective effect of trans-vinylenes has been confirmed and documented by Ventura [4], using both gamma-rays and ion beams.

The aim of the present work is to study the effect of high doses on hydrogen emission and on oxygen consumption, in a polyethylene irradiated under oxidative conditions, using both gamma-rays and Swift Heavy Ions. By comparing our results with the literature, the atmosphere effect on hydrogen emission radiation chemical yields is evaluated. Moreover, comparing results from gamma-rays and ion beam irradiations allows evaluating the role of the dose rate and the dose deposition structures on the mechanisms involved.

By quantifying the oxygen consumption during irradiation and by comparing oxygen consumption radiation yield with oxidation products yields, obtained by Lacoste & Carlsson [5] on a Linear Low Density Polyethylene (LLDPE) radio-oxidized under gamma-rays, the amount of modified methylene groups has also been assessed.

[1] A. Chapiro, Radiation chemistry of polymeric systems, John Wiley & Sons, New York (1962).

[2] H. Mitsui, Y. Shimizu, J. Polym. Sci. Polym. Phys. Ed. 17 (1979), 2805.

[3] T. Seguchi, Nucl. Instrum. Methods Phys. Res., Sect. B 185 (2001), 43.

[4] A. Ventura, thèse de l'Université de Caen Basse-Normandie, Caen (2013).

[5] J. Lacoste, D.J. Carlsson, J. Polym. Sci. Part A: Polym. Chem. 30 (1992), 493.

07 - Polymers + Organic materials

Tu-PB41

Roughness evolution in polymer thin films submitted to ion irradiation and thermal treatments

PAPALÉO, Ricardo 1; ESTEVES, Christian 1*; GUERRA, Danieli 1; TEXERA, Diego 1; GUTIERRES, Leandro 1; THOMAZ, Raquel 1; FEIL, Adriano 1;

1 Pontifical Catholic University of Rio Grande do Sul;

In this work, we investigated the thermal stability of poly(methyl methacrylate) thin films surfaces after exposure to 18 MeV Au+7 at different temperatures. Irradiations and in situ annealings were performed at room temperature, 100°C, 130°C and 150°C. Surface evolution was monitored after irradiation treatments performed in the following conditions: a) fixed fluence at different irradiation temperatures; b) fixed temperature for different fluences; and c) irradiation at a fixed fluence and temperature, followed by in situ annealing (for up to 72h). Depending on the thermal treatment condition, ion fluence, and type of substrate, the films showed either roughening or smoothing. The effect of irradiation only is to increase steadily surface roughness with increasing ion fluence. However, for a given fluence, different surface morphologies were observed when the films were irradiated at different temperatures. Above the glass transition temperature, high spatial frequency features of the surface topography are reduced, and samples presented distinctively different morphologies as compared to the ones irradiated at lower temperatures. Root mean square roughness peaked for irradiations at 100°C, but for $T > T_g$, a smoothing effect was observed. In situ post-irradiation annealing at the irradiation temperature leads to an asymptotic growth of roughness with time. The surface evolution upon irradiation and thermal treatments was more pronounced in the thickest layers investigated (~200nm) as compared to 40nm or 4nm thick films.

Radiolysis of H₂O+CH₄ ices by MeV heavy ions

MEJÍA, Christian 1, 2*; DE BARROS, Ana 3; FROTA DA SILVEIRA, Enio 1; ROTHARD, Hermann 4; BODUCH, Philippe 5

1 PUC-Rio; 2 CIMAP-GANIL; 3 Centro Federal de Educação Tecnológica Celso Suckow da Fonseca; 4 CIMAP-Ganil CNRS; 5 CIMAP-CNRS

In order to analyze the physical–chemical effects produced by fast heavy ions on mixture ice films. Thin films of methane–water ices (thickness around 1 μm) at concentrations of 2:1 and 10:1, respectively were irradiated by 40 MeV 58Ni^{11+} ions at the IRRSUD beamline of GANIL/France. The setup consists of a high vacuum chamber (<107 mbar), equipped with a cryostat capable to reach temperatures as low as 15 K. Ices films are formed from the vapour phase onto CsI (IR transparent) windows and then irradiated. The chemical and physical changes were monitored by infrared (IR) spectroscopy after and before irradiation [1]. The IR bands that appeared during irradiation in the H₂O:CH₄ (2:1) ice are attributed to synthesized compounds: C₂H₂, C₂H₄, C₂H₆ and C₂H₈ hydrocarbons, HCO and H₂CO radicals and the CO, CO₂, H₂O₂, HCOOH; CH₃OH, C₂H₅OH, CH₃CHO, CH₃OCH₃ molecules. It was observed that for the irradiated H₂O:CH₄ (10:1) ice the abundance of the compounds containing two carbons atoms was reduced. In contrast, CH₃OH and H₂O₂ compounds increased when compared to the results obtained with the (2:1) ice. Additionally, after irradiation, the ices were slowly warmed up. After sublimation, the IR spectra reveal new synthesized molecules. Among them are: methyl formate (CH₃OCHO), acetone (CH₃CH₃CO), glycolaldehyde (CH₂OHCHO), and ethylene glycol (HOCH₂CH₂OH). The formation of these complex molecules during the warming up is attributed to the increased mobility of radicals [2]. These findings provide an explanation for the occurrence of methane containing ices in the cold regions of the universe. This process may also explain the observed chemical abundance of the compounds observed in icy grain mantles around protostars.

[1] Mejía, C. F. et al., 2013. MNRAS. 433 (3), 2368.

[2] Bennett, C. J. et al., 2007. ApJ, 660(2), 1588.

[3] Öberg, K. I. et al., 2010. ApJ, 718(2), 832.

Effect of swift 12C irradiation on DNA molecules: a molecular dynamics study using the REAX force field

MÜCKSCH, Christian 1; BOTTLÄNDER, Dominik 1, 2*; URBASSEK, Herbert Michael 1;

1 University of Kaiserslautern; 2 University of Tennessee, Knoxville;

High-energy heavy ions are preferred candidates for external radiotherapy of inner tumors due to their defined local energy deposition and high density of ionization in the target area. The linear stopping power distribution along their path is characterized by an extended section of relatively low energy loss followed by the distinct Bragg maximum of the density of

ionization. This distribution results from the ion energy dependent energy transfer mechanisms between a heavy ion and the penetrated matter. As the location of the Bragg maximum can be controlled by the initial kinetic ion energy, the biological efficiency can be predominantly confined to the tumorous target area. In this context, the presented study is concerned with the structural changes in DNA molecules caused by heavy-ion irradiation. For this purpose, molecular dynamics simulations of a DNA molecule solvated in water were performed. The passage of a swift 12C ion was modeled by kinetic-energy transfer to the atoms in a cylindrical track region. The simulation follows the ensuing processes and comprises the thermal equilibration of the energy as well as chemical processes within the DNA molecule. Our use of a REAX force field allows us to include bond dissociations into our model. The ion track axis ran through the center of mass of the DNA molecule at the time of ion impact. This allowed for an investigation of the directional effect of the ion impact onto the DNA molecule by means of a variation of the orientation of the ion track axis. Our study assesses the effects associated with the biological efficiency of heavy-ion beams for DNA molecules. This involves an analysis of the damage occurring such as single-strand breaks and likely irreparable double-strand breaks as well as of changes in the secondary structure subject to the energy deposition to a DNA molecule.

Upgrading the GSI beamline microscope with a fluorescence lifetime scanner to monitor charged particle induced chromatin decondensation in living cell

ABDOLLAHI, Elham 1*

1 GSI Helmholtzzentrum für Schwerionenforschung GmbH

Advances in a variety of photonic imaging techniques make Fluorescence Lifetime Imaging Microscopy (FLIM) a promising technique for quantitative biophysical measurements as it can provide insight into dynamics of biological processes. Earlier, we showed that single ion micro-irradiation induced a local decondensation of heterochromatin at the sites of ion hits in murine chromocenters. This decondensation is accompanied by a relocation of the induced double-strand breaks (DSB) to an adjacent euchromatin, which might be a requirement for efficient repair [1]. To monitor this particle radiation-induced DNA decondensation quantitatively, we implemented a confocal FLIM scanner into the GSI accelerator beamline microscope [2], which can alternatively be used in combination with a 35 kV X-ray tube. As a primary aim of this study, we investigated a variety of fluorescent DNA dyes, e.g. Nuclear Green and DAPI as candidate probes for the chromatin condensation status. To evaluate the dyes, we set criteria addressing three different properties: (i) the excitation wavelength of the DNA dye has to be compatible with available picosecond lasers; (ii) the DNA dye must show sufficient discrimination between lifetime of condensed and non-condensed areas and (iii) the dye has to be stable over extended time of illumination in measurements of decondensation kinetics. Our results demonstrate that DAPI is a promising DNA dye for FLIM based DNA decondensation measurements in our setup since it exhibits both clear discrimination between lifetime of condensed and non-condensed areas and photostability, whereas, e.g. Nuclear Green reveals superior discrimination between condensation states, but suffers from low photostability. Also, using DAPI we could demonstrate an increased fluorescence lifetime in the euchromatin of living murine cell nuclei indicating chromatin condensation after ATP depletion. In a further step, the DNA dye will be complemented by a

damage marker to identify ion irradiation sites. The feasibility was demonstrated by combining DAPI with XRCC1 using immunocytochemistry.

[1] B. Jakob et al., NAR, 1-11 (2011).

[2] B. Jakob et al., Radiat.Res. 163, 681-690 (2005).

A micro-pattern gaseous detector for beam monitoring in ion-therapy

TERAKAWA, Atsuki 1*; ISHII, Keizo 1; MATSUYAMA, Shigeo 1; MASUYAMA, Masataka 1; KUBO, Ryosuke 1; SATO, Tsuyoshi 1; INANO, Kotaro 1

1 Department of Quantum Science and Energy Engineering, Tohoku University

Recently, gas electron multiplier (GEM) technology has been studied in various fields to develop a new type of a gas detector system and shown significant advantages over a multi-wire proportional chamber such as the excellent special resolution and stable operation at higher counting rate. The aims of this study were to develop a micro-pattern gaseous detector based on GEM technology as a new transmission beam monitor for ion-therapy and to assess its feasibility on the basis of a performance test using therapeutic beams by evaluating two dimensional intensity distribution of the beam. The GEM detector used in this work consisted of a cathode plate, a GEM plate, and two window foils, and filled with a gas mixture (Ne 90% + CF₄ 10%). We used the glass-GEM plate (Hoya CO. LTD., Japan) made of a 680 μm thick glass sandwiched between 9 μm thick copper electrodes, and has holes in 140 μm in diameter with 280 μm distance. The advantage of the glass-GEM is higher gas gain compared to conventional GEM using organic substance as an insulator. An active area of the GEM detector was 100 \times 100 mm. When the GEM plate multiplies electrons induced by an incident ion-beam irradiation, scintillation is generated from the Ne-CF₄ gas and detected with a CCD camera. Thus, it is possible to evaluate a two-dimensional beam-intensity distribution (lateral beam distribution) from the distribution of scintillation. In order to evaluate characteristics of the GEM detector as a beam monitor in ion-therapy, the experiment was performed using an 80-MeV proton beam from the K=110-MeV AVF cyclotron and the proton irradiation system at Cyclotron and Radioisotope Center, Tohoku University. Therapeutic proton beams such as a broad beam for passive irradiation and a spot beam for scanning irradiation were delivered to the GEM detector. The experimental result demonstrated that the GEM detector provides the beam position and the lateral beam-profile simultaneously, and can be used for real-time beam-profile monitoring in ion-therapy.

Radon exposure setup and solubility in different types of tissue

MAIER, Andreas 1*; VAN BEEK, Patrick 1; HELLMUND, Johannes 1; FOURNIER, Claudia 1; DURANTE, Marco 1; KRAFT, Gerhard 1;

1 GSI, Darmstadt

Low doses of ionising radiation and alpha particles are used for therapy of inflammatory diseases. In addition the genetic risk of low dose alpha exposure is of special interest. In both cases the molecular mechanisms of the radon uptake, the chemical path of the decay products and the subsequent biological reaction are not known at a molecular scale. To study the radiobiological effects of Radon exposure in vitro and in vivo under controlled conditions we constructed a Radon exposure chamber. With this device we are able to expose samples at different conditions including the radon galleries in Germany and Austria. Adjustable parameters like Radon activity-concentration, exposure time, temperature and humidity are permanently monitored and controlled. During experiments with cell cultures the chamber provides cell culture conditions. In addition, experiments with small animals can be performed with this setup. To measure the radon kinetics in different types of tissue we exposed tissue samples and mice in the Radon chamber and measured the γ -spectrum of the Radon decay products in the exposed samples with a HPGe-Detector. In these measurements it was possible to distinguish the short living decay products Pb-214 and Bi-214. We recorded the spectra at different time points after exposure and compared the results from different types of tissue like fat or muscle but also activated coal. In an activated coal sample the decay spectra are governed by the life time of the bound Radon (3,8 days). In contrast, in the biological samples the primary Radon diffuses out of the samples and the spectra follow the kinetics of the decay of the daughter products. Therefore in the data analysis their radioactive decay has to be combined with a diffusion term for the primary Radon. First analyses show that the Radon diffusion time constant is in the order of a few minutes but slightly different for different tissues. We want to show the basic concept of the Radon-chamber, the γ -spectroscopy setup as well as first results.

Work is supported by BMBF GREWIS-Projekt (Genetische Risiken und entzündungshemmende Wirkung ionisierender Strahlung 02NUK017A).

Synthesis and characterization of ZnO/TiO₂ nanostructured photo-electrodes by electrodeposition in etched ion-track templates

MOVSESYAN, Liana 1,2*; MAIJENBURG, Albert Wouter 1; SPENDE, Anne 1,2; GOETHALS, Noel 3; SCHUBERT, Ina 1; TRAUTMANN, Christina 1,2; TOIMIL-MOLARES, Maria Eugenia 1

1 GSI Helmholtz Center for Heavy Ion Research, Darmstadt; 2 Technische Universität Darmstadt; 3 Technische Hochschule Mittelhessen

Based on the unique properties of nanoscale materials, three dimensional (3D) assemblies of nanowires are promising structures for applications in various fields such as electronics,

sensorics, photonics, thermoelectrics, and energy applications. We report the synthesis of ZnO/TiO₂ nanowire arrays and interconnected nanowire networks by means of ion-track technology and atomic layer deposition, as well as their application as nanostructured photoelectrodes. Due to their elongated geometry and reduced diameter, nanowire arrays are expected to exhibit higher light absorption and more efficient charge separation and transport than continuous films of same composition and thickness, being thus of great interest for photoelectrochemical applications such as water splitting. First, ZnO nanowires were fabricated by electrodeposition in polycarbonate etched ion-track membranes. This template-based technique allows us to fabricate large arrays of micro- and nanowires with excellent control on wire size and geometry, morphology, crystallographic structure, and composition. ZnO nanowires with lengths up to 30 μm and diameters between 40 and 300 nm were grown from 0.1 M zinc nitrate hexahydrate ($\text{Zn}(\text{NO}_3)_2 \cdot 6\text{H}_2\text{O}$) aqueous solution. We studied the influence of parameters such as applied potential, temperature, electrolyte concentration, and template type (pore diameter or geometry) on the morphology and crystallographic properties of the wires. Integration density and wire diameter were optimized in order to obtain self-supporting 3D nanowire networks after dissolution of the polymer template. In some cases, atomic layer deposition was applied to conformally coat the ZnO wires with a few nm thin TiO₂ layer. ZnO and ZnO/TiO₂ core/shell nanowire networks were tested as photo-electrodes for photoelectrochemical water splitting. Preliminary results showed higher photocurrent for the nanostructures compared to corresponding films.

Ion track etching in PVDF irradiated with uniform ion beam in an oxygen atmosphere

KITAMURA, Akane 1*; YAMAKI, Tetsuya 1; YURI, Yosuke 1; KOSHIKAWA, Hiroshi 1;
SAWADA, Shinichi 1; YUYAMA, Takahiro 1

1 Japan Atomic Energy Agency

A uniform-beam formation/irradiation system using multipole magnets has been developed at TIARA of JAEA. In our previous report, the absolute particle fluence distribution of the beam was microscopically revealed using the track-etching technique, and the measured uniformity was in good agreement with that obtained from the radiochromic films. These results demonstrated that our uniform-beam system would give a useful technique for the mass-production of materials. We have focused on poly(vinylidene fluoride) (PVDF), one of fluoropolymers, because it has excellent properties as super-engineering plastic materials. This study deals with the chemical effect in PVDF films irradiated using our uniform-beam system. Commercially-available PVDF films (25 μm in thickness) were irradiated in an oxygen atmosphere with a 520-MeV 40Ar uniform beam using our system. The beam was extracted through a 30 μm -thick Ti foil window to reach the sample; the kinetic energy on the sample surface was estimated to be approximately 330 MeV by a SRIM code. For comparison, PVDF films were also irradiated in vacuum with 330 MeV 40Ar beam using a conventional system. The fluence was chosen between 1.0E7 and 6.0E11 ions/cm². The irradiated samples were etched in 9 M KOH at 80 °C. The surface morphology was observed with a scanning electron microscope, and the molecular structure was analyzed using Fourier transform infrared spectroscopy. The irradiation with uniform beam in an oxygen atmosphere was found to make the etching rate of pores fast. At a fluence of 6.0E11

ions/cm², more oxygen-containing functional groups were formed. It is well known that oxidation of ion tracks accelerates the etching rate. Therefore, the irradiation in oxygen using our uniform-beam system would promise to develop a rapid track-etching process.

Nano-ARPES on individual electrodeposited Bi₂Te₃ nanowires fabricated by ion-track technology

KRIEG, Janina 1,2; CHEN, Chaoyu 3; AVILA, José 3; TRAUTMANN, Christina 1,2;
ASENSIO, Maria-Carmen 3; TOIMIL-MOLARES, Maria Eugenia 1;

1 GSI Helmholtz Center for Heavy Ion Research, Darmstadt; 2 Technische Universität Darmstadt; 3 Synchrotron Soleil, Gif-sur-Yvette, France

Bi₂Te₃ belongs to a new class of materials, called topological insulators, promising for future dissipationless electronics and spintronic applications. One of their exotic properties is the formation of conductive surface states while the bulk material is an ordinary band insulator. The major challenge to address the surface states is the reduction of the large concentration of residual bulk carriers dominating over the signal of the surface states. Nanowires of high surface-to-volume ratio combined with controllable geometric, crystallographic and morphologic properties are excellent candidates to investigate the surface states. We synthesize Bi₂Te₃ nanowires applying electrodeposition in the channels of ion-track etched polymer templates. The templates are fabricated by irradiating 30 µm thick polycarbonate foils with GeV heavy ions and subsequently creating cylindrical channels with diameters of 100 nm by selective chemical etching of the ion tracks. Followed by electrodeposition of Bi₂Te₃ within the channels, nanowires are fabricated. Their chemical composition and crystallographic structure are analyzed by HRSEM, EDX, TEM, and XRD. After removing the polymer template, the nanowires are transferred onto suitable substrates. X-ray photoemission (XPS) and angle resolved photoemission spectroscopy (ARPES) with sub-micron resolution were conducted on single nanowires at the SOLEIL Synchrotron. Single nanowires were identified by scanning the area of interest and detecting only photoelectrons of a certain energy (corresponding to Bi or Te). The obtained mappings show that our single nanowires can be localized and resolved using the nanoARPES at ANTARES. First experiments focused on XPS analysis of the nanowire surface as a function of time (i.e. oxidation effects), and on studying the influence of different cleaning methods (e.g. annealing, plasma etching) on the nanowire surface quality. By detecting the emission angle of the photoelectrons, the band structure of the nanowires can be investigated. To the best of our knowledge this was done for the first time on individual Bi₂Te₃ nanowires with diameters of 50 nm.

Swift heavy ion induced synthesis of Ag/Pt nanorods in silica matrix

PANNU, Compesh 1; AVASTHI, D. K. 1; KABIRAJ, Debdulal 1; NITYA, Ramanan 2*; LAHIRI, Debdatta 2; SATPATI, Biswarup 3; CHATTOPADHYAY, Soma 4; SHIBATA, Tomohiro 4; TAK, Ritu 2

1 Inter-university Accelerator Center, Aruna Asaf Ali Marg, New Delhi 110067, India; 2 High Pressure & Synchrotron Radiation Physics Division, Bhabha Atomic Research Centre, Mumbai - 400085, India; 3 Surface Physics & Material Science Division, Saha Institute of Nuclear Physics, Kolkata 700 064, India; 4 BCPS Department, Illinois Institute of Technology, Chicago, Illinois 60616, USA and CSRRI-IIT, MRCAT, Advanced Photon Source, Sector 10, Argonne, Illinois 60439, USA

Aligned bimetallic nanorods are of wide practical interest for multiplexing, coding, biophysics applications. Swift Heavy Ion Irradiation (SHII) offers the possibility of generating such nanorods (in insulating matrix) by utilizing the directional reference of the ion track in the matrix. In this work, we investigate the possibility of generating aligned bimetallic nanorods of Ag/Pt, an immiscible binary system, in silica matrix. Thin film of silica containing Ag-Pt nanoparticles were prepared by atom beam cosputtering technique. The thin films were irradiated with 100 MeV Au ions, at fluence ranging from to ions/cm². We have characterized the system both pre- and post-SHII using several characterization techniques to derive its structural and compositional picture: (i) TEM shows well-separated, nanoparticles pre-SHII [average size = 1.5-2.5nm, aspect ratio=1], which elongate post-SHII [average size= 8nm×44nm, aspect ratio~6, irradiation fluence = 1×10^{14} ions/cm²]; (ii) Optical Absorption Spectra show no Surface Plasmon Resonance bands corresponding to Ag or Ag/Pt. Platinum particles lack visible-region plasmon absorption. (iii) Selective Area Diffraction reveals diffuse rings corresponding to amorphous phase; (iv) X-ray Diffraction lacks crystalline peaks and shows strong resemblance to metallic glass; (v) X-ray Absorption Fine Structure (XAFS) at Pt L3 and Ag K edges revealed that both Ag and Pt possess only first nearest neighbors, confirming glassy structure both pre- and post-SHII. XAFS coordination number (N) of pre-SHII thin film was evaluated to be 7, 2, 0 and 11 for Pt-Pt, Pt-Ag, Ag-Pt and Ag-Ag respectively. Which change to 11, 1, 0, 11 in post-SHII samples for Pt-Pt, Pt-Ag, Ag-Pt and Ag-Ag respectively. NAg-Pt=0 due to intrinsic resolution limit (10%) for Pt detection from Ag K edge analysis. The most plausible model for the system is amorphous Ag-Pt alloy, similar to metallic glass, which undergoes SHII-induced elongation. Thus, we establish feasibility of SHII as synthesis method for amorphous (glassy) bimetallic nanorods. We contemplate the influence of amorphous structure on the applications of these nanorods.

**Variation in geometry and electrical conductance properties of asymmetric
Track-etched single nanopores: how uniform are they?**

APEL, Pavel 1,2; OLEJNICZAK, Katarzyna 1,3*; ORELOVITCH, Oleg 1

1 Joint Institute for Nuclear Research, Joliot-Curie str. 6, 141980 Dubna, Russia; 2 Dubna International University, Universitetskaya str. 19, 141980 Dubna, Russia; 3 Nicolaus Copernicus University, Gagarina str. 7, 87-100 Torun, Poland

Recently, artificial single nanopores have been receiving more and more scientific attention due to their applicability in nanofluidics, sensor technology and information processing. Because of this elaboration of a procedure for obtaining single-pore membranes with well-defined and highly-reproducible structural and electrical properties is of particular importance today. Single ion tracks in 12 μm thick polyethylene terephthalate (PET) films were obtained by irradiation of samples with Xe and Au ions at the IC-100 cyclotron (FLNR JINR, Dubna, Russia) and the UNILAC linear accelerator (GSI, Darmstadt, Germany), respectively. The tracked samples were subjected to one-sided exposure to ultraviolet radiation and etched in the presence of a surface-active agent to obtain asymmetric pores with highly-tapered tip. The chemical treatment was carried out in a surfactant-doped 5 mol/L NaOH solution for 6.5 min at 60 °C, identical for all samples. To confirm that the membranes are single-pored the electron microscopy investigations were performed. In parallel, multi-pore samples were examined to characterize the pore geometry. The uniformity of the single pores in PET membranes was determined from electro-conductivity data. The electrical conductance, effective pore diameter and rectification ratio of individual pores were measured. The data were compared with geometrical characteristics of the pores determined by SEM. The shape of the current-voltage curves was asymmetric, typical of negatively charged nanopores with a pronounced diode-like behavior. The maximum rectification ratio for all samples was observed at KCl concentration in the range of 0.05-0.4 mol/L. The variation in properties of individual single pores and the reproducibility of electric current measurements for the same pore were investigated and discussed.

**Ion-track grafting of vinyl benzyl chloride into poly(ethylene-co-tetrafluoroethylene)
film by different ion beams**

YAMAKI, Tetsuya 1; NURYANTHI, Nunung 2*; TERAJ, Takayuki 2; KITAMURA, Akane 1; KOSHIKAWA, Hiroshi 1; ASANO, Masaharu 1; SAWADA, Shin-ichi 1; YOSHIMURA, Kimio 1; HASEGAWA, Shin 1; MAEKAWA, Yasunari 1; SUZUKI, Akihiro 2

1 Japan Atomic Energy Agency; 2 Department of Nuclear Engineering and Management, The University of Tokyo

A swift heavy ion of several hundreds of MeV to a few GeV induces a continuous trail of excitation and ionizations, called a latent track, when passing through a polymer substrate. Each track contains high-density and localized macromolecular radicals, which can act as initiator for graft polymerization. The technique for introducing functional groups directly into

the tracks is known as the ion-track grafting. We have used the ion-track grafting technique for developing an anion exchange membrane for fuel cell applications. In order to obtain the membrane, a vinyl benzyl chloride (VBC) was grafted into an ion-irradiated poly(ethylene-co-tetrafluoroethylene) (ETFE) film. The 25 micrometer-thick ETFE films were irradiated with ^{129}Xe ions at two different energies, i.e., 450 and 560 MeV. In spite of employing the same grafting conditions as well as the very similar beams, the degree of grafting (a measure of reactivity) were found quite different. We attributed this finding to a much greater change in the shape of the membranes grafted with the lower-energy beam; even so, the VBC grafting could largely depend on the irradiation conditions. Therefore, there is a strong motivation to investigate how different ion beams affect a grafting mechanism. This study deals with the ion-track grafting of VBC into the ETFE films irradiated with a variety of ion beams from the cyclotron of Takasaki Ion Accelerators for Advanced Radiation Application (TIARA) facility, JAEA. The accelerated ions with different masses and energies enabled us to clarify the effect of the LET and radial dose distribution in the track on the VBC grafting. Such extensive research will bring us interesting knowledge relating the track structures to the resulting membrane properties.

Characterization of thermoelectric $\text{Bi}_{1-x}\text{Sb}_x$ nanowires electrodeposited in etched ion track membranes

CASSINELLI, Marco 1,2*; TOIMIL MOLARES, Maria Eugenia 1; MÜLLER, Sven 1; VOSS, Kay-Obbe 1; SIGLE, Wilfried 3; TRAUTMANN, Christina 1,2;

1 GSI Helmholtz Center for Heavy Ion Research, Darmstadt; 2 Technische Universität Darmstadt;

3 Max Planck Institute for Intelligence Systems

Nowadays, the negative impact on the environment by energy production based on fossil fuel is a serious concern. Thermoelectrics offers a path for clean and more sustainable energy production by converting thermal energy into electrical power [1, 2]. In the 90s it was predicted that the efficiency of thermoelectric materials can be increased via quantum- and finite size effects, and $\text{Bi}_{1-x}\text{Sb}_x$ nanowires were proposed as suitable model systems to investigate these effects [3, 4]. We have fabricated thermoelectric $\text{Bi}_{1-x}\text{Sb}_x$ ($0 < x < 1$) nanowire arrays by electrodeposition in etched ion-track membranes. 30 μm thick polycarbonate membranes were irradiated with GeV heavy ions at the UNILAC, linear accelerator of GSI, and afterwards, the ion tracks were chemical etched to form cylindrical channels with diameters between 15 and 130 nm [5]. $\text{Bi}_{1-x}\text{Sb}_x$ nanowires were synthesized using both potentiostatic [6] and pulsed electrochemical deposition. X-ray diffraction (XRD) and transmission electron microscopy (TEM) analysis were performed revealing the crystalline structure of such nanowires. The Seebeck coefficient of nanowire arrays embedded in the membrane was measured as a function of the nanowire composition and diameter. Finally, we have studied the thermal stability of $\text{Bi}_{1-x}\text{Sb}_x$ nanowires to assess their reliability towards device applications. Nanowires were transferred onto Si wafers and thin carbon-coated TEM grids. The nanowires were thermally annealed between 100 °C and 250 °C in air for 2, 20 and 100 hours. Morphology and composition of the nanowires were analyzed by both SEM and TEM before and after the annealing process.

- [1] G. Pennelli, Beilstein Journal of Nanotechnology, 5 (2014) 1268-1284.
- [2] M. H. Elsheikh et al., Renewable and Sustainable Energy Rev., 30 (2014) 337-355.
- [3] L. D. Hicks and M. S., Phys. Rev. B 47 (1993) 16631.
- [4] O. Rabin, Y.-M. Lin, and M. S. Dresselhaus, Appl. Phys. Lett. 79 (2001) 81.
- [5] M. E. Toimil-Molares, Beilstein Journal of Nanotechnology, 3 (2012) 860-883.
- [6] S. Müller et al., Journal of Crystal Growth 12 (2012) 615-521.

Atomic layer deposition of Al_2O_3 , TiO_2 , and SiO_2 in etched ion-track polycarbonate membranes

SPENDE, Anne 1,2*; SOBEL, Nicolas 3; HESS, Christian 3; LUKAS, Manuela 4; STÜHN, Bernd 4; MONTERO MORENO, Josep M 5; ZIEROLD, Robert 5; NIELSCH, Kornelius 5; TRAUTMANN, Christina 1,2; TOIMIL-MOLARES, Maria Eugenia 1

1 GSI Helmholtz Center for Heavy Ion Research, Darmstadt; 2 Material- und Geowissenschaften, Technische Universität Darmstadt; 3 Eduard-Zintl-Institute for Anorganic Chemistry and Physical Chemistry, Technische Universität Darmstadt; 4 Experimental condensed matter physics, Technische Universität Darmstadt; 5 Institute for Applied Physics, Universität Hamburg

Inorganic nanochannels integrated in solid state membranes are of high relevance for both basic research and industrial applications in various fields such as nanofluidics, catalysis, and filtration. Tailoring of the characteristic dimensions and surface properties of the nanostructures requires the development of suitable fabrication techniques. We present a novel approach modifying the surface of etched ion-track polycarbonate (PC) membranes by low-temperature atomic layer deposition (ALD). PC membranes with ion tracks of 30 μm length are produced by irradiating PC foils with swift heavy ions at the UNILAC accelerator of GSI. By subsequent chemical track etching cylindrical nanochannels with defined diameter down to 18 nm were obtained. In order to functionalize the surface and reduce the diameter further in a precisely controlled manner, these membranes were coated by ALD with layers of alumina (Al_2O_3), titania (TiO_2), and silicon dioxide (SiO_2). Being a sequential, self-limiting process, ALD coating is controlled layer by layer. Small angle x-ray scattering characterization of average channel diameter, diameter distribution, and ALD layer thickness of all membranes before and after coating evidences a homogeneous and conformal coating of the nanochannels along their entire length. In addition, XPS demonstrates stoichiometric compositions. Furthermore, the grown nanostructures were released from the supporting polymer templates by wet-chemical methods and STEM-in-SEM analysis evidenced the successful fabrication of SiO_2 , TiO_2 , and Al_2O_3 nanotubes with precisely controllable diameter and wall thickness. EDX studies of the nanotubes confirmed the homogeneity of the ALD process inside the nanochannels.

A model of chemical etching of olivine in the vicinity of the trajectory of a swift heavy ion

GORBUNOV, Sergey 1*; RYMZHANOV, Ruslan 2; VOLKOV, Alexander 1-3;

1 LPI of the Russian Academy of Sciences, Leninskij prospekt, 53, 119991 Moscow, Russia;
2 JINR, 141980 Dubna, Russia; 3 1 NRC Kurchatov Institute, Kurchatov Sq. 1, 123182 Moscow, Russia

Searching of superheavy elements, OLYMPIA experiment (LPI, Moscow) investigates the charge spectra of heavy nuclei in Galactic Cosmic Rays using the database of etched ion tracks in meteorite olivine. Etching results in formation of hollow syringe-like channels with the diameter of 1-10 μm depending on the chemical activity of the olivine lattice around the trajectories of these swift heavy ions (SHI). According to the activated complex theory the local chemical activity is determined by an increase of the specific Gibbs energy of the lattice stimulated by structure transformations and long-range elastic fields generated in the vicinity of the ion trajectory. The presented hybrid model is applied to determine this Gibbs energy change enabling a calibration of the etching data e.g. by a comparison with the results of irradiations of olivine at SHI accelerators. At the first stage (≤ 100 fs after the ion impact) the original Monte-Carlo (MC) code TREKIS is applied to describe excitation of the electron subsystem of olivine in a SHI track. The data obtained from MC simulations are used as an input for the model describing energy transfer to the lattice during relaxation the electron ensemble in a track. The cross-sections describing the kinetics of excitations of electron and atomic subsystem are calculated in the framework of the Dynamical Structure Factor – Complex Dielectric Function formalism. This approach automatically takes into account peculiarities of collective responses of the electron subsystem and lattice to perturbations in SHI tracks. The molecular dynamics (MD) approach is applied to describe relaxation of the excited olivine lattice (> 100 fs) causing structure transformations in the nanometric vicinity of the ion trajectory. These transformations result also in long range elastic fields changing the specific lattice Gibbs energy which determines the etching rate of olivine.

Investigations on heavy ion induced Single-Event Transients (SETs) in highly-scaled FinFETs

GAILLARDIN, MARC 1*; FAYNOT, Olivier 2; RAINE, Melanie 1; PHILIPPE, Paillet 3;
GIRARD, Sylvain 4; ADELL, Philippe C. 5; DUHAMEL, Olivier 3; ANDRIEU, Francois 2;
BARRAUD, Sylvain 2

1 CEA; 2 CEA, LETI-Minatec, 17 avenue des Martyrs, 38000 Grenoble, France; 3 CEA, DAM, DIF, F-91297 Arpajon, France; 4 Université de Saint-Etienne, Laboratoire H. Curien, UMR-5516, 42000, Saint-Etienne, France; 5 Jet Propulsion Laboratory, Pasadena, CA 91101, USA

Multiple-gate transistors have been developed to push the limits of silicon-based devices towards the nanometer scale. Several architectures such as FinFET, multiple-gate Field Effect Transistor (FET), or planar double-gate transistors have been proposed by several

research teams to significantly reduce short channel effects and to improve electrical performances compared to their single-gate counterparts. For a long time considered as academic devices, multiple-gate transistors and FinFETs are now included in mainstream applications. Indeed, Intel has recently introduced bulk Tri-Gate FETs to process Integrated Circuits (ICs) at the 22 nm node. Radiation effects in those kinds of devices have been studied since the early 90's. Most studies based on experimental results were devoted to Total Ionizing Dose (TID) effects in multiple-gate transistors. Others were dedicated to heavy ion induced micro-dose effects but only few studies focused on Single-Event Effects (SEE). The objective of this paper is thus to get insights into the Single-Event Transient (SET) phenomena in FinFETs and nanowires as function of the device design in order to estimate their SEE sensitivity for space applications. Charge collection mechanisms are investigated using a statistical analysis of the charge collected on elementary devices irradiated with heavy ion broad beams. Then, the influence of the main geometrical device characteristics on the experimental data is presented. The impact of the amount of injected charge related to the incident particle Linear Energy Transfer (LET), the effect of scaling and the influence of the 3D multiple-gate architecture are analyzed using both experimental and simulation results to separate all physical mechanisms which govern the SET response of innovative multiple-gate transistors. Finally, implications for multiple-gate device design hardening are discussed, leading to the proposition of some guidelines.

High Energy Irradiation Experiments with a modified Paris-Edinburgh-Cell

BURCHARD, Michael 1*; DEDERA, Sebastian 1; TRAUTMANN, Christina 2;
GLASMACHER, Ulrich A. 1

1 University of Heidelberg; 2 GSI, Darmstadt

Originally, Paris-Edinburgh-cells (PE-cells) have been developed for investigations with neutron diffraction under high pressure.

This basis has been used to build a PE-cell, which can be used for irradiation of a high payload (up to 4 mm³) with high energy swift heavy ions. Additionally, it should be possible to measure "in situ" the irradiated samples with a Raman spectroscope to determine the actual pressure impacting on the sample on the one hand, and to investigate material changes of the sample caused by pressure and irradiation on the other hand. Therefore, two new stamps have been developed. The new stamps have the outer dimensions of the old stamps, so they can be used in any available system. To perform Raman measurements of built in samples, the new stamps have been equipped with an aperture closed with a spherical diamond windows per stamp.

In March and August 2014 three irradiation experiments have been performed with the new system, where calcite and malachite crystals have been irradiated with swift heavy ions. The experiments showed, that the preparation of the cells as well as the measurability of the crystals inside the cells work very well and it was possible for the first time, to determine the exact pressure inside the chamber with Raman shifts. Furthermore, all new parts including the diamonds survived the experiment undamaged, which emphasizes the good design of the modifications.

After these first experiments to test the new system, a new tool to irradiate high volumes of matter with swift heavy ions and subsequent in situ measurement of the samples is at hand.

Formation of Nanodroplets in N₂/H₂O/SO₂ under Irradiation of Fast Proton Beams

NAKAI, Yoichi 1*; TOMITA, Shigeo 2*; FUNADA, Shuhei 2; PEDERSEN, Jens Olaf Pepke 3; HVELPLUND, Preben 4; KOBARA, Hitomi 5; SASA, Kimikazu 6;

1 RIKEN Nishina Center; 2 Institute of Applied Physics, University of Tsukuba; 3 National Space Institute, Technical University of Denmark; 4 Department of Physics and Astronomy, Aarhus University; 5 Research Institute for Environmental Management Technology, National Institute of Advanced Industrial Science and Technology (AIST); 6 Tandem Accelerator Complex, University of Tsukuba;

The droplet formation induced by cosmic ray in the terrestrial atmosphere attract certain attention in recent decades because this process could be important to understand the possible relationship between cosmic ray and climate on the earth. The role of energetic ions for the droplet formation would be in both the ion production and oxidation of SO₂ in the air. Attractive polarization forces between ions and molecules decrease energy barrier in droplet growth. On the other hand, the oxidation of SO₂ by radical species in ion irradiation result in the production of H₂SO₄, which also decrease energy barrier of the droplet growth in the binary nucleation process of water and H₂SO₄.

We have performed irradiation of proton beam on the gas mixture of N₂/H₂O/SO₂ and Air/H₂O/SO₂. The reduction of SO₂ concentration by beam irradiation was monitored using an SO₂ meter and the size distributions of generated droplets were measured with a differential mobility analyzer. We found that the mass yield of generated droplets showed linear dependence on the amount of SO₂ oxidation. This behavior is different from binary nucleation theory of water and H₂SO₄. The difference might indicates importance of considering the droplet formation to be a kind of cooperative phenomena by ion processes and oxidation of SO₂.

Symmetric Neutralized Heavy Ion Beam Transport to Material Targets

HICKS, Nathaniel 1*

1 University of Alaska Anchorage

In cases where it is desired to deliver an ion beam with very little net charge to a target, a positive ion beam can be neutralized with electrons. However, it may be beneficial to inject a beam with no electron content. In this case, the beam may be neutralized by using positive and negative ions such that the beam has net electrical neutrality. In particular applications where a transverse magnetic fields is present, such beams may propagate without disturbance if the charge-to-mass ratios of the positive and negative species are identical. Particle-in-cell simulations of a range of such heavy ion beam scenarios are conducted, in order to study beam formation, transport to target, and ultimately interaction with neutrals. Attainable beam parameters are investigated, and applications to deposition in materials and modification of particular material targets are discussed.

Energy loss and charge state measurements of heavy ions in dense weakly coupled plasma

ALEX, Ortnner 1,2*; BLAZEVIC, Abel 1; ROTH, Markus 2; KRAUS, Dominik 1; SCHUMACHER, Dennis 1; CAYZAC, Witold Andrzej 1; HELFRICH, Jan 2; DEPPERT, Oliver 2; WAGNER, Florian 1; BEDACHT, Stefan 2; FALK, Steffen 3; TAUSCHWITZ, Anna 3; RIENECKER, Tim 3; SCHAUMANN, Gabriel 2; FRANK, Alexander 4

1 GSI Darmstadt, 2 TU Darmstadt; 3 Goethe-Universität Frankfurt am Main; 4 Helmholtz-Institute Jena

In this talk we present new experimental results on heavy ion energy loss and charge state measurements of Calcium ions interacting with a dense weakly coupled carbon plasma generated by thermal X-rays.

The energy deposition of ions in plasmas is a key question in ICF simulations, for the evaluation of heavy ions as drivers or ion driven fast ignition concepts. The GSI Helmholtzzentrum für Schwerionenforschung offers the unique possibility to create dense plasma states with the high energy laser PHELIX and to probe it with a heavy ion beam from the UNILAC accelerator. To convert the laser light into X-rays a special double hohlraum configuration has been designed which allows to generate a homogeneous carbon plasma with an electron density of up to 10^{22} cm^{-3} , a temperature of 5-15 eV and an ionization degree of 2-3.

The measurements show an unexpected high increased in energy loss compared to the prediction of common theories.

Multiwalled carbon nanotubes as masks against carbon irradiation. A molecular dynamics study

DENTON, Cristian D. 1*; MORENO-MARÍN, Juan Carlos 2; HEREDIA-AVALOS, Santiago 2

1 Departamento de Física Aplicada, Universidad de Alicante, E-03690, Spain; 2 Departamento de Física, Ingeniería de Sistemas y Teoría de la Señal, Universidad de Alicante, E-03690, Spain

Experiments showed that multiwalled carbon nanotubes (MWCNT) can be used as masks against irradiation to create metallic nanowires in a substrate [1,2]. In order to understand the limitations of this application, it is interesting to know the energy and number of carbon atoms emerging from the MWCNT after the irradiation and how the structure of the MWCNT is modified. Using a molecular dynamics code that we have previously developed [3], we have simulated the continuous irradiation of MWCNT with carbon projectiles.

We have analyzed the number, energy, and spatial distribution of the recoils generated during irradiation and the change of the MWCNT structure as a function of the incident energy, dose and number of shells of the MWCNT. These results determine the effectiveness of MWCNT as a mask, being useful to understand whether the atoms emerging from the MWCNT produce damage in the substrate or not.

- [1] Yun et al., J. Vac. Sci. Technol. A 18 (2000) 1329.
 [2] Krashennnikov et al., Appl. Phys. Lett. 81 (2002) 1101.
 [3] Heredia-Avalos et al., Nucl. Instrum. Meth. Phys. Res. B 326 (2014) 37.

11 - Simulations

Tu-PB62

Monte-Carlo simulations of excitation of the electron subsystem of ZnO and MgO in tracks of swift heavy ions

VOLKOV, Alexander 1,2,3*; RYMZHANOV, Ruslan 4; VORONKOV, Roman 5

1 NRC Kurchatov Institute, Kurchatov Sq. 1, 123182, Moscow, Russia; 2 FLNR, JINR, Joliot-Curie 6, 141980 Dubna, Russia; 3 LPI of the Russian Academy of Sciences, Leninskij prospekt, 53, 119991 Moscow, Russia; 4 Joint Institute for Nuclear Research; 5 NRNU MEPhI, Kashirskoe sh. 31, 115409 Moscow, Russia

Kinetics of material excitation in the nanometric vicinity of the trajectory of a swift heavy ion (SHI track, $E > 1$ MeV/nuc) decelerated in the electronic stopping regime depends crucially on the parameters characterizing the excited electron ensemble of a target at sub-picosecond times after the ion impact.

The original Monte Carlo (MC) code TREKIS is applied for event-by-event simulations of excitation of the electron subsystems of ZnO and MgO by a penetrating SHI and fast electrons generated in ionization cascades. Cross-sections used in this code are calculated within the framework of the dynamical structure factor - complex dielectric function (DSF-CDF) formalism. This enables considering all peculiarities of the collective response of the electron ensemble of a target to perturbation that is important taking into account the intensity and ultra-short temporal and spatial scales on the electron kinetics in a track. The experimental optical data are used for a reconstruction of the dependence of the CDF on the transferred energy. The calculated electron inelastic mean free paths and the energy loss of ions agree well with the NIST database and the results from SRIM code.

The temporal evolutions of the radial distributions of generated free electrons, valence and core holes as well as their energy densities in tracks of different ions in ZnO and MgO have been determined. The simulations demonstrate spatial propagation of two fronts of the electronic excitations. The velocities of these fronts are determined. The obtained data can be used as the initial conditions for quantitative models describing lattice excitation of these materials during relaxation of the excited electron subsystem of these solids in SHI tracks.

11 - Simulations

Tu-PB63

A dewetting picture for the evolution of thin solid films under swift ion irradiation

REPETTO, Luca 1*; LO SAVIO, Roberto 1; ANGELI, Elena 1; FIRPO, Giuseppe 1; VALBUSA, Ugo 1

1 Department of Physics - Università di Genova

Starting from experimental data on the modifications that supported chromium films undergo during 30 keV gallium ion bombardment, we have developed a continuum model where a

liquid-like picture is proposed to explain the surface morphologies that thin solid films show under ion irradiation [1]. In this picture, the film is destabilized by the contrasting actions of surface tension, dispersion forces and sputtering, and is considered only locally free to relax to a more favorable energetic configuration.

The bridge to the atomistic view is provided by the thermal spike model that predicts for the target a local transition to the liquid state upon the impact of a projectile of proper species and energy. The radius of the molten zone defines to which extent the relaxation process is local in nature, and thus plays a relevant role in the induced morphological modifications. As thermal spikes are predicted also for swift heavy ion irradiation, and the liquid-like phenomenology has been reported experimentally in this case too (e.g. [2]), the applicability of our model appears possible also when electronic stopping dominates the collision.

Here we analyze how the size of the track radius, under the hypothesis that it reflects the occurrence of a temporary transition to the liquid state, affects the dewetting of the film by simulating its evolution for several typical situations. In the case of swift heavy ions, the size of the molten zone can be correlated to ion species, their energy and targets by using consolidated models [3], thus providing a tool for further prediction and control of these processes.

[1] L. Repetto, B. Šetina Batič, G. Firpo, E. Piano, U. Valbusa. *Appl. Phys. Lett.* 100, 223113 (2012).

[2] T. Bolse, H. Paulus, W. Bolse. *Nucl. Instrum. Meth. B* 245, 264 (2006).

[3] A. Meftah, F. Brisard, J. M. Costantini, E. Dooryhee, M. Hage-Ali, M. Hervieu, J. P. Stoquert, F. Studer, M. Toulemonde. *Phys. Rev. B* 49, 12457 (1994).

11 - Simulations

Tu-PB64

Effect of electric field on kinetics of electron subsystem in tracks of swift heavy ions

RYMZHANOV, Ruslan 1*; MEDVEDEV, Nikita 2; VOLKOV, Alexander 1,3,4

1 FLNR, JINR, Joliot-Curie 6, 141980 Dubna, Russia; 2 CFEL at DESY, Notkestr. 85, 22607 Hamburg, Germany; 3 NRC Kurchatov Institute, Kurchatov Sq. 1, 123182 Moscow, Russia 4, LPI of the Russian Academy of Sciences, Leninskij prospekt, 53, 119991 Moscow, Russia

Excitation of the electron subsystem in the nanometric vicinity of the trajectory of a swift heavy ion (SHI track) results in temporal spatial separation of electrons and holes causing formation of positively charged track core. This unbalanced charge distribution can produce a strong electric field (so-called track potential). Depending on the charge-neutralization times, this track core potential might affect the kinetics of the electron subsystem or even result in the repulsion of positively charged target ions (Coulomb explosion).

The developed Monte Carlo model (TREKIS) describing the kinetics of the electron subsystem of materials in SHI tracks is used to study this effect in solid Al_2O_3 and SiO_2 targets. To simulate the effect of the track core, the mean electric field approximation of an infinite charged cylinder is applied.

The code uses cross sections of interaction of a charged particle with the electron subsystem of a target calculated via the complex dielectric function formalism. This allows to account for all the collective modes of the electron ensemble of the target. That is important at ultra-short temporal and spatial scales of the kinetics of electrons in a SHI track. Considering the spatial redistribution of excited electrons and valence holes in an ion track

region, the charge-neutralization time is estimated. Temporal and radial distributions of the densities and energies of excited electrons and of valence holes in the presence of the track electric field are compared with our earlier results excluding the track potential effect.

11 - Simulations

Tu-PB65

Computer simulations of ion beam shaping of Au nanocrystals

LEINO, Aleksi 1*; PAKARINEN, Olli 1; DJURABEKOVA, Flyura 2; NORDLUND, Kai 1

1 University of Helsinki; 2 Helsinki Institute of Physics

It is experimentally known that Au nanoparticles embedded in silica elongate under swift heavy ion irradiation. In a typical experiment the particles have a spherical shape before the irradiation and their diameters are ranging from 4 to 30 nm. MeV irradiation shapes the particles into nanorod or prolate shaped particles with the axis of elongation in parallel to the ion beam direction [1-2]. The exact dynamics of the elongation process are not very well understood.

Metal nanoparticles in an insulating matrix give rise to additional conduction electrons. The electrons act in response to external electromagnetic radiation, e.g. light, in a way that is depending on the size, shape, density and the alignment of the nanoparticles. Shaping of the particles by ion beams thus has potential applications in a variety of optical devices such as optical filters. For example, fine-tuning of the absorption maximum of the metal-insulator composite is possible by controlling the shape of the particles.

We use molecular dynamics (MD) and kinetic Monte Carlo simulations to study the elongation. At the MeV energy regime, the ions deposit their energy to the composite mainly through electronic stopping. This results in a highly excited electronic subsystem and in the occurrence of energetic electrons in the nanometric vicinity of the ion track right after the impact. The electrons later transfer their energy to the nuclei, which is typically approximated by inelastic thermal spike model, but the relaxation kinetics of the excited electronic subsystem can be modeled more realistically using Monte Carlo simulations. The current focus in our research lies in utilizing the results from these simulations in MD.

11 - Simulations

Tu-PB66

Stopping powers and ranges for the heaviest atoms

SAGAIK, Roman 1*

1 Joint Institute for Nuclear Research, Dubna, Russia

Notion of energy and angular distributions for heavy atoms of evaporation residues produced in nuclear fusion-evaporation reactions of accelerated heavy ions (HI) interacting with target nuclei is important for the conditioning of HI beam experiments. This notion becomes crucial in experiments on synthesis of superheavy elements (SHE) produced at the rate of several

atoms per month at present day HI beam intensities with the use of recoil separators for their detection. Transmission of SHE through the Dubna Gas-Filled Recoil Separator has been studied using TRIM simulations aiming at estimates of their slowing down and losses inside the separator. Extrapolations of stopping properties of solids and gases for HI with $82 \leq Z \leq 92$ to the region of SHE (around $Z=114$) demonstrate large uncertainties in their final values of ranges in a Si detector ('physical' experiments) as well as in a He+Ar gas mixture ('chemical' experiments). In the light of these uncertainties available experimental data on the stopping powers (SP) of some solids and gases for HI with $18 \leq Z \leq 92$ at energies $E < 20$ MeV/u have been analyzed within different empirical approaches aiming at a reliable extrapolation to the heaviest atoms ($Z > 92$). The analysis has shown that the examined semi-empirical parameterizations lead to the Mylar SP values which differ more than ten times from each other for $Z \geq 100$ in the energy region of interests (~ 0.1 MeV/u). An empirical approach has been proposed for SP estimates. It uses the hydrogen SP and effective charge (EC) together with the HI EC parameterization. Hydrogen data are well determined, whereas for the HI EC parameterization the measured values of HI SP available from a literature have been used, which relate to the same velocity and media as the hydrogen ones. In such a way the SP of the gases and solids can be determined for any moving atom with $Z \geq 18$ at the reduced velocity $V_{red} \leq 5$. In comparison to the examined empirical calculations the SP values derived for the heaviest atoms in this study seem to be more reliable and can be used in the conditioning of experiments on synthesis of SHE.

11 - Simulations

Tu-PB67

Two-temperature molecular dynamic simulations of swift heavy ion irradiation of freestanding graphene sheets

DJURABEKOVA, Flyura 1*; ÅHLGREN, Harriet 2*; LEINO, Alekski 2; DARASZEWICZ, Szymon 3; KRASHENINNIKOV, Arkady 4; NORDLUND, Kai 2; KOTAKOSKI, Jani 5

1 Helsinki Institute of Physics; 2 University of Helsinki; 3 University College London; 4 Aalto University; 5 University of Vienna

Porous graphene can act as a selective filter and an ultra thin sensor. The diameter of the pores has a great impact on the utilization of the membrane. We study the effect of swift heavy ion irradiation of graphene using molecular dynamic simulations augmented by two-temperature (temperatures of electronic and atomic sublattices) model. In the study we correlate the diameters of simulated pores to the stopping power of the ion. As we clearly see that the diameter of the defect can be controlled quite closely by the stopping power. The created defects are approximately round with varying diameters from few nm up to hundreds of nm's. This method provides a precise method for patterning graphene and creating porous graphene membranes for highly sensitive sensors and filters.

Ion-Track Formation at High Pressure: A Theoretical Approach

TOULEMONDE, Marcel 1*; DUFOUR, Christian 1; LANG, Maik 2; SCHAURIES, Daniel 3; ZHANG, Fuxiang 4; LI, Weixing 5; KLUTH, Patrick 3; TRAUTMANN, Christina 6; EWING, Rodney C. 5

1 CIMAP-GANIL, Caen, France; 2 UTK, Knoxville, Tennessee, USA; 3 ANU, Canberra, Australia; 4 Univ of Michigan, Ann Arbor, USA; 5 Stanford University, Stanford, USA; 6 GSI, Darmstadt, Germany

In the recent past, ion-beam irradiations have been combined with high pressure by injecting relativistic heavy ions at the GSI Helmholtz Center through several mm of diamond into solid samples pressurized in diamond anvil cells up to 50 GPa [1,2]. Drastic structural changes such as the formation and stabilization of new phases were observed that are not triggered by the applied pressure or the ions alone. Common for many radiation-induced material modifications at very high pressure is the increased efficiency of a single ion as compared with irradiation experiment at ambient pressure, such as the significantly reduced critical fluence for the monoclinic-to-tetragonal phase transformation in ZrO_2 [3].

While most irradiation experiments at high pressure focused on phase transformations at high fluences, little is known about single ion tracks. The simple question, e.g., whether the ion-track diameter increases or decreases if the irradiation is performed under pressure can currently not be answered. To address this issue, the inelastic thermal spike model was applied to describe track formation at ambient conditions [4] and as a function of increasing pressure. To account for the effect of pressure, the increase of the melting temperature under compression as well as the additional compressional energy in the pressurized solid was implemented. Calculations were performed for quartz (SiO_2) and zircon (ZrSiO_4) and the data are compared with a limited number of available experimental results from high-resolution transmission electron microscopy and small angle x-ray scattering.

[1] U.A. Glasmacher et al. Phys. Rev. Lett. 96, 195701 (2006)

[2] M. Lang et al. Nat. Mat. Lett. 8, 793 (2009)

[3] B. Schuster et al. Nucl. Instr. Meth. B 267, 964 (2009)

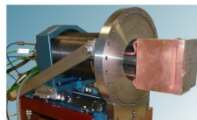
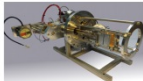
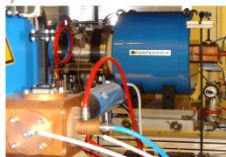
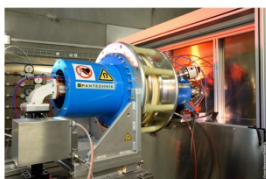
[4] M. Toulemonde et al. Mat Fys. Medd. 52, 263 52(2006).

Supported by



PANTECHNIK

Boost Your Physics



World leader in Electron Cyclotron Resonance (**ECR**) ion sources

- ✓ ECR for **Multiple charged state** beam production
- ✓ **Mono charged state** high intensity ECR Permanent Magnet
- ✓ Full **turn-key** systems for ion beam production
- ✓ Gas or metallic injection
- ✓ Beam Diagnostic systems
- ✓ Complete Command and Control



WWW.PANTECHNIK.COM

13 RUE DE LA RÉSISTANCE, 14400 BAYEUX - FRANCE T: +33 2 31 512 760

Authors index

Abdollahi	PB44	Baizhumanov	PA36
Abe	PA48	Bala	PA15
Adell	PB56	Balanzat	O26 PB20 O10 PB18
Afra	PA66 O25		PB40 I08 PB31 PB36
Agarwal	PA06	Ban d'Etat	PB29 I08 PB36 PA27
Ageev	O20	Banyasz	O30
Åhlgren	PB67	Bardin	PA07
Akbarov	PA61	Barraud	PB56
Akilbekov	PA36 PB32	Barriga-Carrasco	PA5
Alencar	PB25 PB28	Bauer, J. D.	PB28
Alex	PB60	Bauer, M.	O31
Alexander	PA04	Bayarjargal	PB28
Alzanova	PB34	Beceiro Novo	PA14
Amani	PA13	Becht	I01
Amekura	PB26	Bedacht	PB60
Amirthapandian	O31	Behar	PA46
Amroussia	O03	Bender	PA16 PB8 PB14 PB22
Andrieu	PB56		PB10 O12
Angeli	PB63	Benhacine	PA37
Apel	PA52 PB51	Benis	PA68
Arbeitman	PA46	Benyagoub	PA27 O13
Asai, K	PA40 PB38	Bereczky	PA48
Asai, T	PA3	Bergen	PA27
Asano	PA51 PB52	Bernard	PA58
Asdi	O31 PA08	Bernard-Carlsson	PB17
Asensio	PB49	Berneschi	O30
Ashokan	PB19 PA31 PA15 PA22	Bernstorff	PB29
Assmann	PB04	Bertarelli	PB11
Asylbayev	PA36	Beuve	I10
Auge	PA43 PA07 I14	Bizzaro	PB11
Aumayr	I13 PA27 PA69	Blazevic	PA59 PB60
Avasthi	PA06 PB50 PA38 PA15	Boduch	PA10 PA07 PB42 PB07
	PA34 PB26 PB23 PB6		PB8 O24 PB05 I14
	O17 PA39		PA43
Avila	PB49	Boehlert	O03
Avilov	O04 PB10	Bogdanović Radović	PB29
Azuma	I16	Bolse	O31 PA08 PB11
Backman	I09	Bolz	PB11
Bagnoud	PA59	Bordalo	PB8
Bagulya	PA50	Borghesi	I12

Bottländer	PB43				Costa Fraga	I01			
Bouffard	I13				Coughlan	I12			
Boughattas	PB40				Coulon	O16			
Brabetz	PA59				Cunha	I10			
Breuer	O22	PB22	PA11		Currell	I12			
Brucato	PB05				Czasch	I01			
Brunetto	PA07	I14			da Silveira	PA10	PB05	O24	
Bukowska	O08	PB22			DAMAJ	O10			
Buljan	PA60	PB29			Dannoux-Papin	O10			
Burchard	PA24	PB57	PA26	PB27	Daraszewicz	PB67			
	PB30				Dartois	PA07	I14		
Burr	O06				Dash	PB23	PB6		
Busold	PA59				Dauletbekova	PA36	PA37	PB32	PB34
Cao	O05				Dautel	O31			
Cardin	O16				Dauvois	PB40			
Carra	PB11				de Barros	PB42	I14	PA10	
Casas	PA5				de Combarieu	PB40			
Cassimi	PB05	PB36	I13	I01	De Filippo	PB04			
Cassinelli	PB53				Dedera	PA53	PA24	PB57	
Cayzac	PB60				del Grosso	PA46			
Cervera	PB17				Delauche	PA07			
CHABOT	I14				Della-Negra	PA13			
Chae	PA31				Deng	PA04			
Chattopadhyay	PB50				Denton	PB61			
Chen	O05				Deppert	PA59	PB60		
Chen	O14				Deutsch	O18			
Chen	O18				Dimitriou	PA68			
Chen	PA12				DING	I14			
Chen	PB49				Djurabekova	O25	PB67	PB65	I09
Cheng	O02				Dmitriev	PA52			
Cheng	PA04				Dohi	PA12			
Chernyavskii	PA50				Domaracka	I14	PA43	PA10	PA07
Chettah	PB26					PB07	PB8	O24	PB05
Chirtoc	O04				Dörner	I01			
Chisholm	PA32				Doukas	PA68			
Choudhary	PA38				Dromey	I12			
Ciocca	PB01				Du	O05	O14		
Clochard	PA49	I04			Duan	O05			
Cochin	O10	PB40			Dufour	PA69	O16	PB68	I13
Coignet	PB40				Duhamel	PA58	PB56		

Dunlap	PB16				Gafton	PB17			
Dunne	I12				Gaiduk	PA20			
Duprat	PA07				Gaillardin	PA58	PB56		
Durand	PB40				Galassi	PB01	PA64		
Durante	O15	PB46			Gao	O02	PB02	PA01	
Durantel	O03	PB36			Garcia Bermudez	PA46			
Echler	O29				Gardes	PB31	PB36		
Eddrief	PB17				Garmatter	O31			
Egelhof	O29				Gassert	I01			
Endeward	PB28				Gautam	PA31			
Engrand	PA07				Geng	O05			
Ensinger	PA41	PB37	PB35		Gilbert	O09			
Esnouf	PB40	O10			Girard	PB56			
Esteves	PB41				Glasmacher	PA53	PA24	PB57	PA26
Etgens	PB17					PB27	PB30		
Ewing	PB21	O27	O21	PA28	Godard	I14			
	O25	PB68	PB10		Goethals	PB47			
Fafin	O16				Goncharova	PA50			
Faik	PB60				Gorbunov	PA50	PA65	PB55	
Fainstein	PA64				Gorlachev	PA09			
Faynot	PB56				Gou	PA23	PB33		
Fazinić	PA60				Grabitz	O29			
Feil	PB41				Grants	PA25			
Feng	O02	PB02	PA01		Grisenti	I01			
Ferhati	O31	PB11			Gruber	PA27	I13		
Ferlet-Cavrois	I03				Grygiel	O26	PB20	PB18	PA27
Fernandes	O04	PB10				O03	I08	PB31	PB36
Ferry	O10	PB40				I13			
Firpo	PB63				Gu	O05			
Forck	PB35				Guerra	PB41			
Fournier	PB46				Guo, D	O02	PB02	PA01	
Frank	PB60				Guo, J.	O14			
Friedrich	PA44				Guo, N.	O14			
Fromentin	PB40				Gupta	PA15	PA16		
Frota da Silveira	PB42	PB07	I14		Gurbanov	PA61			
Fuchs	O18				Gutierrez	PB41	PA44	O11	PB39
Fujimoto	PA40	PB38			Gütlich	PB37			
Funada	PB58				Güven	PA55			
Furuya	PA47				Haag	O31			
Gacoin	O16				Hagmann	PB04			

Hasanov	PA61	Itoh	PA47	PA17	PA3
Hasegawa	PB52	Ivanov, I.	PA09		
Hashimoto	PA18	Ivanov, O.	PA52		
Haussühl	PB25 PB28	Iwamatsu	PB38		
Havranek	O30	Iwase	PA18	PB13	
Hayashi	PA70	Izumi	PA48		
Helfrich	PB60	Jaggi	PA14		
Hellmund	PB46	Jagutzki	I01		
Herder	PA11	Jahn	PA59		
Heredia-Avalos	PB61	Jahnke	I01		
Hermes	PB11	Jakob	O15		
Hess	PB54	Jakšić	PA60	PB29	
Hicks	PB59	Janis	O04		
Hidki	PB17	Janse van Vuuren	PA33		
Hierzenberger	PB9	Jianming	PB12		
Hijazi	PB05	Jin	PB24		
Himics	O30	Jonder	PB39		
Hirano	PA48	Jublot-Leclerc	I08		
Hiroki	PA42	Jung, A.	I01		
Hlatshwayo	PA21	Jung, D.	I12		
Hoffmann	PB15 PA04	Kabiraj	PA39	PB19	PB50
Hofsäss	PA16 PA13	Kadyrzhanov	PA57		
Hooda	PB19	Kalinina	PA50		
Hori	PA18 PB13	Kamalou	I14		
Horny	O04	Kaneko	PB3		
Hossain	PA41	Kaneno	PA18		
Hou	O05	Kanjilal	PA38	PB19	PB23
Huang	O02	Karlušić	O08	PB29	PA60
Hubert	PB16 PB14	Katba	PA31	PA22	
Hvelplund	PB58	Katrik	PB15		
Ibañez	PA46	Kawatsura	O01	PA2	
Ikeda	PA48	Kettunen	O29		
Ilze	O04	Khan	PA34	O17	PA06 PB19
Imai	O01 PA2	Khomenkov	O16		
Inano	PB45	Khomorenkov	PA69		
Indelicato	PA68	Kim	I01		
Ishii, Keizo	PB45	Kimura, A.	PB38	PA42	
Ishii, Koji	PB13	Kimura, Kazuie	PA40		
Ishikawa	O19 PA18 PB26 PB13	Kimura, Kenji	PA70	O23	
	I15	Kinoshita	PA2		

Kirby	O09	O25			Kurashima	PB38			
Kirilkin	PB32				Kuschel	I12			
Kislitsin	PA09				Lacaze	PB17			
Kitamura, A.	PA51	PB48	PB52		Lafosse	O16			
Kitayama	PA70	O23			Lahiri	PB50			
Kitzmantel	PB11				Laitinen	O29			
Klaumünzer	I05				Lamour	PA64	PB17	I02	
Kluth	I09	O09	O25	PA30	Lang	O27	O25	O21	PA28
	PA66	PB21	PB26	PB68		PB21	PB68	PB10	
Knörr	PA53				Langlinay	PB05			
Kobara	PB58				Lanzano	PB04			
Kobayashi, K.	PB13				Laoutaris	PA68			
Kobayashi, T.	PA48				Lattouf	PA27			
Kobylko	O16				Lebius	O26	PA27	PB29	I08
Kociak	O16					PB31	PB36		
Kodaira	PA62				Lederer	PB37	PB35		
Kojima	PA18				Legand	PB40			
Komaki	O01				Lei	PA04			
Komarov	PB34				Leino	O25	PB67	PB65	
Konovalova	PA50				Lenz	I01			
Koppe	PA13				Levavasseur	PA27			
Kornieieva	O20				Lévy	I02			
Korolkov	PA55				Lewis	I12			
Koshikawa	PA51	PB48	PB52		Li, B.	PA01			
Koshimizu	PA40	PB38			Li, J.-S.	PA62			
Kotakoski	PB67				Li, W.	PB68			
Kovalev	PB32				Li, Z.	PA12			
Kozlovskiy	PA57				Lieberwirth	PB37	PB35		
Kraft	PB46				Liu, Jiande	O05			
Kraft-Bermuth	O29				Liu, Jie	O07	O05		
Krashennikov	PB67				Liu, Tianqi	O05			
Kraus	PB60				Liu, Wenjing	O14			
Krauser	PA16	PA13			Liu, Wenqiang	O05			
Krieg	PB49				Lizunov	PA52			
Kuberkar	PA31	PA22			Lo Savio	PB63			
Kubo	PB45				Losquin	O16			
Kuhn	PA63				Louette	O11	PB39		
Kumar, M.	PA34				Lüdde	I01			
Kumar, N.	PA14				Lukas	PB54			
Kupka	PB16	PB14			Luo	O05			

Lv	PB07	PB8	I14		Mittig	O03	O04	PA14	PB10
Ma	PA04	O02	PB02	PA01	Miyahara	PA47			
Macé	I02				Mo	O05			
Madesis	PA68				Moisy	O26	PB20	PB18	I08
Maekawa	PA51	PB52			Molinelli	PB01			
Maier	PB46				Monini	I10			
Maijenburg	PA54	PB47			Monnet	O26	PB20	O16	PB18
Mailly	O16					O03	I08	PB31	PB36
Mairani	PB01					I13			
Majima	PA47	PA3			Montero Moreno	PB54			
Mallick	PA38				Morais	O11			
Mamonova	PA52				Morales	PA5			
Manakova	PA57				Moreno-Marín	PB61			
Manika	PA25				Moribayashi	PA45			
Maniks	PA36	PA25			Morita	O23			
Marangolo	PB17				Mota Santiago	O09	O25	PB26	PA30
Marlena	O06				Movsesyan	PA54	PB47		
Marquardt	PB31				Mücksch	PB43			
Marques	PA68				Müller, K.	O29			
Martinez, M.	PA58				Müller, R.	PA63			
Martinez, R.	PA07	PB8	PB05		Müller, S.	PB53			
Martins	PA68				Muniz	PA07	PA43		
Mashentseva	PA55				Murakami	PA12			
Masuyama	PB45				Murase	PA17			
Matsubara	PA3				Mustafin	PB15			
Matsuda	PA70	O23	O01	PA2	Nadzri	O25	PA30		
Matsumura	I15				Nagasawa	PA42			
Matsuyama	PB45				Nagy	O30			
Meckel	I01				Nakai	PB58			
Medvedev	PA67	PB64	I07	PA65	Nakajima	PA70	O23		
Meinerzhagen	O22	O08	PB22	PA11	Name	ID			
Mejia	PA43	PA10	PA07	PB42	Narumi	PA70	O23		
	PB07	PB8	I14		Nasibov	PA61			
Melilli	PA49				Nechaev	PA52			
Merabet	I01				Neethling	O20	PA29		
Metz	I01				Nersisyan	I12			
Meyer	PB9				Neubauer	PB11			
Minagawa	PA17				Neumann	I01			
Mirandola	PB01				Ngono-Ravache	O10	PB40		
Mishra	PA38	PB23	PB6		Nielsch	PB54			

Nikitina	O20				Perlov	PA28	PB21
Nishida	PA12				Perruchas	O16	
Nishio	O01				Persaud	O12	
Nitya	PB50				Petridis	I01	
Nomura	PA47				Philippe	PB56	
Nordlund	PA66	O25	PB67	PB65	Pilling	O24	
	I09				Pino	I14	
Nunzi Conti	O30				Pireaux	O11	PB39
Nuryanthi	PA51	PB52			Polukhina	PA50	
Nylandsted	PA20				Ponciano	PB05	
O'Connell	PA33	O20	PA29		Prakash	PA38	
Ochedowski	PA27	O08	PB9		Prigent	PA64	PB17 I02
Odenweller	I01				Prisner	PB28	
Ogawa	PB3				Proft	O25	
Ojha	PA22	PA06			Qian	O02	PA01
Okamoto	PA18				Quaranta	PB11	
Okateva	PA50				Quiroga	PB01	
Okayasu	O01				Radić	PB29	
Okubo	O19	PB26			Raine	PA58	PB56
Olejniczak	PA52	PB51			Rajta	O30	
Olivares Villegas	O30				Ramirez	PA64	
Orelovitch	PB51				Rangama	I01	PA27
Ozernoy	PA57				Rath	PB23	
Paillet	PA58				Ravalia	PA31	PA22
Pakarinen	O25	PB65	I09		Redaelli	PB11	
Palomares	O21	PA28			Ren	PA04	
Palumbo	PB05				Repetto	PB63	
Pandey, A.	PA34				Ridgway	I09	PA30
Pandey, R.	PA34				Ridley	I12	
Pannu	PA39	PA06	PB50		Rienecker	PB60	
Papaléo	PB41	PA44	O11	PB39	Righini	O30	
Parente	PA68				Rivarola	PA64	
Parkhomenko	PB34				Rizza	O16	
Pavlova	PA50				Romanenko	PB16	PB14
Pavlovič	PB15				Ropars	PB05	PB36
Pedersen	PB58				Rossi, A.	PB11	
Pellemoine	O03	O04	PA14	PB10	Rossi, M.	O29	
Pelli	O30				Roth	PA59	PB60
Pellizzi	PB40				Rothard	PB04	PA43 PA10 PA07
Peña Rodriguez	O30					PB42	PB07 PB8 PA13
						O24	PB05 I14

Rozet	PA64	PB17	I02		Sellaiyan	PB19			
Rusakov	PA57				Senboshi	PA18			
Rymzhanov	PA67	PB64	PA65	PB62	Senje	I12			
	PB55	PA29			Severin	PA16	PA24	PB8	PA51
Sachan	PA32	PB24				O11	PB39	PB25	PB14
Sagaidak	PB66					PB22	PB10	O12	
Sahoo	PB6				Shah	PA22			
Saifulin	PA33				Shamblin	PA28	PB21		
Saito	PA18				Shchedrina	PA50			
Saitoh	PA70	O23			Shibata, H.	O01			
Sakai	PA48				Shibata, T.	PB50			
Sall	O26	PB20	PB18	I08	Shiina	PA2			
Sann	I01				Sigle	PB53			
Šantić	PA60	PB29			Siketić	PA60			
Santos	PA68				Simon	PB20			
Sasa	PB58	PA2			Singh	PB23	PB6	PA39	PA06
Sataka	PA70	O23	O01	PA2	Skuratov	PA33	O20	PA20	PB32
Sato	PB45					PA29			
Satpati	PB50				Sobel	PB54			
Sawada	PA51	PB52	PB48		Soe	PA50			
Schaumann	PB60				Sohatsky	O20			
Schauries	O09	O25	PA30	PB21	Solanki, P.S.	PA22			
	PB68				Solanki, V.	PB6			
Schein	O04	PB10			Soneda	PA12			
Schenkel	O12				Song	PB33			
Schleberger	PA27	O08	PA60	PB29	Sorokin	PA35	PA36	PA37	
	PB9	PB22	PB36		Spende	PB54	PB47		
Schlüter	PA63				Srivastava, N.	O31			
Schmidt-Böcking	I01				Srivastava, S. K.	PA39			
Schmidt, H.	PA13				Starkov	PA50			
Schmidt, L.	I01				Stefanuik	I12			
Schöffler	I01				Steydli	PB17	I02		
Schöppner	PA26	PB27	PB30		Stodel	PA14			
Schössler	I01				Stöhlker	I06			
Schubert	PB47	O06			Strasik	PB15			
Schumacher	PA59	PB60			Strazzulla	O24	PB05		
Schwartz, J.	O12				Stuck	I01			
Schwartz, K.	PA35	PA36	PA37	PA25	Stühn	PB54			
Seidl	PA51				Su	O05			
Sekimura	PA12				Sun, J.	PA19			

Sun, J. R.	I13				Trinter	I01			
Sun, Y.	O07	O05			Tripathi, A.	PA34			
Suzuki	PB52				Tripathi, S.K.	PA15			
Taguchi, M.	PB38	PA42			Tripathi, T.S.	PA15			
Taguchi, T.	O19				Trivedi	PA31	PA22		
Tak	PB50				Trzaska	O29			
Takahiro	O01				Tsuchida	PA47	PA17	PA3	
Takaki	I15				Tsujimoto	PA70			
Tamanis	PA25				Turchanin	O08			
Taucher-Scholz	O15				Udeshi	PA22			
Tauschwitz	PB60				Uedono	PB19			
Taylor	I12				Uglov	O20			
Teixeira	PA44				Ulbricht	PB9			
ten Elshof	PA54				Ullmann-Pleger	I01			
Terai	PB52				Ulrich	I01			
Terakawa	PB45				Ulysse	O16			
Terekhin	PA65				Urbassek	PB43			
Tessaro	PB01				Utsugi	PA48			
Testa	I10				Vacik	PA52			
Texera	PB41				Vagadia	PA31			
Thomas	I14				Valbusa	PB63			
Thomaz	PB41	PA44	O11	PB39	Van Beek	PB46			
Titze	I01				Varentsov	O28			
Toimil Molares	PB53	PA56	PA54	PB54	Veres	O30			
	PB9	PB47	PB49	O06	Vernhet	PA64	PB17	I02	
Tomita	PB58	PA2			Vetter	PA13			
Tomut	PA63	PB16	PB14	O04	Vilches-Freixas	PB01			
	PB10	PB11	O12		Virtanen	O29			
Toulemonde	PA69	PA70	O23	I08	Vladymyrov	PA50			
	PB68	I13			Vlasukova	PB34			
Tracy	O27	PA28			Voigtsberger	I01			
Trassinelli	PA64	PB17	I02		Volant	PB04			
Trautmann	O09	O27	O25	PA16	Völklein	PA56			
	PA63	PA56	PA54	PA53	Volkov	PA67	PB64	PA50	PA65
	O21	PA24	PB54	PB8		PB62	PB55	PA29	PB32
	PA51	PA13	PA28	PB10	Voronkov	PB62			
	PB25	PA26	PB27	PB28	Vosecek	O30			
	PB68	O11	PB39	PB57	Voss	PA51	PB25	PB14	PB53
	PB30	PB16	PB14	PB53	Vyas	PA22			
	PB47	PB49	O04	PB11	Wagner, F.	PB60			
	O06	O12			Wagner, M.	PA56			

Wahlstrom	I12				Zdorovets	PA57	PA55	PA09
Waitz	I01				Zeng	O07	O05	
Wang, B.	O05				Zepf	I12		
Wang, H.	O02				Zhai	O07	O05	
Wang, Y.	PA69	PA27	PA04	I13	Zhanbotin	PA57		
Wang, Z.G.	I13	PA69	PA19		Zhang, C.	PA23	PB33	
Weber	PA32	PB24	I09		Zhang, D.-H.	PA62		
Wegrowe	PA49				Zhang, F.	O27	O21	PA28 PB68
Weisen	PB12				Zhang, P.	PA01		
Widmann	O31	PA08			Zhang, R.	O02	PB02	PA01
Winkler	PB25	PB28			Zhang, X.	O02		
Wu	O14				Zhang, Y.	PA32	PB24	I09
Wucher	O22	PA11			Zhang, Z.	O05		
Xi	O05				Zhao, D.	O02		
Xiao	I13	PA04			Zhao, Y.T.	I13	PA04	
Xie	O07				Zheng	PB17		
Xu	PA04				Zhou, C.L.	I01		
Xu, S.	PA01	O02			Zhou, Xianming	PA04		
Xu, Y.	PB11				Zhu, Xiaolong	O02	PB02	PA01
Xue	PB24				Zhu, Y.	PA19		
Yadav	PA34				Zierold	PB54		
Yamaki	PA51	PB48	PB52		Zimmermann	PB37		
Yamamoto	I15				Zolnai	O30		
Yamashita	PA42				Zouros	PA68		
Yan	O02	PA01						
Yanagida	PB38							
Yao, C.	PA19							
Yao, H.	O07	O05						
Yasuda, K.	I15							
Yasuda, N.	PA62							
Ye	O05							
Yokoyama	PB13							
Yoshida	PA3							
Yoshimura	PB52							
Yoshizakil	PA18							
Yuri	PB48							
Yuvchenko	PB34							
Yuyama	PB48							
Zabels	O04	PA25						
Zarkadoula	PB24							

